The Effect of Heterogeneity in Risk-Aversion on Transportation Networks

Bachelor's Project Thesis

Britt Derksen, S4404750, b.l.derksen@student.rug.nl
Supervisors: Cherukuri & Hübl

Abstract: This thesis investigates the impact of heterogeneous risk aversion on equilibrium traffic flows and network performance in stochastic transportation networks. While existing models typically assume homogeneous risk preferences, this study extends the Conditional Value-at-Risk (CVaR)-based Wardrop equilibrium framework to account for multiple traveler groups with distinct risk aversion levels. The analysis compares the equilibrium outcomes under heterogeneous risk preferences to those obtained under a homogeneous risk assumption, with a focus on assessing whether heterogeneity leads to more efficient network performance. To explore these effects, the study evaluates different network structures, starting with simple parallel-path networks and extending to more complex configurations such as the Wheatstone network and the Sioux Falls network. The results show that heterogeneous risk preferences significantly alter equilibrium flows in smaller networks, with heterogeneity either improving or harming network performance depending on the network's structure and risk aversion configurations. However, these effects do not persist in the larger, more realistic Sioux Falls network, where the influence of heterogeneous risk aversion is minimal. These findings highlight the complex relationship between risk preferences and network performance, showing that the impact of risk heterogeneity depends on network size and complexity. Therefore, this research offers valuable insights into the effect of heterogeneity of risk aversion on transportation network equilibria and overall performance.

Contents

1 Introduction **3**

2 Problem Analysis **4**
2.1 Literature Review 4

3 System description **6**
3.1 Transportation network setup 6
3.2 Theoretical Background 8
3.3 Homogeneous CVaR-based Wardrop equilibrium 8
3.4 Heterogeneous CVaR-based Wardrop equilibrium 9
3.5 Comparison heterogeneous versus homogeneous 11

4 Networks **13**
4.1 One-OD 3-paths network 13
4.2 Two-OD 5-paths Network 16
4.3 Wheatstone Network 19
4.4 Sioux Falls network 23

5 Results **28**
5.1 One-OD 3-paths network 28
5.2 Two-OD 5-paths network 33
5.3 Wheatstone Network 37
5.4 Sioux Falls Network 40

6 Conclusion **46**

7 Discussion **47**
7.1 Limitations 47
7.2 Future research 48

A Appendix **53**
A.1 Results 54
A.2 One-OD 3-paths network 54
A.3 $\bar{\alpha} = 0.3$ 54
A.4 $\bar{\alpha} = 0.5$ 57
A.5 $\bar{\alpha} = 0.7$ 61
A.6 Two-OD 5-paths network 63
A.7 $\bar{\alpha} = 0.3$ 63
A.8 $\bar{\alpha} = 0.5$ 66
A.9 $\bar{\alpha} = 0.7$ 69
A.10 Wheatstone Network 72
A.11 $\bar{\alpha} = 0.3$ 72
A.12 $\bar{\alpha} = 0.5$ 75
A.13 $\bar{\alpha} = 0.7$ 78
A.14 Sioux Falls 81

B Matlab Codes **89**

1 Introduction

In real-world transportation networks, uncertainty arises from a wide range of sources, including traffic incidents, weather conditions, and construction activities (Siu and Lo, 2006; Chen, Zhou, Chootinan, Ryu, Yang, and Wong, 2011). Travel time uncertainty represents a fundamental challenge in transportation networks that affects both traveler behavior and system performance. Uncertainty impacts network equilibrium patterns, with actual travel times often deviating substantially from expected values (Chen, 2010). Studies demonstrate that travelers actively incorporate uncertainty into their decision-making, perceiving travel time uncertainty as a substantial risk that influences their route choices (Bell and Cassir, 2002).

In addition to uncertainty in travel times, travelers differ in how they perceive and respond to such uncertainty. Individuals vary in their tolerance for uncertainty and the possibility of extreme delays, depending on characteristics such as trip purpose, scheduling constraints, and personal preferences (Zeng, Miwa, and Morikawa, 2018; Recker, Chung, Park, Wang, Chen, Ji, Liu, Horrocks, and Oh, 2005). As a result, travelers may evaluate the same uncertain route differently, even when facing identical network conditions. Assuming a homogeneous attitude toward risk for the entire population may therefore fail to capture important aspects of real-world routing behavior.

Allowing for heterogeneity in risk preferences can have important implications for network performance. Differences in risk attitudes affect how travelers trade off expected travel time against uncertainty and therefore influence route choice decisions. When such differences are present, the resulting equilibrium traffic patterns may differ from those obtained under homogeneous risk preferences. It is therefore interesting to analyze whether heterogeneity in risk preferences may benefit or harm overall network performance, or whether it has no effect at all.

Therefore, this paper investigates the effect of heterogeneous risk aversion on equilibrium traffic flows and network performance in stochastic transportation networks. The analysis builds on a Conditional Value-at-Risk (CVaR)-based Wardrop equilibrium framework from Cherukuri (2019) and extends it to allow multiple traveler groups with distinct risk-aversion parameters. Equilibrium outcomes under heterogeneous risk preferences are compared to those obtained under homogeneous risk aversion with the same average level of risk sensitivity. This comparison isolates the impact of heterogeneity itself and allows an assessment of whether heterogeneity in risk preferences leads to differences in system-level performance.

To examine these effects across different network structures, the analysis considers networks of increasing complexity. First, a simple parallel-path network is studied to analyze the effects of heterogeneous risk preferences in a setting with limited structural interaction and purely parallel flows. Second, a non-parallel Wheatstone network is considered to investigate how heterogeneity interacts with shared congestion and network topology, including the presence of a shortcut link. Finally, the framework is applied to the Sioux Falls network to assess whether the observed effects persist in a larger and more realistic transportation network.

The remainder of the paper is organized as follows. Section 2 presents the problem analysis. Section 3 describes the system description and equilibrium framework. Section 4 introduces the networks considered in the analysis. Section 5 shows the MATLAB implementation. Section 6 reports and discusses the results. Section 7 is the conclusion, and Section 8 presents the discussion.

2 Problem Analysis

2.1 Literature Review

Traffic assignment problems study how travel demand in a transportation network is distributed across available paths. The standard analytical framework models users as selfish decision-makers who minimize their individual travel costs (Saltan, Wang, Kosay, Lin, and Sayin, 2025). In nonatomic routing games, this behavior leads to the Wardrop equilibrium (WE). Wardrop's first principle states that, at equilibrium, no traveler can reduce their journey time by unilaterally switching routes (Wardrop, 1952). As a result, all routes that are actually used between an origin–destination (OD) pair have equal and minimal travel times. The second principle states that the resulting flow pattern minimizes the total travel time experienced by all users, corresponding to an optimal state at system level (Wardrop, 1952).

However, the classical Wardrop framework relies on a deterministic perception of travel costs. Travel times are assumed to be known and identical for all users, represented by fixed or flow-dependent travel time functions. However, this assumption expects that travelers have perfect knowledge of network travel costs, and are able to identify the minimum travel cost route (Sheffi, 1984). As a result, deterministic equilibrium models may fail to accurately predict route choices and network costs given the stochastic nature of travel times in real-world traffic networks.

Deterministic equilibrium models can be extended by explicitly treating travel times as random variables. The Stochastic User Equilibrium was proposed by Daganzo and Sheffi (1977) to relax the perfect knowledge assumption that is used in the classic WE. This leads to stochastic user equilibrium formulations in which route costs are given by the expectation of the underlying random travel time (van der Weijde and van den Berg (2013)). Under this assumption, equilibrium conditions remain similar to the deterministic Wardrop equilibrium, now with used routes having equal expected costs.

In many of these models, the travelers are assumed to be risk-neutral. The assumption of risk neutrality implies that travelers evaluate routes solely on the basis of average travel time. However, in practice, travelers can be influenced by uncertainty in travel times and may select routes that provide less uncertainty, even when these involve longer expected travel times. As a result, two routes with identical expected travel times may be perceived differently if they differ in uncertainty of travel time outcomes. Therefore, the risk neutrality assumption does not reflect real-world travel conditions, where travel times are inherently uncertain due to accidents, weather variability, and construction work (Chen et al., 2011; Ordonez and Stier-Moses, 2010b). Thus, expected travel time alone cannot fully characterize route performance under uncertainty.

To address this limitation, several studies incorporate risk-sensitive route choice by modify-

ing how route costs are evaluated under uncertainty. For example, Nikolova and Stier-Moses (2015) introduce the notion of the price of risk aversion, which measures the inefficiency of risk-averse equilibria relative to risk-neutral equilibria. Numerous studies employ diverse methods for incorporating risk aversion into traffic assignment models. Moment-based methods extend expected travel time by incorporating measures of variability, such as variance or standard deviation (Nikolova and Stier-Moses, 2014; Seshadri and Srinivasan, 2017). Percentile-based methods model risk aversion by letting agents minimize a specified percentile of the uncertain cost (Pel and Nicholson, 2013; Ordonez and Stier-Moses, 2010a). Robust optimization approaches represent risk aversion by protecting against worst-case or bounded deviations from expected travel times through safety margins or uncertainty sets (Ordonez and Stier-Moses, 2010a).

Within the class of tail-risk approaches, a widely used measure is Conditional Value-at-Risk (CVaR). CVaR focuses on minimizing the potential for extreme losses. It accounts for outcomes in the worst part of the distribution (Gbadegoye, Camur, and Li, 2025). For a given confidence level, CVaR evaluates the expected travel time conditional on realizations exceeding that level, and therefore captures the severity of extreme delays. An advantage is that CVaR allows the degree of risk aversion to be adjusted through the confidence level.

Building on this idea, Cherukuri (2019) and Cherukuri (2022) formally introduce and analyze a CVaR-based Wardrop equilibrium for transportation networks under travel time uncertainty. In this formulation, the classical Wardrop equilibrium condition is extended by replacing deterministic or expected travel time with CVaR as the perceived route cost. At equilibrium, all routes used between an OD pair have equal and minimal CVaR values. The authors provide a precise mathematical definition of the equilibrium, establish its existence, and show that it can be computed by formulating the problem as a variational inequality that admits a linear complementarity representation. To address the fact that the underlying travel time distribution is typically unknown, they propose a sample average approximation approach and establish asymptotic consistency and exponential convergence of the resulting sample-based equilibrium.

A key simplifying assumption in their CVaR-based Wardrop equilibrium framework is that all travelers share the same degree of risk aversion, represented by a single CVaR confidence parameter. (Cherukuri, 2019) The authors state that their results extend to the general case with heterogeneous risk aversion. However, they do not investigate how heterogeneity in risk aversion affects network performance. In practice, travelers differ substantially in their tolerance for travel time uncertainty, depending on factors such as trip purpose, age, and individual preferences (Zeng et al., 2018; Recker et al., 2005). Some users behave nearly risk-neutral, while others strongly avoid routes with even small probabilities of severe delay. As a result, different travelers may perceive the same uncertain route very differently.

Ignoring heterogeneity in risk aversion may therefore affect equilibrium predictions. When travelers have different risk preferences, routes that are attractive to risk-tolerant users may be avoided by highly risk-averse users, leading to a segmentation of traffic across the network. Such differences in route choice behavior could alter congestion patterns and benefit or hurt aggregate network outcomes, including total expected travel time and overall reliability. For example, when travelers exhibit heterogeneous levels of risk aversion, their differing route preferences could possibly lead to a more dispersed use

of available routes. This could potentially reduce congestion on heavily used links and improve network performance. Interestingly, (Knoop, Bell, and van Zuylen, 2008) show that route choices for a given user class are directly influenced by the risk aversion of other users in the network. This implies that heterogeneous risk preferences can shape equilibrium flows and influence aggregate network outcomes.

Several studies have incorporated heterogeneity in risk aversion within traffic assignment models (Shao, Lam, and Tam, 2006; Wu and (Marco) Nie, 2011)). However, none of these studies explicitly examine how system performance differs between a fully homogeneous population and a population with heterogeneous risk preferences. Furthermore, within the CVaR-based Wardrop equilibrium framework, heterogeneous risk aversion has not been explicitly analyzed. This study therefore investigates how heterogeneity in risk aversion within the CVaR-based Wardrop equilibrium framework of Cherukuri (2019) affects equilibrium flows and network-level performance under travel time uncertainty. In particular, it examines whether the presence of heterogeneous risk preferences improves or degrades overall system performance relative to the homogeneous case.

Research Objective

The objective of this research is to examine how heterogeneity in risk aversion affects equilibrium traffic flows and network performance in stochastic transportation networks. The study extends the CVaR-based Wardrop equilibrium framework of (Cherukuri, 2019) by allowing multiple user groups with different CVaR confidence levels and compares the resulting equilibria with those obtained under homogeneous risk aversion. The central focus is to assess whether heterogeneity in risk aversion leads to different, and potentially beneficial, equilibrium outcomes in terms of congestion patterns and aggregate network costs compared to homogeneous risk aversion.

3 System description

3.1 Transportation network setup

Consider a nonatomic transportation network in which travelers choose routes selfishly. The network is represented as a directed graph

$$G = (V, E), \tag{3.1}$$

where V is the set of nodes and E is the set of directed links. A finite set of origin–destination (OD) pairs is denoted by $\mathcal{W} \subseteq \mathcal{O} \times \mathcal{D}$. For each OD pair $w = (o, d) \in \mathcal{W}$, a fixed demand $d_w > 0$ must be transported from o to d.

Let $\mathcal{P}_w$ denote the set of feasible paths connecting OD pair w, and let $\mathcal{P} = \bigcup_{w \in \mathcal{W}} \mathcal{P}_w$ be the set of all paths in the network. Each path $p \in \mathcal{P}$ carries a nonnegative flow $h_p \geq 0$. Collecting all path flows in the vector $h = (h_p)_{p \in \mathcal{P}}$, feasibility requires that total demand is met for every OD pair:

$$\sum_{p \in \mathcal{P}_w} h_p = d_w, \qquad \forall w \in \mathcal{W}. \tag{3.2}$$

The corresponding feasible set of aggregate path flows is

$$H = \left\{ h \in \mathbb{R}^{|\mathcal{P}|}_{\geq 0} \;\middle|\; \sum_{p \in \mathcal{P}_w} h_p = d_w,\ \forall w \in \mathcal{W} \right\}. \tag{3.3}$$

This set describes all admissible aggregate flow patterns in the network. In the heterogeneous model introduced later, this aggregate flow will be decomposed into group-specific flows.

To connect paths, links, and OD pairs, two incidence matrices are introduced.

Let $Q \in \{0,1\}^{|E|\times|\mathcal{P}|}$ denote the edge–path incidence matrix, where $Q_{ep} = 1$ if link e lies on path p. ℓ_e is the flow on edge $e \in E$. The resulting vector of edge flows is

$$\ell = Qh. \tag{3.4}$$

Let $B \in \{0,1\}^{|\mathcal{W}|\times|\mathcal{P}|}$ denote the OD–path incidence matrix, where $B_{wp} = 1$ if $p \in \mathcal{P}_w$. Then the OD constraints can be written compactly as

$$Bh = d, \qquad h \geq 0, \tag{3.5}$$

where $d = (d_w)_{w\in\mathcal{W}}$.

Travel times may be subject to uncertainty. Each link $e \in E$ has a deterministic travel time component and a possible additive uncertainty term. The realized link cost is modeled as

$$J_e(\ell_e, u_e) = f_e(\ell_e) + u_e, \tag{3.6}$$

where $f_e(\ell_e)$ denotes the deterministic travel time on edge e and u_e is a bounded random variable representing uncertainty. Let $u = (u_e)_{e\in E}$ denote the random network state with probability distribution $\mathbb{P}$. For links without uncertainty, $u_e = 0$ with probability one.

The random travel cost of a path p is obtained by summing the costs of its constituent links:

$$C_p(h,u) = \sum_{e\in p} J_e(\ell_e, u_e). \tag{3.7}$$

Thus, path costs depend on the aggregate flow h through congestion and on the realization of uncertainty u.

The deterministic travel time component consists of a free-flow travel time and a flow-dependent congestion term. Specifically, $t \in \mathbb{R}^{|E|}$ collects the free-flow travel times of all edges, and $R \in \mathbb{R}^{|E|\times|E|}$ is a diagonal matrix containing the congestion coefficients. The deterministic edge travel times are therefore linear functions of the aggregate edge flows.

Stacking the edge travel times into a vector, the realized edge cost vector can be written as

$$J(h,u) = RQh + t + u. \tag{3.8}$$

Then, the vector of path costs satisfies

$$C(h,u) = Q^\top RQh + Q^\top t + Q^\top u. \tag{3.9}$$

This network and cost structure applies to both the homogeneous and heterogeneous equilibrium models.

3.2 Theoretical Background

Wardrop's first principle states that, at equilibrium, no traveler can reduce their journey time by unilaterally switching routes (Wardrop, 1952). This leads to the user equilibrium, in which all used paths between an OD pair have equal and minimal travel times, while unused paths have higher travel times.
Mathematically, for an OD pair $w = (o, d)$, a flow h^* is a Wardrop equilibrium if, for every used path $p \in \mathcal{P}_w$,

$$h_p^* > 0 \;\Rightarrow\; C_p(h^*) = \min_{q \in \mathcal{P}_w} C_q(h^*), \tag{3.10}$$

where $C_p(h^*)$ denotes the travel cost of path p at equilibrium.
Wardrop's Second Principle complements the first by stating that the total travel cost in the network is minimized at this equilibrium, taking into account the aggregate flow (Wardrop, 1952).

In Wardrop's formulation, travelers are assumed to be risk-neutral, as route choices are based solely on expected travel costs. When travel times are uncertain, the risk-neutral assumption underlying Wardrop's equilibrium may no longer be appropriate. Following Cherukuri (2019), travelers evaluate path costs using CVaR to incorporate risk aversion in the model.

For a given path $p \in \mathcal{P}$ and confidence level $\alpha \in (0, 1)$, the CVaR associated with path p as a function of the flow is defined following Rockafellar and Uryasev (2000) as

$$\mathrm{CVaR}_\alpha[C_p(h, u)] = \inf_{t \in \mathbb{R}} \left\{ t + \frac{1}{\alpha}\, \mathbb{E}_{\mathbb{P}}\big[(C_p(h, u) - t)^+\big] \right\}, \tag{3.11}$$

where $(x)^+ = \max\{x, 0\}$. The CVaR captures the expected cost in the worst α-fraction of the distribution of Z, reflecting the risk associated with unfavorable outcomes. Using this formulation, the equilibrium follows Wardrop's principle, with the cost associated to each path given by its CVaR (Cherukuri, 2019).

As α decreases, travelers exhibit greater risk aversion by placing increased weight on adverse realizations of travel costs. When $\alpha = 1$, CVaR reduces to the expected value, which corresponds to the risk-neutral Wardrop equilibrium.

3.3 Homogeneous CVaR-based Wardrop equilibrium

Following the CVaR-based extension of Wardrop equilibrium proposed by Cherukuri (2019), this section considers a homogeneous population of travelers who share the same attitude toward risk. All travelers are assumed to have the same degree of risk aversion, characterized by a common risk parameter $\alpha \in (0, 1)$.

A feasible flow $h^* \in H$ is said to be a CVaR-based Wardrop equilibrium if, for every OD pair $w \in \mathcal{W}$, all used paths attain minimal CVaR cost:

$$h_p^* > 0 \;\Rightarrow\; \mathrm{CVaR}_\alpha[C_p(h^*, u)] \le \mathrm{CVaR}_\alpha[C_q(h^*, u)], \qquad \forall q \in \mathcal{P}_w. \tag{3.12}$$

This condition ensures that no traveler can reduce their perceived risk-adjusted cost by unilaterally switching routes, while simultaneously satisfying all OD demand constraints.

Cherukuri (2019) shows that the homogeneous CWE can be characterized as the solution to a variational inequality (VI): find $h^* \in H$ such that

$$(h - h^*)^\top F(h^*) \ge 0, \qquad \forall h \in H, \tag{3.13}$$

where the perceived cost mapping is defined pathwise as

$$F_p(h) := \mathrm{CVaR}_\alpha[C_p(h,u)]\,, \qquad p \in \mathcal{P}. \tag{3.14}$$

Using Equation 3.9 , the perceived cost vector can be written as

$$F(h) = Q^\top RQh + Q^\top t + \mathrm{CVaR}_\alpha\left[Q^\top u\right], \tag{3.15}$$

where the CVaR operator is applied component-wise. The final term is the vector of element-wise CVaRs associated with the random path costs induced by network uncertainty.

For computation, the VI is reformulated as a linear complementarity problem (LCP) by introducing OD potential variables $v \in \mathbb{R}^{|\mathcal{W}|}$. $v = (v_w)_{w\in\mathcal{W}}$ is the vector of minimum travel costs between any OD pair (Xie and Shanbhag, 2015).

This results in the following optimization problem:

Let $x = [h; v]$. The equilibrium can be obtained by solving

$$\min_x \; x^\top M(x) \qquad \text{subject to} \qquad M(x) \geq 0, \;\; x \geq 0, \tag{3.16}$$

where the mapping $M^(x)$ is defined as

$$M(x) = \begin{bmatrix} Q^\top RQ & -B^\top \\ B & 0 \end{bmatrix} x + \begin{bmatrix} Q^\top t + \mathrm{CVaR}_\alpha[Q^\top u] \\ -d \end{bmatrix}. \tag{3.17}$$

The structure of the LCP ensures that the equilibrium conditions are satisfied. The nonnegativity constraint $h \geq 0$ enforces feasibility of path flows, while the lower block $Bh - d$ of $M(x)$ ensures satisfaction of OD demand constraints. The upper block of $M(x)$ represents the difference between the path costs and the corresponding OD potential (Xie and Shanbhag, 2015). The complementary slackness condition $x^\top M(x) = 0$ implies that a path carries positive flow only if its CVaR cost equals the minimum CVaR cost for the associated OD pair, whereas paths with strictly higher CVaR cost carry zero flow. This reproduces Wardrop's equilibrium conditions with perceived costs given by CVaR.

In his research, Cherukuri (2019) uses a sample average approximation (SAA) to estimate the CVaR term under stochastic realizations of network uncertainty. However, this research uses an analytical representation of CVaR, which allows the equilibrium structure to be studied directly. It isolates the impact of risk aversion on network flows, which is the focus of this analysis.

3.4 Heterogeneous CVaR-based Wardrop equilibrium

The homogeneous model is extended by allowing multiple traveler groups with heterogeneous attitudes toward risk.

Let K denote the number of traveler groups, and let $\alpha_k \in (0,1)$ be the CVaR confidence level associated with group k. For each OD pair $w \in \mathcal{W}$, group-specific demands $d_w^{(k)} \geq 0$ satisfy

$$\sum_{k=1}^{K} d_w^{(k)} = d_w. \tag{3.18}$$

Each group k is associated with its own path-flow vector $h^{(k)} = (h_p^{(k)})_{p\in\mathcal{P}}$, subject to the group-specific feasibility constraints

$$\sum_{p\in\mathcal{P}_w} h_p^{(k)} = d_w^{(k)}, \qquad \forall w \in \mathcal{W}. \tag{3.19}$$

The aggregate path flow is obtained by summing across groups,

$$h = \sum_{k=1}^{K} h^{(k)}, \tag{3.20}$$

and the corresponding edge flows are still given by $\ell = Qh$. Thus, congestion and uncertainty depend on total network usage, while perceived costs differ across groups through their risk attitudes.

For group k, the perceived cost of path p is defined as

$$F_p^{(k)}(h) = \mathrm{CVaR}_{\alpha_k}[C_p(h,u)]\,, \tag{3.21}$$

where h denotes the aggregate flow.

A collection of group flows $\{h^{(k)}\}_{k=1}^K$ constitutes a heterogeneous CVaR-based Wardrop equilibrium if, for every OD pair $w \in \mathcal{W}$ and every group k,

$$h_p^{(k)} > 0 \;\Rightarrow\; \mathrm{CVaR}_{\alpha_k}[C_p(h,u)] \le \mathrm{CVaR}_{\alpha_k}[C_q(h,u)]\,, \qquad \forall q \in \mathcal{P}_w. \tag{3.22}$$

This condition ensures that no traveler, given their group-specific risk preference, can reduce perceived risk-adjusted cost by unilaterally switching routes.

The heterogeneous equilibrium is again formulated as a linear complementarity problem. Group-specific path flows and OD potentials are stacked into a single decision vector

$$x = \big[h^{(1)}; \ldots; h^{(K)}; v^{(1)}; \ldots; v^{(K)}\big],$$

where $v^{(k)} = (v_w^{(k)})_{w\in\mathcal{W}}$ denotes the vector of minimum perceived travel costs for group k.

The OD demand constraints remain group-specific and are therefore represented by block-diagonal matrices $\mathrm{blkdiag}(B,\ldots,B)$ and $\mathrm{blkdiag}(B^\top,\ldots,B^\top)$. These matrices are defined as

$$\mathrm{blkdiag}(\underbrace{B,\ldots,B}_{K}) = \begin{bmatrix} B & 0 & \cdots & 0 \\ 0 & B & \cdots & 0 \\ \vdots & \vdots & \ddots & \vdots \\ 0 & 0 & \cdots & B \end{bmatrix} \in \mathbb{R}^{K|\mathcal{W}|\times K|\mathcal{P}|}, \tag{2.23}$$

and

$$\mathrm{blkdiag}(\underbrace{B^\top,\ldots,B^\top}_{K}) = \begin{bmatrix} B^\top & 0 & \cdots & 0 \\ 0 & B^\top & \cdots & 0 \\ \vdots & \vdots & \ddots & \vdots \\ 0 & 0 & \cdots & B^\top \end{bmatrix} \in \mathbb{R}^{K|\mathcal{P}|\times K|\mathcal{W}|}. \tag{3.23}$$

In contrast, congestion affects all groups simultaneously, as it depends on the aggregate flow. This shared congestion effect is captured by the Kronecker product $J_K \otimes (Q^\top RQ)$, where J_K denotes the $K \times K$ all-ones matrix. This results in the following matrix

$$J_K \otimes (Q^\top RQ) = \begin{bmatrix} Q^\top RQ & \cdots & Q^\top RQ \\ \vdots & \ddots & \vdots \\ Q^\top RQ & \cdots & Q^\top RQ \end{bmatrix} \in \mathbb{R}^{K|\mathcal{P}| \times K|\mathcal{P}|}. \tag{3.24}$$

Each block of this matrix equals $Q^\top RQ$, reflecting that every group experiences congestion generated by the total flow contributed by all groups.

With this structure, the heterogeneous equilibrium can be computed by solving the following optimization problem:

$$\min_x \; x^\top M(x) \qquad \text{subject to} \qquad M(x) \geq 0, \;\; x \geq 0, \tag{3.25}$$

where $x = \left[h^{(1)}; \ldots; h^{(K)}; v^{(1)}; \ldots; v^{(K)}\right]$ and $M(x)$ is given by

$$M(x) = \begin{bmatrix} J_K \otimes (Q^\top RQ) & -\operatorname{blkdiag}(B^\top, \ldots, B^\top) \\ \operatorname{blkdiag}(B, \ldots, B) & 0 \end{bmatrix} x + \begin{bmatrix} Q^\top t + \mathrm{CVaR}_{\alpha_1}\left[Q^\top u\right] \\ \vdots \\ Q^\top t + \mathrm{CVaR}_{\alpha_K}\left[Q^\top u\right] \\ -d^{(1)} \\ \vdots \\ -d^{(K)} \end{bmatrix}. \tag{3.26}$$

When $K = 1$, the formulation reduces to the homogeneous CVaR-based Wardrop equilibrium.

3.5 Comparison heterogeneous versus homogeneous

To study the impact of heterogeneous risk preferences on equilibrium outcomes, the framework is extended by allowing travelers to differ in their level of risk aversion. Travelers are partitioned into $K = 3$ equally sized groups, each characterized by a CVaR confidence parameter $\alpha_k \in (0, 1)$. For each group k, perceived travel costs are constructed using the CVaR formulation introduced earlier, while congestion effects are shared across all groups through aggregate link or path flows.

Let $\bar{\alpha}$ denote the benchmark level of risk aversion used in the homogeneous model. All heterogeneous configurations are constructed such that the weighted average of the group-specific parameters equals this benchmark value. With equal group sizes, this condition reduces to

$$\frac{1}{K} \sum_{k=1}^{K} \alpha_k = \bar{\alpha}.$$

This constraint ensures that heterogeneous and homogeneous scenarios exhibit the same average attitude toward risk, so that any observed differences in equilibrium outcomes arise solely from heterogeneity in preferences rather than from changes in overall risk aversion.

For a given average risk aversion $\bar{\alpha}$, all possible heterogeneous configurations $(\alpha_1, \alpha_2, \alpha_3)$ are generated by calculating all combinations within the bounds $0 < \alpha_k < 1$, with each α_k taking values in a grid with a 0.01 step size. To guarantee that configurations reflect heterogeneity, the parameters are ordered and required to satisfy a minimum separation condition,

$$\alpha_{(k+1)} - \alpha_{(k)} \geq \delta$$

with $\delta = 0.1$. This restriction excludes configurations that are close to the homogeneous case and ensures sufficient dispersion of risk preferences across groups.

For each configuration, the heterogeneous CVaR-based Wardrop equilibrium is computed by solving the LCP that accounts for group-specific perceived costs and shared congestion effects. Let h^k denote the equilibrium flow vector for group k, and let

$$h = \sum_{k=1}^{K} h^k$$

be the resulting aggregate flow. Expected travel costs are then evaluated using the realized equilibrium flows and the mean of the uncertainty distributions, yielding a total expected system cost C_{het}.

The heterogeneous equilibrium is evaluated relative to the homogeneous benchmark by computing the cost difference

$$\Delta C = C_{\text{het}} - C_{\text{hom}},$$

where C_{hom} denotes the total expected cost obtained from the homogeneous equilibrium with $\alpha = \bar{\alpha}$. A negative value of ΔC indicates that heterogeneity in risk preferences improves system performance.

The overall degree of heterogeneity is quantified by the standard deviation of the risk-aversion parameters,

$$\text{Spread} = \sqrt{\frac{1}{K} \sum_{k=1}^{K} (\alpha_k - \bar{\alpha})^2}.$$

This methodology is applied consistently across all networks and average risk aversion values of $\bar{\alpha}$. The values $\bar{\alpha} = \{0.3, 0.5, 0.7\}$ are selected as representative average risk aversion levels to study the effect of heterogeneity in risk aversion on network performance. For each case, heterogeneous equilibria with identical average risk aversion are compared to the corresponding homogeneous equilibrium.

4 Networks

To analyze the effects of risk aversion and heterogeneity in routing behavior, several transportation networks are considered. Each network is introduced separately, together with its corresponding graph structure and associated matrices.

4.1 One-OD 3-paths network

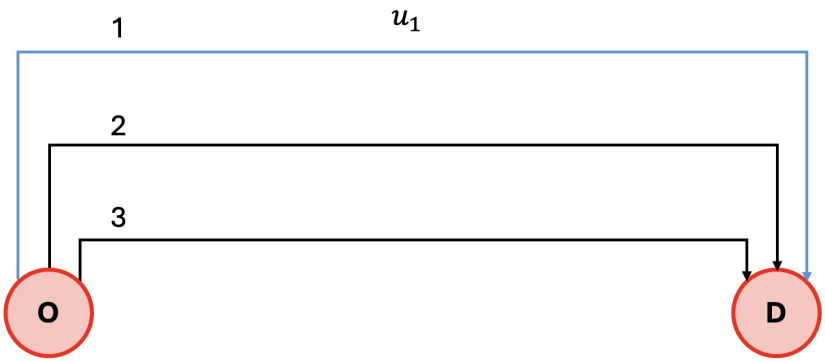

Figure 4.1: One-OD three-path network.

4.1.1 Homogeneous model

The network consists of two nodes $V = \{O, D\}$ connected by three parallel paths $\mathcal{P} = \{1, 2, 3\}$ from O to D. There is a single OD pair $w = (O, D)$ with fixed demand $d = 260$. Path flows are denoted by $h = (h_1, h_2, h_3)^\top$ and satisfy

$$h_1 + h_2 + h_3 = d, \qquad h \geq 0.$$

Since each path consists of a single edge, the edge–path incidence matrix is

$$Q = I_3,$$

and, because all three paths belong to the same OD pair, the OD–path incidence matrix is

$$B = \begin{bmatrix} 1 & 1 & 1 \end{bmatrix}.$$

The network and cost functions are adapted from Xie and Shanbhag (2015), restricted to only the three parallel paths from O to D. The random path cost function is affine in the flow and additive in the uncertainty:

$$C(h, u) = \begin{pmatrix} 40h_1 + 1000 + 3000u_1 \\ 60h_2 + 950 \\ 80h_3 + 3000 \end{pmatrix}, \tag{4.1}$$

where path 1 is uncertain with $u_1 \sim \text{Unif}[0,1]$ and paths 2 and 3 are deterministic.

Travelers evaluate paths using CVaR. For $\alpha \in (0,1]$, the perceived cost vector is defined component-wise as

$$F(h) = \text{CVaR}_\alpha[C(h,u)]\,.$$

Since uncertainty enters additively in the first path only, the perceived costs satisfy

$$\text{CVaR}_\alpha[C(h,u)] = \begin{pmatrix} 40h_1 \\ 60h_2 \\ 80h_3 \end{pmatrix} + \begin{pmatrix} 1000 + 3000\text{CVaR}_\alpha[u_1] \\ 950 \\ 3000 \end{pmatrix}. \tag{4.2}$$

For computation, the LCP is written in terms of the stacked variable $x = [h; v] \in \mathbb{R}^4$, where $v \in \mathbb{R}$ denotes the OD potential. With $Q = I_3$ and $B = [1\ 1\ 1]$, the mapping $M(x) = Ax + q$ has the explicit form

$$M(x) = \begin{bmatrix} 40 & 0 & 0 & -1 \\ 0 & 60 & 0 & -1 \\ 0 & 0 & 80 & -1 \\ 1 & 1 & 1 & 0 \end{bmatrix} \begin{pmatrix} h_1 \\ h_2 \\ h_3 \\ v \end{pmatrix} + \begin{pmatrix} 1000 + 3000\text{CVaR}_\alpha[u_1] \\ 950 \\ 3000 \\ -260 \end{pmatrix}.$$

To evaluate the perceived cost of path 1, the analytical solution to $\text{CVaR}_\alpha[u_1]$ is required. Using the Rockafellar and Uryasev (2000) representation,

$$\text{CVaR}_\alpha[u_1] = \inf_{t \in \mathbb{R}} \left\{ t + \frac{1}{\alpha}\mathbb{E}\big[(u_1 - t)^+\big] \right\}, \qquad \alpha \in (0,1], \tag{4.3}$$

the expectation can be computed explicitly.

Furthermore, the uncertainty follows the uniform distribution $u_1 \sim \text{Unif}[0,1]$. For t, the term $(u_1 - t)^+$ is nonzero only when $u_1 \geq t$. Hence, for $t \in [0,1]$,

$$\mathbb{E}\big[(u_1 - t)^+\big] = \int_t^1 (u - t)\, du = \frac{(1-t)^2}{2}, \tag{4.4}$$

and for $t \geq 1$ the expectation equals 0. Hence the objective becomes

$$\phi(t) = t + \frac{1}{2\alpha}(1-t)^2, \qquad t \in [0,1]. \tag{4.5}$$

Minimizing ϕ yields

$$\phi'(t) = 1 - \frac{1}{\alpha}(1-t) = 0 \quad \Rightarrow \quad t^* = 1 - \alpha, \tag{4.6}$$

which lies in $[0,1]$ for all $\alpha \in (0,1]$.

Evaluating ϕ at t^* therefore yields

$$\text{CVaR}_\alpha[u_1] = \phi(t^*) = 1 - \frac{\alpha}{2}. \tag{4.7}$$

4.1.2 Heterogeneous model

The network structure is unchanged: one OD pair $w = (O, D)$ with demand $d = 260$ and three parallel paths $\mathcal{P} = \{1, 2, 3\}$. Heterogeneity is introduced by splitting the demand over $K = 3$ groups with group demands

$$d^{(1)} = d^{(2)} = d^{(3)} = \frac{260}{3}.$$

Group-specific path flows are denoted by $h^{(k)} = (h_1^{(k)}, h_2^{(k)}, h_3^{(k)})^\top$ and satisfy

$$h_1^{(k)} + h_2^{(k)} + h_3^{(k)} = d^{(k)}, \qquad h^{(k)} \geq 0, \qquad k = 1, 2, 3.$$

Aggregate path flow is $h = \sum_{k=1}^{3} h^{(k)}$, so that each path cost depends on the total usage of that path. The incidence matrices remain

$$Q = I_3, \qquad B = \begin{bmatrix} 1 & 1 & 1 \end{bmatrix}.$$

The random path cost function remains

$$C(h, u) = \begin{pmatrix} 40h_1 + 1000 + 3000u_1 \\ 60h_2 + 950 \\ 80h_3 + 3000 \end{pmatrix},$$

where $u_1 \sim \text{Unif}[0, 1]$.

Each group k evaluates costs using CVaR_{α_k}, resulting in the group-specific perceived constants

$$c^{(k)} = \begin{pmatrix} 1000 + 3000\text{CVaR}_{\alpha_k}[u_1] \\ 950 \\ 3000 \end{pmatrix}, \qquad k = 1, 2, 3.$$

In the heterogeneous model, the analytical expression for the risk term remains unchanged, so that for each group k the CVaR of the uncertainty satisfies

$$\text{CVaR}_{\alpha_k}[u_1] = 1 - \frac{\alpha_k}{2}. \tag{4.8}$$

For the LCP formulation, the stacked variable is

$$x = \begin{pmatrix} h^{(1)} \\ h^{(2)} \\ h^{(3)} \\ v^{(1)} \\ v^{(2)} \\ v^{(3)} \end{pmatrix} = \begin{pmatrix} h_1^{(1)} \\ h_2^{(1)} \\ h_3^{(1)} \\ h_1^{(2)} \\ h_2^{(2)} \\ h_3^{(2)} \\ h_1^{(3)} \\ h_2^{(3)} \\ h_3^{(3)} \\ v^{(1)} \\ v^{(2)} \\ v^{(3)} \end{pmatrix} \in \mathbb{R}^{12},$$

where $v^{(k)}$ denotes the OD potential for group k. The linear complementarity mapping has the affine form $M(x) = Ax + q$ with

$$A = \begin{bmatrix} 40 & 0 & 0 & 40 & 0 & 0 & 40 & 0 & 0 & -1 & 0 & 0 \\ 0 & 60 & 0 & 0 & 60 & 0 & 0 & 60 & 0 & -1 & 0 & 0 \\ 0 & 0 & 80 & 0 & 0 & 80 & 0 & 0 & 80 & -1 & 0 & 0 \\ 40 & 0 & 0 & 40 & 0 & 0 & 40 & 0 & 0 & 0 & -1 & 0 \\ 0 & 60 & 0 & 0 & 60 & 0 & 0 & 60 & 0 & 0 & -1 & 0 \\ 0 & 0 & 80 & 0 & 0 & 80 & 0 & 0 & 80 & 0 & -1 & 0 \\ 40 & 0 & 0 & 40 & 0 & 0 & 40 & 0 & 0 & 0 & 0 & -1 \\ 0 & 60 & 0 & 0 & 60 & 0 & 0 & 60 & 0 & 0 & 0 & -1 \\ 0 & 0 & 80 & 0 & 0 & 80 & 0 & 0 & 80 & 0 & 0 & -1 \\ 1 & 1 & 1 & 0 & 0 & 0 & 0 & 0 & 0 & 0 & 0 & 0 \\ 0 & 0 & 0 & 1 & 1 & 1 & 0 & 0 & 0 & 0 & 0 & 0 \\ 0 & 0 & 0 & 0 & 0 & 0 & 1 & 1 & 1 & 0 & 0 & 0 \end{bmatrix}, \qquad q = \begin{bmatrix} 1000 + 3000\mathrm{CVaR}_{\alpha_1}[u_1] \\ 950 \\ 3000 \\ 1000 + 3000\mathrm{CVaR}_{\alpha_2}[u_1] \\ 950 \\ 3000 \\ 1000 + 3000\mathrm{CVaR}_{\alpha_3}[u_1] \\ 950 \\ 3000 \\ -\frac{260}{3} \\ -\frac{260}{3} \\ -\frac{260}{3} \end{bmatrix}.$$

4.2 Two-OD 5-paths Network

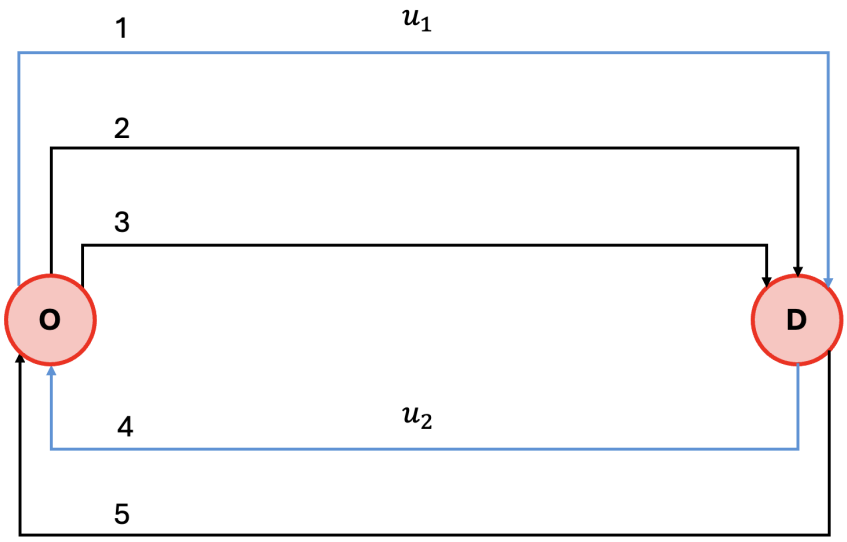

Figure 4.2: Two-OD five-path network.

4.2.1 Homogeneous model

Next, the single OD network is extended by allowing travel in both directions between the two nodes. The network consists of two nodes $V = \{O, D\}$ connected by five parallel paths $\mathcal{P} = \{1, \ldots, 5\}$. There are two OD pairs: $w_1 = (O, D)$ and $w_2 = (D, O)$, with demands

$$d = \begin{pmatrix} 260 \\ 170 \end{pmatrix}.$$

Path flows are denoted by $h = (h_1, \ldots, h_5)^\top$ and satisfy

$$h_1 + h_2 + h_3 = 260, \qquad h_4 + h_5 = 170, \qquad h \geq 0. \tag{4.9}$$

Paths 1–3 serve OD pair (O, D), while paths 4–5 serve OD pair (D, O). The OD–path incidence matrix is

$$B = \begin{bmatrix} 1 & 1 & 1 & 0 & 0 \\ 0 & 0 & 0 & 1 & 1 \end{bmatrix},$$

and, since each path consists of a single edge,

$$Q = I_5.$$

The network and cost functions are adapted from Xie and Shanbhag (2015). In this network, all the paths are considered.

Congestion interactions are captured by the matrix

$$R = \begin{bmatrix} 40 & 0 & 0 & 20 & 0 \\ 0 & 60 & 0 & 0 & 20 \\ 0 & 0 & 80 & 0 & 0 \\ 8 & 0 & 0 & 80 & 0 \\ 0 & 4 & 0 & 0 & 100 \end{bmatrix}.$$

R captures cross-path congestion effects, reflecting that traffic on certain paths influences the travel times on other paths.

Uncertainty now affects paths 1 and 4 through random variables $u_1, u_2 \sim \mathrm{Unif}[0, 1]$. Travelers evaluate paths using CVaR_α, so the perceived constant path costs are

$$c = \begin{pmatrix} 1000 + 3000\,\mathrm{CVaR}_\alpha(u_1) \\ 950 \\ 3000 \\ 1000 + 4000\,\mathrm{CVaR}_\alpha(u_2) \\ 1300 \end{pmatrix}.$$

As established in the previous section, for $U \sim \mathrm{Unif}[0, 1]$, the CVaR term evaluates to

$$\mathrm{CVaR}_\alpha(U) = 1 - \frac{\alpha}{2}.$$

For computation, the LCP is written in terms of the stacked variable $x = [h; v] \in \mathbb{R}^7$, where $v = (v_1, v_2)^\top \in \mathbb{R}^2$ denotes the OD potentials. With Q, B and R defined above, the mapping $M(x) = Ax + q$ has the form

$$M(x) = \begin{bmatrix} 40 & 0 & 0 & 20 & 0 & -1 & 0 \\ 0 & 60 & 0 & 0 & 20 & -1 & 0 \\ 0 & 0 & 80 & 0 & 0 & -1 & 0 \\ 8 & 0 & 0 & 80 & 0 & 0 & -1 \\ 0 & 4 & 0 & 0 & 100 & 0 & -1 \\ 1 & 1 & 1 & 0 & 0 & 0 & 0 \\ 0 & 0 & 0 & 1 & 1 & 0 & 0 \end{bmatrix} \begin{pmatrix} h_1 \\ h_2 \\ h_3 \\ h_4 \\ h_5 \\ v_1 \\ v_2 \end{pmatrix} + \begin{pmatrix} 1000 + 3000\,\mathrm{CVaR}_\alpha(u_1) \\ 950 \\ 3000 \\ 1000 + 4000\,\mathrm{CVaR}_\alpha(u_2) \\ 1300 \\ -260 \\ -170 \end{pmatrix}.$$

4.2.2 Heterogeneous model

The network structure is unchanged. Heterogeneity is introduced by splitting demand equally across $K = 3$ traveler groups with risk parameters α_k. For each group $k = 1, 2, 3$,

$$d^{(k)} = \frac{1}{3}\begin{pmatrix}260\\170\end{pmatrix}.$$

Group-specific path flows are denoted by $h^{(k)} = (h_1^{(k)}, \dots, h_5^{(k)})^\top$ and satisfy

$$Bh^{(k)} = d^{(k)}, \qquad h^{(k)} \geq 0, \qquad k = 1, 2, 3,$$

where

$$B = \begin{bmatrix}1 & 1 & 1 & 0 & 0\\ 0 & 0 & 0 & 1 & 1\end{bmatrix}.$$

Each group k evaluates costs using CVaR_{α_k}, leading to group-specific perceived constant path costs

$$c^{(k)} = \begin{pmatrix}1000 + 3000\,\mathrm{CVaR}_{\alpha_k}(u_1)\\ 950\\ 3000\\ 1000 + 4000\,\mathrm{CVaR}_{\alpha_k}(u_2)\\ 1300\end{pmatrix}, \qquad k = 1, 2, 3.$$

As established in the previous section, for $U \sim \mathrm{Unif}[0, 1]$,

$$\mathrm{CVaR}_{\alpha_k}(U) = 1 - \frac{\alpha_k}{2}.$$

For the LCP formulation, the stacked variable is

$$x = \begin{pmatrix}h^{(1)}\\ h^{(2)}\\ h^{(3)}\\ v^{(1)}\\ v^{(2)}\\ v^{(3)}\end{pmatrix} \in \mathbb{R}^{21}.$$

The affine mapping defining the heterogeneous equilibrium has the form

$$M(x) = Ax + q,$$

with the matrix A defined as

$$A = \begin{bmatrix}J_3 \otimes R & -\,\mathrm{blkdiag}(B^\top, B^\top, B^\top)\\ \mathrm{blkdiag}(B, B, B) & 0\end{bmatrix}.$$

The Kronecker product $J_3 \otimes R$ is given by

$$J_3 \otimes R = \begin{bmatrix} R & R & R \\ R & R & R \\ R & R & R \end{bmatrix},$$

and the block-diagonal matrices are defined as

$$\operatorname{blkdiag}(B, B, B) = \begin{bmatrix} B & 0 & 0 \\ 0 & B & 0 \\ 0 & 0 & B \end{bmatrix}, \qquad \operatorname{blkdiag}(B^\top, B^\top, B^\top) = \begin{bmatrix} B^\top & 0 & 0 \\ 0 & B^\top & 0 \\ 0 & 0 & B^\top \end{bmatrix}.$$

Lastly, the vector q is given by

$$q = \begin{bmatrix} 1000 + 3000\,\mathrm{CVaR}_{\alpha_1}(u_1) \\ 950 \\ 3000 \\ 1000 + 4000\,\mathrm{CVaR}_{\alpha_1}(u_2) \\ 1300 \\ 1000 + 3000\,\mathrm{CVaR}_{\alpha_2}(u_1) \\ 950 \\ 3000 \\ 1000 + 4000\,\mathrm{CVaR}_{\alpha_2}(u_2) \\ 1300 \\ 1000 + 3000\,\mathrm{CVaR}_{\alpha_3}(u_1) \\ 950 \\ 3000 \\ 1000 + 4000\,\mathrm{CVaR}_{\alpha_3}(u_2) \\ 1300 \\ -\frac{260}{3} \\ -\frac{170}{3} \\ -\frac{260}{3} \\ -\frac{170}{3} \\ -\frac{260}{3} \\ -\frac{170}{3} \end{bmatrix}.$$

4.3 Wheatstone Network

4.3.1 Homogeneous model

The Wheatstone network is introduced to examine the interaction between risk aversion and the classical Braess paradox. Unlike the previously considered networks, the Wheatstone network is not a parallel path network. Instead, it consists of interacting routes that share links and include an additional shortcut between intermediate nodes.

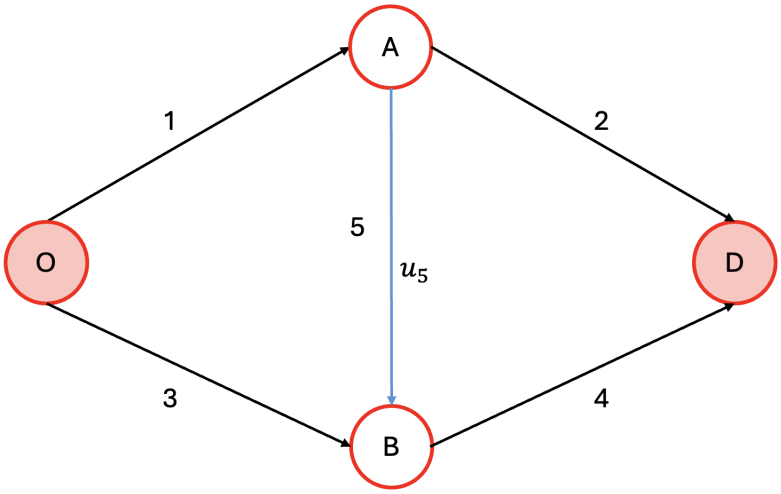

Figure 4.3: Wheatstone network (with shortcut link).

Under deterministic conditions ($U \equiv 0$), the Wheatstone network exhibits the Braess paradox (Verbree and Cherukuri, 2023). In this setting, adding the shortcut edge can increase equilibrium travel time and total system cost compared to the network without the shortcut (Abdulhafedh, 2022). The mechanism is that selfish routing shifts flow toward the shortcut path, increasing congestion on shared links and thereby worsening overall network performance.

The network consists of four nodes $V = \{O, A, B, D\}$ and five directed edges. A single OD pair $w = (O, D)$ is considered with fixed demand $d = 4000$.

The directed edges are defined as

$$e_1 : O \to A, \quad e_2 : A \to D, \quad e_3 : O \to B, \quad e_4 : B \to D, \quad e_5 : A \to B.$$

Three feasible paths connect O to D:

$$p_1 : O \to A \to D, \qquad p_2 : O \to B \to D, \qquad p_3 : O \to A \to B \to D.$$

Let $h = (h_1, h_2, h_3)^\top$ denote the path-flow vector. Feasibility requires

$$h_1 + h_2 + h_3 = d, \qquad h \geq 0.$$

The edge–path incidence matrix is

$$Q = \begin{pmatrix} 1 & 0 & 1 \\ 1 & 0 & 0 \\ 0 & 1 & 0 \\ 0 & 1 & 1 \\ 0 & 0 & 1 \end{pmatrix},$$

and the OD–path incidence matrix is

$$B = \begin{pmatrix} 1 & 1 & 1 \end{pmatrix}.$$

Edge costs follow an affine congestion model with additive uncertainty. For each edge e, the realized travel cost is

$$J_e(\ell_e, u_e) = a_e \ell_e + t_e + u_e.$$

The network and cost functions are adapted from Abdulhafedh (2022), with

$$a = \begin{pmatrix} \frac{1}{100} \\ 0 \\ 0 \\ \frac{1}{100} \\ 0 \end{pmatrix}, \qquad t = \begin{pmatrix} 0 \\ 45 \\ 45 \\ 0 \\ 0 \end{pmatrix}.$$

The network assumes that uncertainty affects only the shortcut edge e_5. Then,

$$u = \begin{pmatrix} 0 \\ 0 \\ 0 \\ 0 \\ u_5 \end{pmatrix}, \qquad u_5 \sim \mathrm{Unif}[0,1],$$

while all other edges are deterministic.

Since uncertainty enters additively only through the shortcut path p_3, the perceived cost vector can be written as

$$C(h,u) = \begin{pmatrix} \frac{1}{100}h_1 + \frac{1}{100}h_3 + 45 \\ \frac{1}{100}h_2 + \frac{1}{100}h_3 + 45 \\ \frac{1}{100}h_1 + \frac{1}{100}h_2 + \frac{2}{100}h_3 + 20u_5 \end{pmatrix}. \tag{4.10}$$

Travelers evaluate paths using the CVaR risk measure. The perceived cost vector is therefore

$$\mathrm{CVaR}_\alpha[C(h,u)] = \begin{pmatrix} \frac{1}{100}h_1 + \frac{1}{100}h_3 \\ \frac{1}{100}h_2 + \frac{1}{100}h_3 \\ \frac{1}{100}h_1 + \frac{1}{100}h_2 + \frac{2}{100}h_3 \end{pmatrix} + \begin{pmatrix} 45 \\ 45 \\ 20\mathrm{CVaR}_\alpha[u_5] \end{pmatrix}. \tag{4.11}$$

As in this network, $u_5 \sim \mathrm{Unif}[0,1]$, the CVaR term again evaluates to

$$\mathrm{CVaR}_\alpha(U) = 1 - \frac{\alpha}{2}.$$

Finally, with the stacked variable defined as

$$x = (h_1, h_2, h_3, v)^\top,$$

the homogeneous CVaR-based Wardrop equilibrium conditions are written in LCP form as

$$M(x) = \begin{pmatrix} \frac{1}{100} & 0 & \frac{1}{100} & -1 \\ 0 & \frac{1}{100} & \frac{1}{100} & -1 \\ \frac{1}{100} & \frac{1}{100} & \frac{2}{100} & -1 \\ 1 & 1 & 1 & 0 \end{pmatrix} \begin{pmatrix} h_1 \\ h_2 \\ h_3 \\ v \end{pmatrix} + \begin{pmatrix} 45 \\ 45 \\ 20\mathrm{CVaR}_\alpha(u_5) \\ -400 \end{pmatrix}.$$

4.3.2 Heterogeneous analysis

The Wheatstone network structure remains unchanged. Heterogeneity is introduced by partitioning the single OD demand over $K = 3$ traveler groups, each characterized by a group-specific CVaR confidence level $\alpha_k \in (0, 1)$. The total OD demand $d = 4000$ is split equally across groups, such that

$$d^{(1)} = d^{(2)} = d^{(3)} = \frac{4000}{3}.$$

Group-specific path flows are denoted by

$$h^{(k)} = \left(h_1^{(k)}, h_2^{(k)}, h_3^{(k)}\right)^\top, \qquad k = 1, 2, 3,$$

and satisfy

$$h_1^{(k)} + h_2^{(k)} + h_3^{(k)} = d^{(k)}, \qquad h^{(k)} \geq 0.$$

Congestion depends on the aggregate path flow

$$h = \sum_{k=1}^{3} h^{(k)},$$

where $h = (h_1, h_2, h_3)^\top$ denotes the aggregate path-flow vector. The incidence matrices remain the same as in the homogeneous case.

Each group evaluates paths using its own CVaR risk measure. Using the homogeneous path cost specification $C(h, u)$, the perceived cost vector for group k is given by

$$\mathrm{CVaR}_{\alpha_k}[C(h,u)] = \begin{pmatrix} \frac{1}{100}h_1 + \frac{1}{100}h_3 \\ \frac{1}{100}h_2 + \frac{1}{100}h_3 \\ \frac{1}{100}h_1 + \frac{1}{100}h_2 + \frac{2}{100}h_3 \end{pmatrix} + \begin{pmatrix} 45 \\ 45 \\ 20\,\mathrm{CVaR}_{\alpha_k}(u_5) \end{pmatrix}. \tag{4.12}$$

As in the homogeneous case, $u_5 \sim \mathrm{Unif}[0, 1]$, and therefore

$$\mathrm{CVaR}_{\alpha_k}(u_5) = 1 - \frac{\alpha_k}{2}, \qquad k = 1, 2, 3.$$

Introducing the stacked decision variable

$$x = \begin{pmatrix} h^{(1)} \\ h^{(2)} \\ h^{(3)} \\ v^{(1)} \\ v^{(2)} \\ v^{(3)} \end{pmatrix} \in \mathbb{R}^{12},$$

the heterogeneous CVaR-based Wardrop equilibrium is characterized by the mapping $M(x) = Ax + q$.

The matrix $A \in \mathbb{R}^{12\times 12}$ has the same block structure as in the previous heterogeneous network formulations, with network-specific congestion captured through the matrix

$$M_{\text{base}} = Q^\top R Q.$$

Accordingly,

$$A = \begin{pmatrix} J_3 \otimes M_{\text{base}} & -\text{blkdiag}(B^\top, B^\top, B^\top) \\ \text{blkdiag}(B, B, B) & 0_{3\times 3} \end{pmatrix}.$$

The vector q collects the group-specific perceived constant costs and OD demands:

$$q = \begin{pmatrix} 45 \\ 45 \\ 20\,\text{CVaR}_{\alpha_1}(u_5) \\ 45 \\ 45 \\ 20\,\text{CVaR}_{\alpha_2}(u_5) \\ 45 \\ 45 \\ 20\,\text{CVaR}_{\alpha_3}(u_5) \\ -\frac{4000}{3} \\ -\frac{4000}{3} \\ -\frac{4000}{3} \end{pmatrix}.$$

4.4 Sioux Falls network

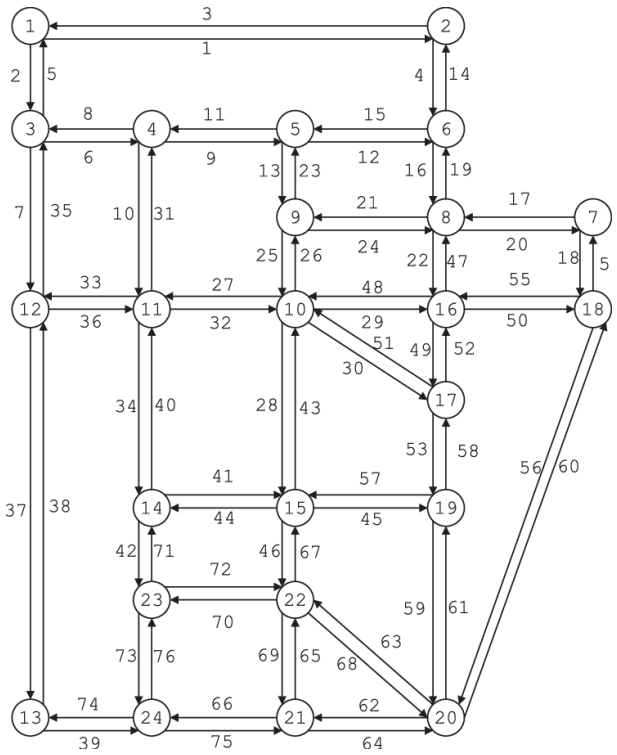

Figure 4.4: Sioux Falls network.

4.4.1 Homogeneous model

Following the simpler networks, the larger network of Sioux Falls is evaluated. The Sioux Falls traffic network consists of 24 nodes and 76 directed edges (Long, Szeto, Shi, Gao, and Huang, 2015). Each directed edge e represents a road segment carrying flow ℓ_e. The deterministic component of the edge travel time is modeled as

$$f_e(\ell_e) = t_e^0 \left(1 + b_e \frac{\ell_e}{c_e}\right),$$

where t_e^0 denotes the free-flow travel time, c_e the edge capacity, and $b_e = 100$ for all edges. The values for t_e^0 and c_e are taken from the Transportation Networks for Research Core Team (2024) repository.

For simplicity, the network is evaluated for the three origin–destination (OD) pairs (Cherukuri, 2022):

$$(1, 19), \quad (13, 8), \quad (12, 18),$$

with corresponding travel demands

$$d_{(1,19)} = 300, \qquad d_{(13,8)} = 600, \qquad d_{(12,18)} = 200.$$

For each OD pair, a finite path set is obtained by enumerating all simple directed paths up to a prescribed maximum length and retaining the ten paths with the smallest free-flow travel time. This yields a total of $P = 30$ paths, ordered first by OD pair. The selected paths are listed in Appendix A.

Let $h \in \mathbb{R}_+^{30}$ denote the vector of path flows. Edge flows $\ell \in \mathbb{R}_+^{76}$ are obtained as

$$\ell = Qh,$$

where $Q \in \{0, 1\}^{76\times 30}$ is the path–edge incidence matrix.

The OD–path incidence matrix is given by

$$B \in \{0, 1\}^{3\times 30}, \qquad B = \begin{bmatrix} \mathbf{1}_{1\times 10} & \mathbf{0}_{1\times 10} & \mathbf{0}_{1\times 10} \\ \mathbf{0}_{1\times 10} & \mathbf{1}_{1\times 10} & \mathbf{0}_{1\times 10} \\ \mathbf{0}_{1\times 10} & \mathbf{0}_{1\times 10} & \mathbf{1}_{1\times 10} \end{bmatrix}.$$

This structure reflects the fact that each path belongs to exactly one OD pair and that ten paths are associated with each OD pair.

Congestion effects are captured through the diagonal matrix

$$R = \operatorname{diag}\left(b_e \frac{t_e^0}{c_e}\right) \in \mathbb{R}^{76\times 76},$$

.

Furthermore, there is uncertainty in the travel time on edges incident to nodes 10, 16, or 17. Let

$$u = \begin{pmatrix} u_1 \\ \vdots \\ u_{76} \end{pmatrix} \in \mathbb{R}^{76}$$

denote the vector of uncertainties. For edges incident to nodes 10, 16, or 17, the uncertainty satisfies

$$u_e \sim \text{Unif}\left[0, \tfrac{1}{2}t_e^0\right],$$

while for the remaining edges $u_e = 0$.

Perceived costs are evaluated using the CVaR. To evaluate the perceived cost of the uncertain costs, the analytical expression for CVaR is required. Using Rockafellar and Uryasev (2000) representation:

$$\text{CVaR}_\alpha[u_e] = \inf_{t\in\mathbb{R}} \left\{ t + \frac{1}{\alpha}\mathbb{E}[(u_e - t)_+] \right\}, \quad \alpha \in (0, 1] \tag{4.13}$$

The uncertainty follows the uniform distribution $u_e \sim \text{Unif}[0, \frac{1}{2}t_0]$. For t, the term $(u_e - t)_+$ is then nonzero only when $u_e \geq t$. Hence, for $t \in [0, \frac{1}{2}t_0]$:

$$\mathbb{E}[(u_e - t)_+] = \int_t^{\frac{1}{2}t_0} (u_e - t) \cdot \frac{2}{t_0}\, du_e$$

Evaluating the integral:

$$\mathbb{E}[(u_e - t)_+] = \frac{2}{t_0}\int_t^{\frac{1}{2}t_0} (u_e - t)\, du_e = \frac{1}{t_0}\left(\frac{\left(\frac{1}{2}t_0 - t\right)^2}{2}\right)$$

For $t \geq \frac{1}{2}t_0$, the expectation equals 0. Hence, the objective becomes:

$$\phi(t) = t + \frac{1}{2\alpha}\left(\frac{\left(\frac{1}{2}t_0 - t\right)^2}{2}\right), \quad t \in [0, \frac{1}{2}t_0]$$

Minimizing $\phi(t)$ yields:

$$\phi'(t) = 1 - \frac{1}{\alpha t_0}\left(\frac{1}{2}t_0 - t\right) = 0 \quad \Rightarrow \quad t^* = 1 - \alpha$$

Evaluating ϕ at t^* therefore yields:

$$\text{CVaR}_\alpha[u_e] = \frac{t_0(2-\alpha)}{4} \tag{4.14}$$

The constant component of perceived path costs is therefore

$$c_{\text{path}} = Q^\top t + \text{CVaR}_\alpha(Q^\top u) \in \mathbb{R}^{30}.$$

Introducing OD potentials $v \in \mathbb{R}^3_+$ and defining the stacked variable

$$x = \begin{pmatrix} h \\ v \end{pmatrix} \in \mathbb{R}^{33},$$

the equilibrium conditions are written in affine form $M(x) = Ax + q$, where

$$A = \begin{bmatrix} Q^\top RQ & -B^\top \\ B & 0 \end{bmatrix}, \qquad q = \begin{pmatrix} Q^\top t^0 + Q^\top \mathrm{CVaR}_\alpha(u) \\ -300 \\ -600 \\ -200 \end{pmatrix}.$$

4.4.2 Heterogeneous model

The Sioux Falls network structure is unchanged. Heterogeneity is introduced by splitting each OD demand equally across $K = 3$ traveler groups with group-specific CVaR confidence levels $\alpha_k \in (0, 1)$. For each group $k = 1, 2, 3$, the group-specific OD demand vector is

$$d^{(k)} = \frac{1}{3}\begin{pmatrix} 300 \\ 600 \\ 200 \end{pmatrix} = \begin{pmatrix} 100 \\ 200 \\ \frac{200}{3} \end{pmatrix}.$$

Group-specific path flows are denoted by $h^{(k)} \in \mathbb{R}^{30}_+$ and satisfy $Bh^{(k)} = d^{(k)}$, with $h^{(k)} \geq 0$. The aggregate path flow is

$$h = \sum_{k=1}^{3} h^{(k)},$$

so that congestion depends on total network usage. The incidence matrices Q and B remain the same as in the homogeneous model.

Each group evaluates perceived costs using its own CVaR risk measure. Let $u \in \mathbb{R}^{76}$ denote the edge-level travel-time uncertainty vector defined in the homogeneous Sioux Falls model. The perceived constant path costs for group k are given by

$$c^{(k)}_{\text{path}} = Q^\top t + \mathrm{CVaR}_{\alpha_k}(Q^\top u) \in \mathbb{R}^{30}, \qquad k = 1, 2, 3.$$

For the LCP formulation, the stacked decision variable is

$$x = \begin{pmatrix} h^{(1)} \\ h^{(2)} \\ h^{(3)} \\ v^{(1)} \\ v^{(2)} \\ v^{(3)} \end{pmatrix} \in \mathbb{R}^{99}.$$

The heterogeneous complementarity mapping $M(x) = Ax + q$ has the same block structure as in the Wheatstone network formulation. Accordingly,

$$A = \begin{bmatrix} J_3 \otimes (Q^\top RQ) & -\mathrm{blkdiag}(B^\top, B^\top, B^\top) \\ \mathrm{blkdiag}(B, B, B) & 0 \end{bmatrix} \in \mathbb{R}^{99\times 99}.$$

The vector q is defined as

$$q = \begin{pmatrix} c_{\text{path}}^{(1)} \\ c_{\text{path}}^{(2)} \\ c_{\text{path}}^{(3)} \\ -100 \\ -200 \\ -\frac{200}{3} \\ -100 \\ -200 \\ -\frac{200}{3} \\ -100 \\ -200 \\ -\frac{200}{3} \end{pmatrix} \in \mathbb{R}^{99}.$$

5 Results

This section presents the equilibrium outcomes for the networks introduced in the previous section. For each network, the homogeneous CVaR-based Wardrop equilibrium is analyzed first in order to establish a baseline and to illustrate the effects of risk aversion under homogeneous risk aversion. Subsequently, the heterogeneous case is examined, in which travelers differ in their degree of risk aversion. This comparison makes it possible to assess how heterogeneity in risk preferences affects network performance. Spread–performance figures are reported in Appendix A. Furthermore, the best and worst performing heterogeneous configurations, along with their corresponding costs and cost differences, are reported in Appendix A. This section focuses on the key patterns and findings for each network.

5.1 One-OD 3-paths network

5.1.1 Homogeneous analysis

Figures 5.1a and 5.1b show the equilibrium path flows and total network cost for the homogeneous one-OD three-path network as functions of the risk aversion parameter α. Travelers with a higher degree of risk aversion (low α) behave more conservatively and allocate relatively more flow to deterministic paths, while the stochastic path carries less flow. At $\alpha = 0.1$, Path 1 carries approximately 93 units of flow, compared to about 110 units on Path 2 and 57 units on Path 3. As α increases and travelers become less risk-averse, flow shifts toward the uncertain path, which carries approximately 111 units at $\alpha = 1$, while flows on Path 2 and Path 3 decrease to around 100 and 49 units, respectively. This corresponds to an increase 19.3% in flow on Path 1, while flows on Path 2 and Path 3 decrease by 9.1% and 14.0%, respectively.

This routing behavior follows from how risk-averse travelers evaluate route costs under uncertainty. Path 1 has the lowest congestion coefficient but involves uncertainty, whereas Paths 2 and 3 offer predictable travel times at the expense of higher congestion. Travelers with higher risk aversion place greater emphasis on uncertainty in the CVaR-based cost evaluation and therefore prefer more reliable but more congested routes. As risk aversion decreases, congestion costs become relatively more important, making the stochastic path increasingly attractive.

Thus, these routing choices affect the overall network performance. As shown in Figure 5.2, total network cost decreases from 1,840,740 at $\alpha = 0.1$ to 1,804,000 at $\alpha = 1$, corresponding to a reduction of approximately 2% as travelers become less risk-averse. This indicates that higher risk aversion leads to more conservative routing behavior that increases congestion and total network cost, whereas lower risk aversion results in more cost-efficient equilibrium outcomes in this network.

5.1.2 Heterogeneous analysis

For the three-path network, the heterogeneous analysis is first conducted for an average risk-aversion level of $\bar{\alpha} = 0.3$. The corresponding homogeneous equilibrium yields a total expected system cost of

$$C_{\text{hom}} = 1{,}828{,}331.$$

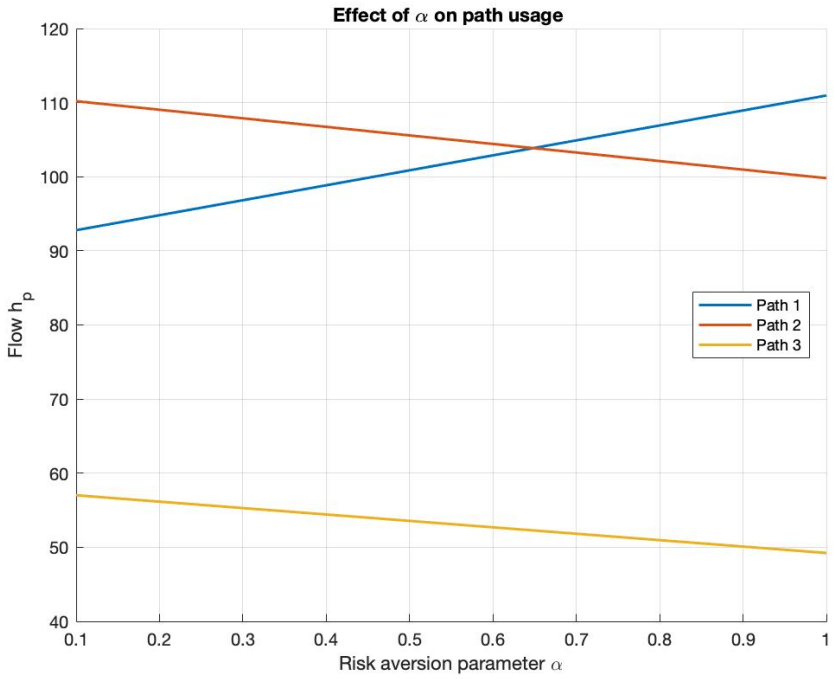

(a) Equilibrium path flows as a function of the risk aversion parameter α.

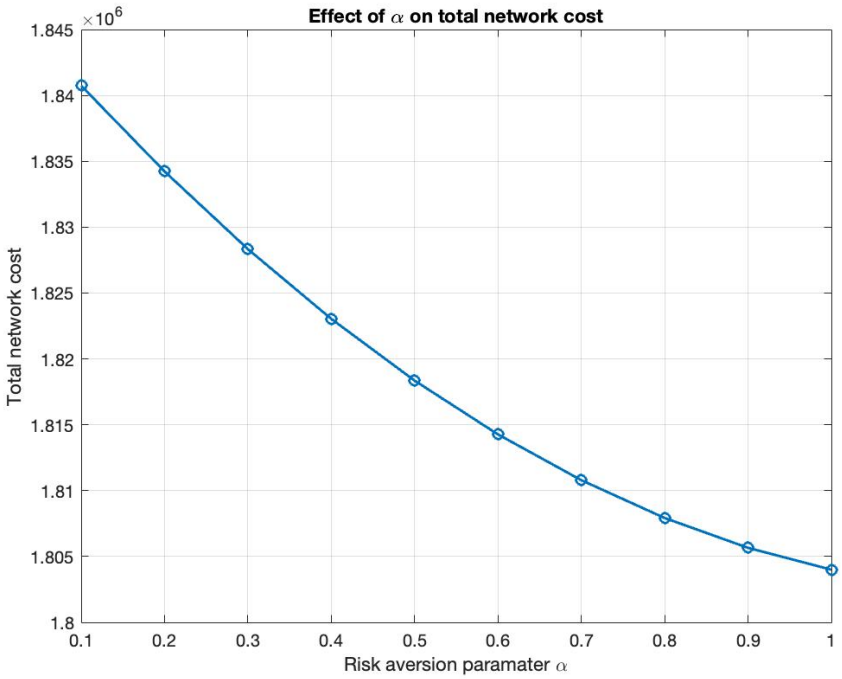

(b) Total network cost as a function of the risk aversion parameter α.

Figure 5.1: Effect of risk aversion on equilibrium flows and total network cost in the homogeneous one-OD network.

Across all heterogeneous configurations, the average cost difference relative to the homogeneous equilibrium equals $\mathbb{E}[\Delta C] = 2{,}016$, indicating that heterogeneity increases total expected cost on average. At the same time, heterogeneity does not uniformly worsen performance: 30% of all configurations yield a lower total cost than the homogeneous equilibrium. The largest observed improvement corresponds to a cost reduction of 4,791 (-0.26%), while the worst configuration increases total cost by 11,726 ($+0.64\%$).

Figure A.1 (see Appendix A) relates the cost difference ΔC to the spread of risk preferences, measured as the standard deviation of the group-specific α values. While large spread values are more frequently associated with positive cost differences, the relationship is not monotonic. Configurations with similar spread levels can result in both improvements and deteriorations relative to the homogeneous equilibrium. This indicates that the magnitude of heterogeneity is insufficient to explain system performance.

Instead, performance differences are explained by the relative position of group-specific risk aversion levels with respect to the average risk-aversion level $\bar{\alpha}$. All cost-reducing configurations share the same structure: two of the three groups have risk-aversion parameters above $\bar{\alpha} = 0.3$, while the remaining group has a lower α. Conversely, the worst-performing configurations arise when two groups have α values below the average level, implying that a majority of users are more risk-averse than in the homogeneous case. When one group's risk aversion equals the average level $\bar{\alpha}$, the configuration is effectively centered: the opposing effects of the other two groups cancel out, and total cost is equal to the homogeneous outcome.

As shown in the homogeneous analysis, higher risk aversion is associated with higher perceived travel costs. When two groups are less risk-averse than the average level, they allocate more flow to the uncertain path, while the remaining more risk-averse group avoids it. This differentiation across groups spreads demand more evenly across the network and reduces congestion on the safer alternatives. When two groups are more risk-averse than the average level, the opposite occurs: a share of demand shifts away from the uncertain path toward the same alternative, leading to higher congestion and increased total cost.

Table 5.1 illustrates this mechanism by comparing total path flows in the best and worst heterogeneous configurations. In the best configuration ($\alpha = [0.02, 0.39, 0.49]$), the uncertain path (Path 1) carries a larger share of the total flow, while flows on the safer paths are reduced. In contrast, the worst configuration ($\alpha = [0.01, 0.11, 0.78]$) shows a lower utilization of the uncertain path and a stronger concentration on the safer alternatives. These flow reallocations explain the observed cost differences and confirm that, for $\bar{\alpha} = 0.3$, heterogeneity affects system performance primarily through he relative positioning of group-specific risk aversion levels around the average, rather than through the overall magnitude of dispersion.

Table 5.1: Total path flows in the best and worst configurations for $\bar{\alpha} = 0.3$.

	Path 1†	Path 2	Path 3
Homogeneous	97	108	55
Best configuration	99	107	55
Worst configuration	93	110	57
Difference (Best – Worst)	+6	−3	−2

† Path 1 is the uncertain path.

Out of all evaluated heterogeneous configurations, 30 % fall into the first category, with two groups having $\alpha > \bar{\alpha}$, and these configurations account for the observed cost reductions. 63.33% of the configurations have two groups with $\alpha < \bar{\alpha}$, and these configurations are associated with higher total costs than in the homogeneous equilibrium. The remaining configurations include one group with $\alpha = \bar{\alpha}$ and therefore behave in a largely symmetric manner around the average level, resulting in cost differences close to zero. Together, this composition explains why heterogeneity increases total cost on average for $\bar{\alpha} = 0.3$, despite the presence of cost-reducing configurations.

Next, an average risk-aversion level of $\bar{\alpha} = 0.5$ is considered. The corresponding homogeneous equilibrium yields a total expected system cost of

$$C_{\text{hom}} = 1{,}818{,}351.$$

Across all heterogeneous configurations, the average cost difference relative to the homogeneous equilibrium equals $\mathbb{E}[\Delta C] = 201$. Heterogeneity does not consistently improve or worsen performance: 47.5% of configurations yield a lower total cost than the homogeneous equilibrium. The largest observed improvement equals 7,237 (−0.40%), while the worst configuration increases total cost by 9,424 (+0.52%).

Figure A.2 (See Appendix A again relates the cost difference ΔC to the spread of risk preferences. As in the case $\bar{\alpha} = 0.3$, no monotonic relationship is observed. Configurations with similar spread values lead to both cost reductions and cost increases, confirming that the magnitude of heterogeneity alone remains insufficient to explain system performance.

The configuration patterns identified for $\bar{\alpha} = 0.3$ are also observed for $\bar{\alpha} = 0.5$. Cost-reducing outcomes arise when two groups have risk-aversion parameters above the average level $\bar{\alpha} = 0.5$, while configurations with two groups below the average level are associated with higher total costs. Configurations that include one group with $\alpha = \bar{\alpha}$ remain effectively centered and yield outcomes close to the homogeneous equilibrium.

Table 5.2 illustrates this mechanism by comparing total path flows in the homogenous, best and worst heterogeneous configurations. In the best configuration ($\alpha = [0.01, 0.69, 0.80]$), the uncertain path carries a larger share of total flow, while congestion on the safer alternatives is reduced. In contrast, the worst configuration ($\alpha = [0.21, 0.31, 0.98]$) shows lower utilization of the uncertain path and a stronger concentration of demand on the safer routes. These flow reallocations explain the observed cost differences and confirm that, for $\bar{\alpha} = 0.5$, heterogeneity affects system performance through the relative positioning of group-specific risk aversion levels around the average.

Table 5.2: Total path flows in the best and worst configurations for $\bar{\alpha} = 0.5$.

	Path 1†	Path 2	Path 3
Homogeneous	101	106	54
Best configuration	105	103	52
Worst configuration	97	108	55
Difference (Best – Worst)	+8	+5	+3

† Path 1 is the uncertain path.

Finally, the heterogeneous analysis is conducted for an average risk-aversion level of $\bar{\alpha} = 0.7$. The corresponding homogeneous equilibrium yields a total expected system cost of

$$C_{\text{hom}} = 1{,}810{,}793.$$

Across all heterogeneous configurations, the mean cost difference equals $\mathbb{E}[\Delta C] = -907$, so heterogeneity reduces total expected cost on average. In fact, 63.33% of configurations yield a lower total cost than the homogeneous equilibrium. The best configuration achieves a cost reduction of 4,935 (-0.27%), while the worst configuration increases total cost by 3,101 ($+0.17\%$).

Figure A.3 (see Appendix A shows the relationship between the cost difference ΔC and the spread of risk aversion for $\bar{\alpha} = 0.7$. As in the previous cases, the relationship is non-monotonic: configurations with similar spread levels generate both cost increases and cost reductions.

As before, performance differences depend on how the group-specific risk aversion levels are positioned around $\bar{\alpha}$. Cost-reducing outcomes arise when two groups have risk-aversion parameters above the average level, whereas configurations with two groups below $\bar{\alpha}$ are associated with higher total costs. Table 5.3 compares the best and worst heterogeneous configurations. In the best configuration ($\alpha = [0.22, 0.89, 0.99]$), a larger share of total demand is assigned to the uncertain path (Path 1), while flows on the safer paths are reduced. In the worst configuration ($\alpha = [0.51, 0.61, 0.98]$, demand shifts away from the uncertain path toward the same safer alternatives, increasing congestion.

Table 5.3: Total path flows in the best and worst configurations for $\bar{\alpha} = 0.7$.

	Path 1†	Path 2	Path 3
Homogeneous	105	103	52
Best configuration	109	101	50
Worst configuration	103	104	53
Difference (Best – Worst)	+6	−3	−3

† Path 1 is the uncertain path.

Overall, the results show that heterogeneity can both benefit and harm network performance. Across all cases, cost reductions arise when two groups are less risk-averse than the average, which increases utilization of the uncertain path and reduces congestion on the safer alternatives. This mechanism is consistent with the homogeneous analysis, where higher risk aversion was shown to carry a system-level cost. Heterogeneity, therefore,

improves performance when it allows risk-tolerant users to exploit the uncertain path while more risk-averse users self-select away from it. However, it amplifies inefficiencies when a majority of users respond in the same risk-averse direction. For lower values of α, fewer admissible configurations satisfy the condition that two group-specific risk-aversion parameters exceed the average, whereas for higher values of α this condition is satisfied by a larger share of configurations. Differences in the fraction of cost-reducing configurations across average risk-aversion levels therefore primarily reflect the composition of the configuration set, rather than changes in equilibrium behavior.

5.2 Two-OD 5-paths network

5.2.1 Homogeneous Analysis

Figures 5.2a and 5.2b show the equilibrium path flows and total network cost for the homogeneous two-OD five-path network as functions of the risk aversion parameter α. As in the one-OD case, higher risk aversion (low α) leads travelers to allocate more flow to deterministic paths, while paths subject to uncertainty attract more flow as α increases.

Across both OD pairs, a consistent shift in path usage is observed as α increases. Paths with lower congestion coefficients but exposure to uncertainty carry increasing flow, whereas more congested deterministic paths carry decreasing flow. This reflects a change in route choice as the weight placed on uncertainty in the CVaR-based cost evaluation decreases relative to congestion costs.

As shown in Figure 5.5c, total network cost decreases from 3,978,400 at $\alpha = 0.1$ to 3,913,130 at $\alpha = 1$, corresponding to a reduction of approximately 1.6%. Higher risk aversion is therefore associated with flow allocations that place greater emphasis on reliability at the expense of higher congestion, while lower risk aversion leads to lower total network cost in this network.

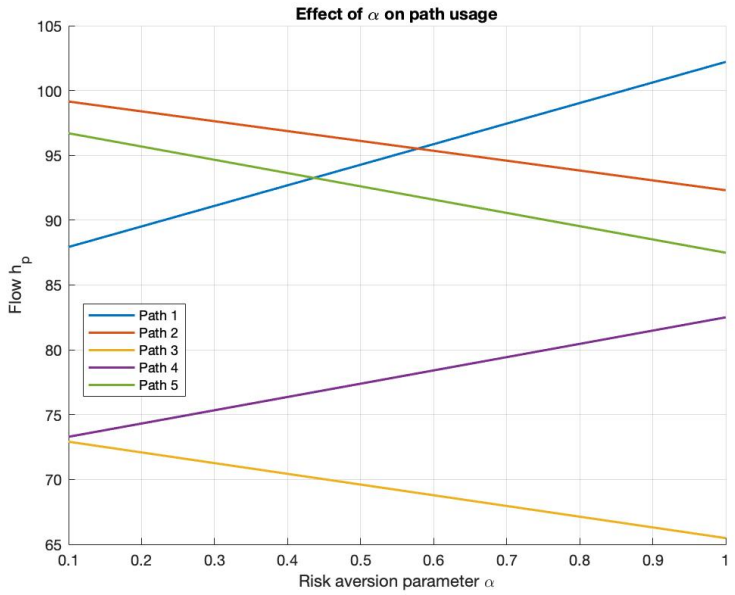

(a) Equilibrium path flows as a function of the risk aversion parameter α.

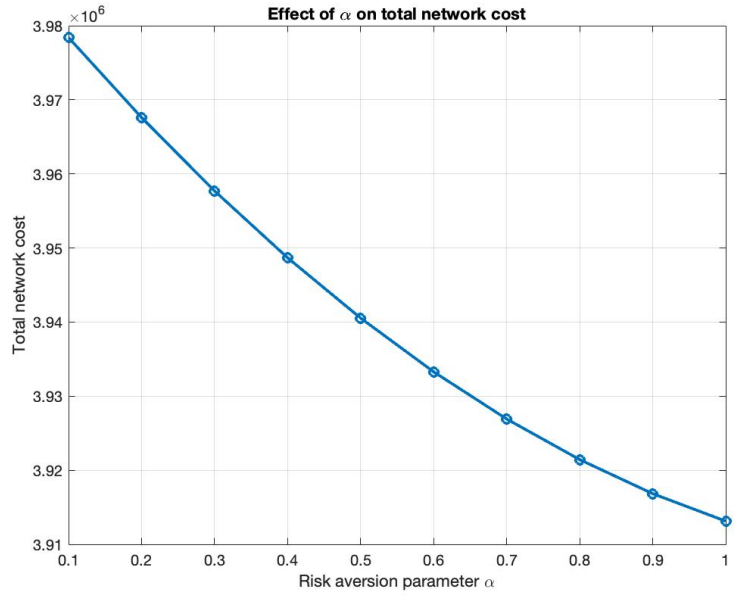

(b) Total network cost as a function of the risk aversion parameter α.

Figure 5.2: Effect of risk aversion on equilibrium flows and total network cost in the homogeneous two-OD network.

5.2.2 Heterogeneous Analysis

Similair to before, the heterogeneous CVaR-based equilibrium is evaluated for three levels of average risk aversion: $\bar{\alpha} \in \{0.3, 0.5, 0.7\}$.

The heterogeneous analysis of the two-OD five-path network confirms the same configuration mechanism identified in the one-OD three-path network. For all average risk-aversion levels considered, the configurations that minimize total system cost are those in which two

groups have risk-aversion parameters above the average level $\bar{\alpha}$, while the cost-maximizing configurations arise when two groups have risk-aversion parameters below $\bar{\alpha}$. The same alpha configurations that characterize the best and worst outcomes in the one-OD network reappear in this network. Therefore, the second OD pair does not alter the underlying structure through which heterogeneity affects equilibrium outcomes.

For $\bar{\alpha} = 0.3$, the homogeneous equilibrium yields a total expected system cost of

$$C_{\text{hom}} = 3,957,698$$

The best heterogeneous configuration reduces total cost by 8,160 (-0.21%), while the worst configuration increases total cost by 19,583 ($+0.49\%$). In the best configuration, approximately 4,470 of the cost reduction (54.8%) is attributable to OD-1 and 3,691 (45.2%) to OD-2. In the worst configuration, OD-1 accounts for 10,702 of the cost increase (54.7%), with the remaining 8,880 (45.3%) attributable to OD-2. The OD-level cost difference remains stable across best and worst outcomes.

Given the demand levels of 260 travelers for OD-1 and 170 travelers for OD-2, these absolute cost changes translate into different effects at the traveler level. In the best configuration, the cost reduction corresponds to approximately 17.2 per traveler for OD-1 and 21.7 per traveler for OD-2. In the worst configuration, the cost increase equals approximately 41.2 per traveler for OD-1 and 52.2 per traveler for OD-2. Although OD-1 contributes slightly more to total system cost changes in absolute terms, the impact of heterogeneity per traveler is larger for OD-2.

Table 5.4 shows the equilibrium path flows in the homogeneous case and in the best and worst heterogeneous configurations. Again, heterogeneity benefits the system by shifting flow toward the uncertain paths. In contrast, heterogeneity deteriorates system performance when flow is shifted away from the uncertain paths.

Table 5.4: Total path flows in the homogeneous, best and worst configurations for $\bar{\alpha} = 0.3$.

	Path 1†	Path 2	Path 3	Path 4‡	Path 5
Homogeneous	91	98	71	75	95
Best configuration	93	97	71	76	94
Worst configuration	88	99	73	73	97
Difference (Best – Worst)	+4	−2	−2	+3	−3

† Path 1 is the uncertain path for OD-1.

‡ Path 4 is the uncertain path for OD-2.

For $\bar{\alpha} = 0.5$, the homogeneous equilibrium cost equals

$$C_{\text{hom}} = 3,940,537$$

The best configuration reduces total cost by 13,022 (-0.33%), whereas the worst configuration increases total cost by 16,218 ($+0.41\%$). Of the improvement in the best configuration, 7,176 (55.1%) is attributable to OD-1 and 5,842 (44.9%) to OD-2. In the

worst configuration, OD-1 contributes around 8,894 (54.8%) and OD-2 7,324 (45.2%) to the total cost increase.

Expressed per traveler, the best configuration corresponds to a cost reduction of approximately 27.6 for OD-1 and 34.4 for OD-2, while the worst configuration results in cost increases of approximately 34.2 for OD-1 and 43.1 for OD-2. Again, the impact per traveler is larger for OD-2. Table 5.5 shows that the associated flow reallocations again involve shifts toward the uncertain paths in the best configuration and away from them in the worst configuration.

Table 5.5: Total path flows in the homogeneous, best and worst configurations for $\bar{\alpha} = 0.5$.

	Path 1†	Path 2	Path 3	Path 4‡	Path 5
Homogeneous	94	96	70	78	93
Best configuration	97	95	68	79	91
Worst configuration	91	98	71	75	95
Difference (Best – Worst)	+6	−3	−3	+4	−4

† Path 1 is the uncertain path for OD-1.

‡ Path 4 is the uncertain path for OD-2.

For $\bar{\alpha} = 0.7$, the homogeneous equilibrium yields

$$C_{\text{hom}} = 3,926,918$$

The best configuration reduces total cost by 9,658 (−0.25%), while the worst configuration increases cost by 5,690 (+0.15%). In the best configuration, OD-1 accounts for 5,368 (55.6%) of the cost reduction and OD-2 for 4,290 (44.4%). In the worst configuration, the corresponding contributions are 3,142 (55.2%) for OD-1 and 2,548 (44.8%) for OD-2.

Normalizing these cost changes by demand shows that the best configuration yields a reduction of approximately 21 per traveler for OD-1 and 25 per traveler for OD-2, whereas the worst configuration increases costs by approximately 12 per traveler for OD-1 and 15 per traveler for OD-2. The associated flow reallocations, reported in Table 5.6, follow the same qualitative pattern as for lower average risk-aversion levels.

Table 5.6: Total path flows in the homogeneous, best and worst configurations for $\bar{\alpha} = 0.7$.

	Path 1†	Path 2	Path 3	Path 4‡	Path 5
Homogeneous	97	95	68	79	90
Best configuration	100	93	66	81	89
Worst configuration	96	95	69	79	91
Difference (Best – Worst)	+4	−2	−2	+3	−3

† Path 1 is the uncertain path for OD-1.

‡ Path 4 is the uncertain path for OD-2.

Similar to the three-path network analysis, heterogeneity in the two-OD five-path network affects costs by shifting flow to the uncertain paths, even though the average

risk-aversion level remains the same. When risk preferences are balanced across groups, flow is more efficiently distributed, which can reduce congestion and total costs. However, when a majority of travelers are more risk-averse, the flow becomes overly concentrated on deterministic paths, leading to higher congestion and increased costs.

5.3 Wheatstone Network

Figures 5.3 and 5.4 show the equilibrium path flows and total network costs for the homogeneous Wheatstone network as a function of the risk aversion parameter α. When α is low (indicating higher risk aversion), travelers avoid the shortcut (O $\rightarrow$ A $\rightarrow$ B $\rightarrow$ D) due to its uncertainty. At $\alpha = 0.1$, both Path 1 (O $\rightarrow$ A $\rightarrow$ D) and Path 2 (O $\rightarrow$ B $\rightarrow$ D) carry approximately 1,400 units of flow, while Path 3 (the shortcut) carries about 1,200 units. As α increases (less risk aversion), flow shifts toward the shortcut, with Path 3 carrying approximately 3,000 units at $\alpha = 1$, while the flow on the deterministic paths (Paths 1 and 2) drops to about 500 units each. Thus flow on the shortcut path increases by 150%, while the flowns on the other two paths decrease by 64.3%.

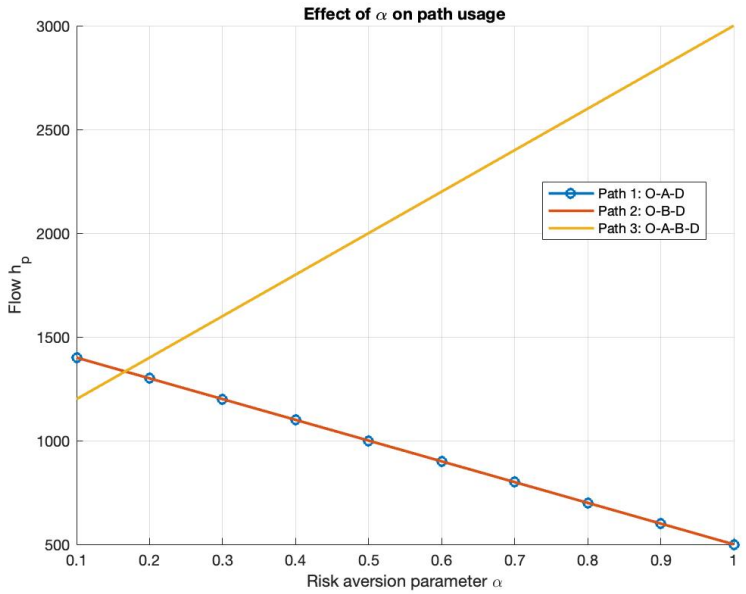

Figure 5.3: Equilibrium path flows as a function of the risk aversion parameter α.

Total network cost increases from 273,200 at $\alpha = 0.1$ to 320,000 at $\alpha = 1$, reflecting an increase of approximately 17.1%. This increase in costs shows that the network becomes less efficient as travelers become less risk-averse (higher α) and start to use the shortcut more, resulting in higher congestion on that path.

In a normal Wheatstone network without uncertainty, Braess' Paradox shows that adding an extra link to the network can lead to higher overall costs (Verbree and Cherukuri, 2023). This occurs because the additional shortcut attracts more flow, which increases congestion on that new link, thereby increasing travel times for all network users. The paradox is counter-intuitive: adding a road can increase congestion and travel times for everyone.

However, when uncertainty is placed on the shortcut (O $\rightarrow$ A $\rightarrow$ B $\rightarrow$ D) in the Wheatstone

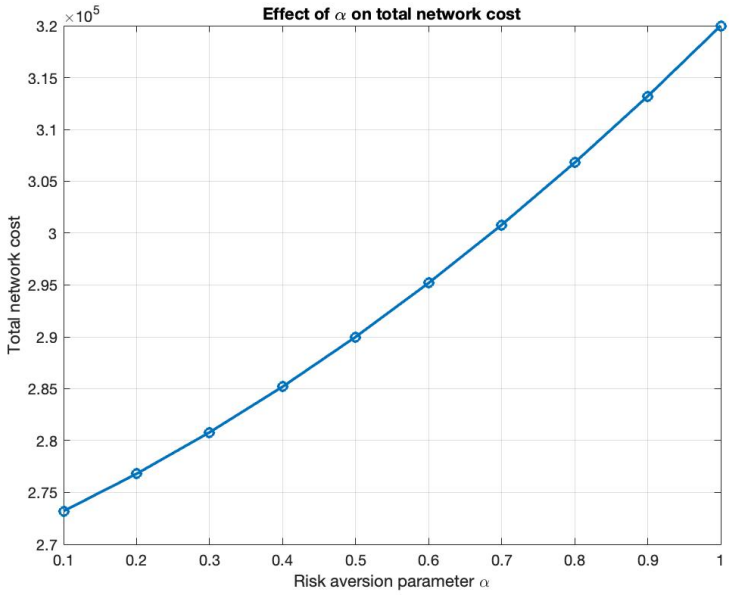

Figure 5.4: Total network cost as a function of the risk aversion parameter α.

network, the situation changes. As risk aversion increases, travelers perceive the shortcut as less reliable due to its uncertain travel times. As a result, fewer travelers use the shortcut, reducing congestion on this path and leading to a more efficient distribution of flow across the network. Therefore, the uncertainty on the shortcut leads to lower overall network costs as more travelers avoid it. Thus, risk aversion can make the Wheatstone network more efficient by reducing congestion on the shortcut.

This outcome contrasts with earlier networks, where higher risk aversion typically led to higher costs. In those cases, travelers chose less optimal, more congested paths, increasing overall costs. However, in the Wheatstone network, uncertainty on the shortcut causes risk-averse travelers to avoid it, resulting in a more efficient network and lower costs.

5.3.1 Heterogeneous Analysis

For the Wheatstone network, the heterogeneous analysis is first conducted for the average $\bar{\alpha} = 0.3$. The corresponding homogeneous equilibrium yields a total expected system cost of

$$C_{\text{hom}} = 280{,}800$$

Across the 300 heterogeneous configurations that satisfy the average constraint, heterogeneity is beneficial on average. The mean cost difference equals $\mathbb{E}[\Delta C] = -1241.52$, corresponding to a change of -0.44% relative to the homogeneous benchmark. 63.33% of configurations outperform the homogeneous case. The best configuration attains $\Delta C = -5244.44$ (-1.87%), whereas the worst configuration yields $\Delta C = 3942.00$ ($+1.40\%$).

As in the other networks, spread alone does not explain performance differences (See Appendix A. The relationship between the standard deviation of α and ΔC is non-monotonic: configurations with similar spread can lead to both improvements and deteriorations. This indicates that outcomes are primarily driven by how risk parameters are positioned relative to $\bar{\alpha}$, rather than by dispersion itself.

Compared to the earlier networks, the configuration pattern is reversed. The best-performing configurations occur when two groups have $\alpha_k < \bar{\alpha}$ and the remaining group has $\alpha_k > \bar{\alpha}$. In contrast, the worst outcomes arise when two groups have $\alpha_k > \bar{\alpha}$ and only one group is more risk-averse than average. As in the other networks, configurations in which one group has $\alpha_k = \bar{\alpha} = 0.3$ average out, since the remaining two groups are symmetrically positioned around the benchmark and induce equilibrium outcomes close to the homogeneous case

The flows between the paths are summarised in Table 5.7. In the homogeneous benchmark, the shortcut (Path 3) carries the highest flow, reflecting the inefficiency of the Braess paradox. The worst heterogeneous configuration concentrates even more flow on the shortcut than in the homogeneous case, leading to higher congestion and higher total cost. The best heterogeneous configuration corresponds to an equal division of total flow across all three paths. At this point, total flow is evenly distributed across all three paths, so that all routes have equal equilibrium cost. This configuration represents the maximum attainable improvement under heterogeneity. Around this point, multiple distinct $(\alpha_1, \alpha_2, \alpha_3)$ combinations lead to the same equilibrium cost. Once flows are evenly distributed, further changes in the composition of risk parameters do not alter the equilibrium.

Table 5.7: Total path flows in the homogeneous, best and worst configurations for $\bar{\alpha} = 0.3$.

	Path 1	Path 2	Path 3[†]
Homogeneous	1200	1200	1600
Best configuration	1333.3	1333.3	1333.3
Worst configuration	1110	1110	1780
Difference (Best – Worst)	+223.3	+223.3	–446.7

[†]Path 3 denotes the shortcut path.

This heterogeneous pattern is consistent with the homogeneous Wheatstone results. In the homogeneous analysis, increasing risk aversion improves performance by discouraging the use of the risky shortcut path and thereby weakening the Braess Paradox. The heterogeneous outcomes reflect the same mechanism through the shortcut share. In the homogeneous benchmark, the shortcut share equals 0.4. The best heterogeneous configuration is associated with a substantially lower shortcut usage (0.33), while the worst configuration corresponds to a higher shortcut usage (0.445). Thus, heterogeneity improves the Wheatstone network precisely when it shifts sufficient flow away from the shortcut. This is the same manner through which risk aversion was shown to be beneficial in the homogeneous case.

For $\bar{\alpha} = 0.5$, the homogeneous equilibrium yields a total system cost of

$$C_{\text{hom}} = 290{,}000,$$

and a shortcut share of 0.5000. Across heterogeneous configurations, 47.5% of cases outperform the homogeneous benchmark. The best configuration achieves $\Delta C = -8778.0$ (-3.03%), while the worst configuration yields $\Delta C = 10222.0$ ($+3.52\%$).

As before, configurations in which multiple groups have $\alpha_k < \bar{\alpha}$ reduce shortcut usage and improve performance, whereas configurations with multiple groups having $\alpha_k > \bar{\alpha}$ increase shortcut usage and worsen performance. In the best heterogeneous configuration, shortcut flow decreases from 2000 to 1620, corresponding to a shortcut share of 0.405. In contrast, the worst configuration increases shortcut flow to 2380, yielding a shortcut share of 0.595. The corresponding flow patterns are reported in Table 5.8.

Table 5.8: Total path flows in the homogeneous, best and worst configurations for $\bar{\alpha} = 0.5$.

	Path 1	Path 2	Path 3†
Homogeneous	1000	1000	2000
Best configuration	1190	1190	1620
Worst configuration	810	810	2380
Difference (Best – Worst)	+380	+380	–760

†Path 3 denotes the shortcut path.

For $\bar{\alpha} = 0.7$, the homogeneous equilibrium yields a total system cost of $C_{\text{hom}} = 300{,}800$ and a shortcut share of 0.6. Across the heterogeneous configurations that satisfy the mean constraint, 37% of cases outperform the homogeneous benchmark. The best configuration achieves $\Delta C = -5058.0$ (-1.68%), while the worst configuration yields $\Delta C = 8088.9$ ($+2.69\%$). As in the $\bar{\alpha} = 0.5$ case, configurations that decrease shortcut usage improve performance, whereas configurations that increase shortcut usage worsen performance. In the best configuration (e.g., $(\alpha_1, \alpha_2, \alpha_3) = (0.50, 0.61, 0.99)$), shortcut flow drops from 2400 to 2220 (shortcut share 0.555). In contrast, the worst configuration ($(0.31, 0.84, 0.95)$) increases shortcut flow to 2666.7 (shortcut share 0.6667). The corresponding equilibrium path flows are reported in Table 5.9.

Table 5.9: Total path flows in the homogeneous, best and worst configurations for $\bar{\alpha} = 0.7$.

	Path 1	Path 2	Path 3†
Homogeneous	800	800	2400
Best configuration	890	890	2220
Worst configuration	666.7	666.7	2666.7
Difference (Best – Worst)	223.3	223.3	-446.7

† Path 3 is the shortcut path.

5.4 Sioux Falls Network

5.4.1 Homogeneous analysis

For the Sioux Falls network, the results again show that changes in risk aversion lead to re-allocations of flow across available paths. As risk aversion decreases (higher α). These effects are visible across all considered OD pairs, although their magnitude differs depending on the relative costs and initial usage of the paths.

For OD pair (1,19), the paths that include uncertain edges are path 1 (1–2–6–8–16–17–19), path 9 (1–3–4–5–9–10–15–19), and path 10 (1–3–4–11–10–16–17–19). Among these, path 1 increases from approximately 24 vehicles at low α to about 32 at $\alpha = 1$ (+33%), and path 9 increases from roughly 145 to 153 vehicles (+6%). In contrast, path 10 carries zero flow for all values of α. Paths without uncertain edges lose flow: path 4 (1–2–6–8–7–18–20–19) declines from about 32 to 28 vehicles (−12%), and path 6 (1–3–4–11–14–15–19) decreases from approximately 87 to 83 vehicles (−5%). Therefore, the dominant paths experience smaller changes than the paths with less flow.

For OD pair (13,8), the paths that include uncertain edges are path 7 (13–24–21–22–15–19–17–16–8) and path 10 (13–24–23–22–15–19–17–16–8). Both gain flow as α increases: path 10 rises from approximately 30 to 35 vehicles (+17%), and path 7 increases from about 17 to 22 vehicles (+22%). Path 5 (13–24–21–22–20–18–7–8), which does not include uncertain edges, also increases from roughly 23 to 29 vehicles (+26%), indicating that some deterministic paths benefit indirectly as congestion patterns change. In contrast, several higher-flow paths without uncertain edges decline slightly: path 1 (13–12–3–4–5–6–8) decreases from about 222 to 217 vehicles (−2%), path 6 (13–12–3–1–2–6–8) declines from roughly 147 to 140 vehicles (−5%), and path 8 (13–24–23–22–20–18–7–8) decreases from around 60 to 56 vehicles (−7%). Path 3 (13–12–11–4–5–6–8) remains almost constant at approximately 101 vehicles, while path 9 (13–24–21–20–18–16–8) carries zero flow for all values of α.

For OD pair (12,18), the paths that include uncertain edges are path 1 (12–11–10–16–18) and path 7 (12–3–4–5–6–8–16–18). Of these, path 7 shows a clear increase in usage, rising from approximately 12 to 18 vehicles (+50%). Path 1 changes only marginally, increasing from about 160 to 162 vehicles (+1%) and continuing to carry the majority of demand. Paths without uncertain edges experience declining flows: path 2 (12–13–24–21–20–18) decreases from about 11 to 7 vehicles (−36%), path 4 (12–13–24–21–22–20–18) declines from 8 to 6 vehicles (−25%), and path 5 (12–13–24–23–22–20–18) falls from 10 to 7 vehicles (−30%). Paths 8–10 carry zero flow for all values of α.

Across all OD pairs, the limited variation observed on dominant paths indicates that their relatively low base travel costs remain more important than changes in risk preferences. In contrast, paths with lower initial flow levels tend to exhibit larger relative changes. Some paths carry zero flow for all values of α, indicating that their relatively high base cost prevents them from becoming attractive under any risk preference.

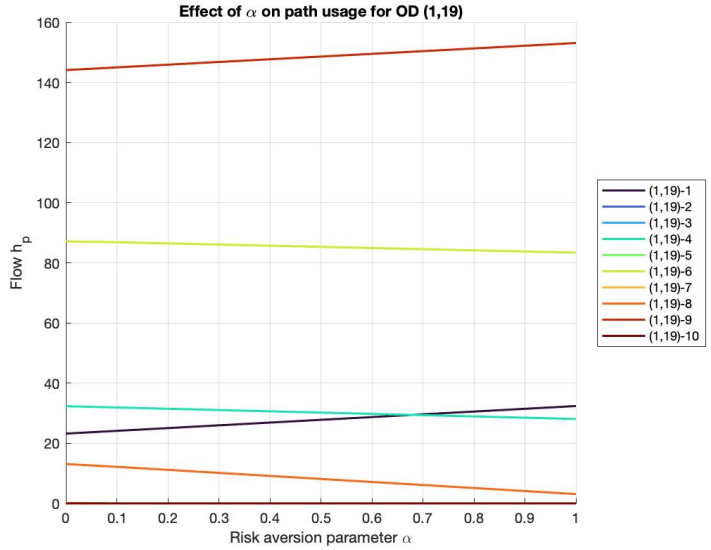

(a) OD 1: Equilibrium path flows.

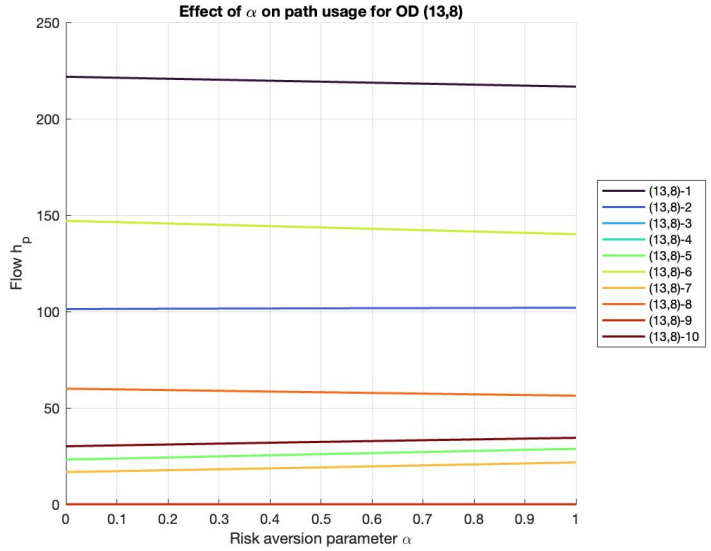

(b) OD 2: Equilibrium path flows.

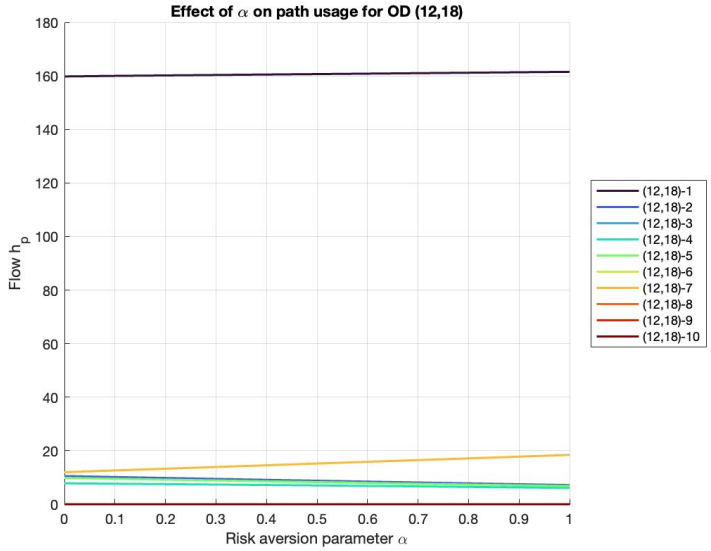

(c) OD 3: Equilibrium path flows.

Figure 5.5: Effect of risk aversion on equilibrium flows in the Sioux Falls network.

Figure 5.6 shows a steady decline in total network cost as the risk aversion parameter α increases. When $\alpha = 1$, the total cost is approximately 82 510, decreasing to about 82 301 when α=1. This represents a reduction of roughly 209 units, corresponding to about 0.25% of the total network cost. This reduction again suggests that lower risk aversion leads to a more efficient use of the network. Although the absolute change in total cost is small, the decrease is consistent over the entire range of α, indicating improvement in network performance as users become less risk-averse.

The relationship between α and total network cost is not linear. The reduction in cost is larger at lower values of α and becomes more gradual as α increases. This indicates that changes in risk aversion have a stronger impact on network efficiency at low values of α.

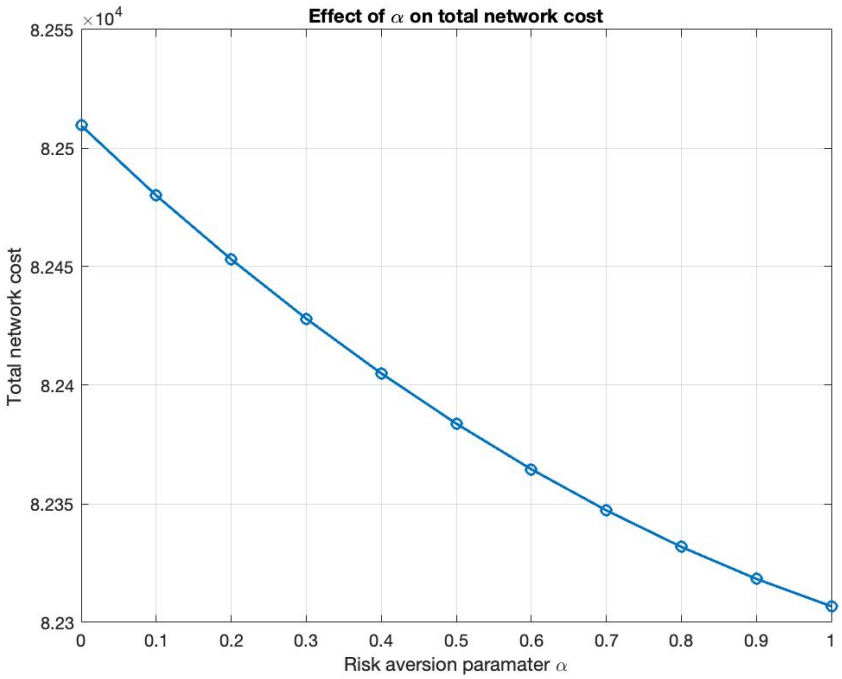

Figure 5.6: Sioux Falls: Total network cost as a function of the risk aversion parameter α

5.4.2 Heterogeneous Analysis

As before, the heterogeneous equilibrium outcomes for the Sioux Falls network are compared to the corresponding homogeneous equilibria for three benchmark levels of average risk aversion, $\bar{\alpha} \in \{0.3, 0.5, 0.7\}$. For the Sioux Falls network, the heterogeneous analysis differs from that of the smaller benchmark networks.The equilibrium outcomes do not display the clear distinguishable configuration patterns observed previously.

Across all heterogeneous configurations, the cost difference ΔC remains negative. That is, heterogeneity in risk preferences never leads to an increase in total network cost. In fact, 100% of heterogeneous configurations yield a lower total cost than the homogeneous equilibrium.

Despite this consistent direction, the magnitude of the effect is very limited. For $\bar{\alpha} = 0.3$, the homogeneous equilibrium yields a total system cost of

$$C_{\text{hom}} = 82{,}428,$$

. The largest observed reduction in the heterogeneous case equals approximately 11.6 ($a = [0.04, 0.18, 0.68]$). The least favorable heterogeneous configuration still improves upon the homogeneous benchmark by roughly 5.0 ($a = [0.20, 0.30, 0.40]$). In relative terms, these correspond to improvements of approximately 0.014% and 0.006%, respectively.

In addition to aggregate cost outcomes, equilibrium path flows were compared between the homogeneous, best and worst heterogeneous configurations. Table 5.10 reports total path flows for both cases. While small reallocations across individual paths can be observed, the overall flow patterns remain highly similar. Differences are limited to a small number of paths and do not result in substantial changes in congestion, which is consistent with the very small differences in total system cost.

To examine how these changes are distributed across the network, OD-level costs were considered. For $\bar{\alpha} = 0.3$, this decomposition indicates that the aggregate improvement is not shared uniformly across OD pairs. Relative to the homogeneous equilibrium, the best heterogeneous configuration increases the allocated cost for OD $1 \rightarrow 19$ and OD $13 \rightarrow 8$ by approximately 42.2 and 60.0, respectively, while reducing the allocated cost for OD $12 \rightarrow 18$ by approximately 112.5. The same pattern is observed for the worst heterogeneous configuration, where OD $1 \rightarrow 19$ and OD $13 \rightarrow 8$ increase by approximately 14.5 and 20.3, and OD $12 \rightarrow 18$ decreases by approximately 39.3. Hence, the overall reduction in total system cost is primarily driven by a cost decrease on OD $12 \rightarrow 18$, which outweighs the small cost increases for the other OD pairs.

Similar patterns are observed for higher average levels of risk aversion. For $\bar{\alpha} = 0.5$, all heterogeneous configurations again outperform the homogeneous benchmark of

$$C_{\text{hom}} = 82{,}383$$

Cost reductions range from approximately 4.7 ($a = [0.13, 0.44, 0.93]$) to 13.3 ($a = [0.40, 0.50, 0.60]$). The overall reduction in total system cost is driven by a decrease in OD $12 \rightarrow 18$, as OD $1 \rightarrow 19$ and OD $13 \rightarrow 8$ experience small cost increases. The corresponding relative improvements remain below 0.016%, and equilibrium path flows differ only marginally between configurations.

For $\bar{\alpha} = 0.7$, the results are qualitatively identical. Heterogeneity never increases total system cost, and the magnitude of the observed improvements remains small. The best-performing configuration yields a reduction of approximately 10.3 ($a = [0.41, 0.70, 0.99]$), while the least favorable heterogeneous configuration improves upon the homogeneous benchmark by approximately 4.5 ($a = 0.60, 0.70, 0.80]$). This corresponds to a maximum cost reduction of 0.012%. Again, the total reduction in system cost is driven by a decrease in OD $12 \rightarrow 18$. As before, differences in equilibrium path flows between configurations are minor.

These results align with the homogeneous Sioux Falls analysis, in which variations in the level of risk aversion already led to only limited changes in total system cost. As a

result, introducing heterogeneity does not significantly alter equilibrium outcomes. While heterogeneous risk preferences do not hurt system performance, they do not lead to meaningful improvements in network efficiency for the Sioux Falls network.

Table 5.10: Sioux Falls equilibrium path flows for $\bar{\alpha} = 0.3$: homogeneous, best heterogeneous, and worst heterogeneous configurations

OD	Path	Homogeneous	Best hetero	Worst hetero
1	1	26	26	26
	2	0	0	0
	3	0	0	0
	4	31	32	31
	5	0	0	0
	6	86	87	86
	7	0	0	0
	8	10	9	9
	9	147	146	147
	10	0	0	0
2	11	220	220	220
	12	102	99	100
	13	0	0	0
	14	0	0	0
	15	25	31	31
	16	145	144	145
	17	18	15	14
	18	59	53	54
	19	0	0	0
	20	31	38	36
3	21	160	157	159
	22	9	12	11
	23	0	0	0
	24	7	7	6
	25	9	9	9
	26	0	0	0
	27	14	15	14
	28	0	0	0
	29	0	0	0
	30	0	0	0

6 Conclusion

This thesis studied how heterogeneity in risk aversion affects equilibrium flows and system performance in transportation networks. Building on the CVaR-based Wardrop equilibrium framework of (Cherukuri, 2019, 2022), the model was extended to allow multiple user groups with different degrees of risk aversion while keeping the average level of risk aversion fixed. Homogeneous and heterogeneous equilibria were compared across networks of increasing structural complexity, ranging from simple parallel-path networks to the Wheatstone network and the larger-scale Sioux Falls network.

Before introducing heterogeneity, the homogeneous analysis already shows that risk aversion has a clear and systematic effect on equilibrium flows and costs. In the parallel-path networks, higher risk aversion shifts flow away from uncertain routes toward deterministic alternatives. Users place less weight on expected travel time and avoid uncertainty, which concentrates demand on safer routes. This leads to a less efficient allocation of traffic and a higher total expected system cost, illustrating a clear price of risk aversion. In contrast, in the Wheatstone network, higher risk aversion reduces usage of the uncertain shortcut, which weakens the Braess paradox and results in a lower total cost. In the Sioux Falls network, changes in risk aversion also lead to lower costs, but the effect is much smaller, reflecting a limited sensitivity of equilibrium flows to risk attitudes.

Heterogeneity in risk aversion can affect equilibrium flows and system costs even when the average level of risk aversion is held fixed. Group-specific differences in risk attitudes change how traffic is distributed across routes, which affects equilibrium flows and total expected cost. This confirms that heterogeneous equilibria are not equivalent to homogeneous equilibria with the same average risk aversion. Across all networks, heterogeneity does not lead to a single or systematic effect on system performance. For a fixed average level of risk aversion, heterogeneous equilibria can result in either higher or lower total expected system cost than the homogeneous equilibrium. Heterogeneity is therefore neither inherently beneficial nor inherently harmful. Its effect depends on how it interacts with congestion, uncertainty, and network structure. Importantly, there is no monotonic relationship between the degree of dispersion in risk preferences and system performance: heterogeneous configurations with similar spread can lead to opposite outcomes, indicating that dispersion alone is not sufficient to explain the observed effects.

A second interesting finding is that heterogeneity affects system performance by reinforcing the flow mechanisms already present in the homogeneous model. Heterogeneity does not introduce a new type of routing behavior, but redistributes demand across the same mechanisms that govern the homogeneous equilibrium, depending on how many users are more or less risk-averse than in the homogeneous benchmark. As a result, heterogeneous outcomes move in the same direction as the effect of risk aversion observed in the homogeneous case.

This is clearly visible in the simple parallel-path networks. In the homogeneous model, higher risk aversion increases costs because flow concentrates on deterministic routes. In the heterogeneous model, when a larger share of the population is more risk-averse than in the homogeneous benchmark, this concentration becomes stronger: more flow is shifted away from the uncertain route, congestion on deterministic routes increases further, and

total cost rises.

The Wheatstone network shows the same reinforcing role of heterogeneity, but with the opposite underlying mechanism. In the homogeneous analysis, risk aversion improves system performance by reducing shortcut usage and weakening the Braess paradox. Heterogeneity again strengthens or weakens this effect depending on the composition of the population. When a sufficiently large share of users is risk-averse, shortcut usage decreases further and total network cost is reduced even more. Thus, also in this network, heterogeneity operates through the same flow reallocations that determine the homogeneous outcome.

However, the magnitude of heterogeneous effects depends on how strongly risk aversion influences the homogeneous equilibrium. In networks where homogeneous risk aversion leads to substantial changes in route choice and costs, heterogeneity produces noticeable differences in system performance. In networks where homogeneous risk aversion has only a limited effect, heterogeneity is correspondingly weak. This explains the contrast with the Sioux Falls network, where equilibrium flows are relatively insensitive to risk aversion and heterogeneous configurations lead to extremely small cost differences. In this network, heterogeneity also does not lead to worse performance. Therefore, the observed effects in the smaller networks do not persist in the larger, more realistic transportation network of Sioux Falls.

Overall, the results confirm that heterogeneity in risk aversion can influence network performance. Even when the average level of risk aversion is the same, group-specific preferences affect equilibrium flows and costs. However, heterogeneity does not automatically improve or worsen system performance. The impact of heterogeneity depends on network characteristics, including network size and structure. These characteristics are ultimately decisive in determining how differences in risk attitudes are reflected in equilibrium flows and overall system performance.

7 Discussion

7.1 Limitations

This study is subject to several limitations that should be considered when interpreting the results. First of all, the analysis is conducted on a limited set of network topologies. Although this allows for controlled comparisons and insights into underlying mechanisms, the results remain network-dependent. Consequently, the conclusions cannot be directly generalized to all transportation networks, particularly those with different structural properties, demand patterns, or congestion characteristics.

Furthermore, heterogeneity in risk aversion is introduced through equally sized traveler groups. While this design isolates the effect of heterogeneity itself, actual traveler populations are unlikely to be evenly distributed across risk-preference levels. Skewed distributions of risk aversion could lead to different equilibrium patterns and system-level outcomes, potentially altering the impact of heterogeneity observed in this study.

Third, travel time uncertainty is modeled using independent uniform distributions on

selected links. This assumption enables closed-form expressions for CVaR. In reality, travel time uncertainty is often characterized by asymmetry, extreme delays, correlation across links, and time-of-day effects. As a result, the findings may not fully capture the complexity of uncertainty in real transportation networks.

7.2 Future research

The results show that heterogeneity in risk aversion can either improve or deteriorate system performance, depending on the relative positioning of group-specific risk preferences and the network structure. An interesting next step would be to examine how robust these effects are under variations in key modeling parameters. In particular, a sensitivity analysis could be conducted with respect to the magnitude of travel time uncertainty, as well as demand and congestion parameters. This would provide further insight into the robustness of the observed performance differences between homogeneous and heterogeneous equilibria.

In addition, future research could extend the analysis to a broader class of network topologies. This includes other larger real-world networks beyond Sioux Falls, as well as synthetic or randomly generated networks that allow structural characteristics to be varied in a controlled manner. Such analyses would help clarify how network structure influences the impact of heterogeneous risk aversion on equilibrium outcomes.

Finally, rather than modeling heterogeneity through a small number of discrete groups, risk aversion could be represented as a continuous distribution across travelers. This would allow a more realistic representation of population heterogeneity and help assess whether the insights obtained with three groups persist in a more general setting.

The author acknowledges the use of AI models in the writing of this thesis. AI tools were mainly employed to assist with drafting, editing, and refining the written text. The content, research design, data analysis, and final conclusions remain the responsibility of the author.

References

Azad Abdulhafedh. Addressing traffic congestion by using of the counter-intuitive phenomenon of braess' paradox in transportation networks. *Open Access Library Journal*, 09:1–12, 09 2022. doi:10.4236/oalib.1109229.

Michael G.H. Bell and Chris Cassir. Risk-averse user equilibrium traffic assignment: an application of game theory. *Transportation Research Part B: Methodological*, 36(8):671–681, 2002. ISSN 0191-2615. doi:https://doi.org/10.1016/S0191-2615(01)00022-4. URL https://www.sciencedirect.com/science/article/pii/S0191261501000224.

Anthony Chen, Zhong Zhou, Piya Chootinan, Seungkyu Ryu, Chao Yang, and S. Wong. Transport network design problem under uncertainty: A review and new developments. *Transport Reviews*, 31:743–768, 11 2011. doi:10.1080/01441647.2011.589539.

Daizhuo Chen. *Modeling Travel Time Uncertainty in Traffic Networks*. PhD thesis, Massachusetts Institute of Technology, Cambridge, MA, 2010. URL http://hdl.handle.net/1721.1/61889.

Ashish Cherukuri. Sample average approximation of cvar-based wardrop equilibrium in routing under uncertain costs, 2019. URL https://arxiv.org/abs/1909.03783.

Ashish Cherukuri. Sample average approximation of conditional value-at-risk based variational inequalities, 2022. URL https://arxiv.org/abs/2208.11403.

Carlos F. Daganzo and Yosef Sheffi. On stochastic models of traffic assignment. *Transportation Science*, 11(3):253–274, August 1977. doi:10.1287/trsc.11.3.253. URL https://ideas.repec.org/a/inm/ortrsc/v11y1977i3p253-274.html.

Jeremiah Gbadegoye, Mustafa Can Camur, and Xueping Li. A two-stage stochastic model for road-rail intermodal freight transportation under demand and capacity uncertainty. *International Journal of Transportation Science and Technology*, 2025. ISSN 2046-0430. doi:https://doi.org/10.1016/j.ijtst.2025.07.004. URL https://www.sciencedirect.com/science/article/pii/S2046043025001029.

Victor Knoop, Michael Bell, and Henk van Zuylen. Traffic assignment based on individual risk-attitude. pages 1 – 2, 12 2008. doi:10.1109/INFRA.2008.5439672.

Jiancheng Long, W. Szeto, Qin Shi, Ziyou Gao, and Hai-Jun Huang. A nonlinear equation system approach to the dynamic stochastic user equilibrium simultaneous route and departure time choice problem. *Transportmetrica A: Transport Science*, 11:388–419, 02 2015. doi:10.1080/23249935.2014.1003112.

E. Nikolova and Nicolas Stier-Moses. A mean-risk model for the traffic assignment problem with stochastic travel times. *Operations Research*, 62, 04 2014. doi:10.1287/opre.2013.1246.

Evdokia Nikolova and Nicolas E. Stier-Moses. The burden of risk aversion in mean-risk selfish routing. In *Proceedings of the Sixteenth ACM Conference on Economics and Computation*, EC '15, page 489–506. ACM, June 2015. doi:10.1145/2764468.2764485. URL http://dx.doi.org/10.1145/2764468.2764485.

Fernando Ordonez and Nicolas Stier-Moses. Wardrop equilibria with risk-averse users. *Transportation Science*, 44:63–86, 02 2010a. doi:10.1287/trsc.1090.0292.

Fernando Ordonez and Nicolas Stier-Moses. Wardrop equilibria with risk-averse users. *Transportation Science*, 44:63–86, 02 2010b. doi:10.1287/trsc.1090.0292.

Adam J. Pel and Alan J. Nicholson. Network effects of percentile-based route choice behavior for stochastic travel times under exogenous capacity variations. In *16th International IEEE Conference on Intelligent Transportation Systems (ITSC 2013)*, pages 1864–1869, 2013. doi:10.1109/ITSC.2013.6728500.

Will Recker, Younshik Chung, JiYoung Park, Lesley Wang, Anthony Chen, Zhaowang Ji, Henry X. Liu, Matthew Rodney Horrocks, and Jun-Seok Oh. Considering risk-taking behavior in travel time reliability. *PATH research report*, 2005. URL `https://api.semanticscholar.org/CorpusID:168067136`.

R. Tyrrell Rockafellar and Stanislav Uryasev. Optimization of conditional value-at risk. *Journal of Risk*, 3:21–41, 2000. URL `https://api.semanticscholar.org/CorpusID:854622`.

Yusuf Saltan, Jyun-Jhe Wang, Arda Kosay, Chung-Wei Lin, and Muhammed Sayin. Designing non-monetary intersection control mechanisms for efficient selfish routing, 11 2025.

Ravi Seshadri and Karthik K. Srinivasan. Robust traffic assignment model: Formulation, solution algorithms and empirical application. *Journal of Intelligent Transportation Systems*, 21(6):507–524, 2017. doi:10.1080/15472450.2017.1358624. URL `https://doi.org/10.1080/15472450.2017.1358624`.

Hu Shao, William Lam, and Mei Tam. A reliability-based stochastic traffic assignment model for network with multiple user classes under uncertainty in demand. *Networks and Spatial Economics*, 6:173–204, 09 2006. doi:10.1007/s11067-006-9279-6.

Yossi Sheffi. *Urban Transportation Networks: Equilibrium Analysis With Mathematical Programming Methods*. 01 1984. ISBN 0139397299.

Barbara W. Y. Siu and Hong K. Lo. Doubly uncertain transport network: Degradable link capacity and perception variations in traffic conditions. *Transportation Research Record*, 1964(1):59–69, 2006. doi:10.1177/0361198106196400108. URL `https://doi.org/10.1177/0361198106196400108`.

Transportation Networks for Research Core Team. Transportation networks for research. `https://github.com/bstabler/TransportationNetworks`, 2024. Accessed January 15, 2026.

A.H. van der Weijde and V.A.C. van den Berg. Stochastic user equilibrium traffic assignment with price-sensitive demand: Do methods matter (much)? WorkingPaper 13-209/VIII, Tinbergen Institute, 2013.

Jasper Verbree and Ashish Cherukuri. Wardrop equilibrium and braess's paradox for varying demand, 2023. URL `https://arxiv.org/abs/2310.04256`.

JG Wardrop. Some theoretical aspects of road traffic research. *Proceedings of the Institute of Civil Engineers*, (Part II):325–378, 1952.

Xing Wu and Yu (Marco) Nie. Modeling heterogeneous risk-taking behavior in route choice: A stochastic dominance approach. *Transportation Research Part A: Policy and Practice*, 45(9):896–915, 2011. ISSN 0965-8564. doi:https://doi.org/10.1016/j.tra.2011.04.009. URL https://www.sciencedirect.com/science/article/pii/S096585641100067X. Select Papers from the 19th International Symposium on Transportation and Traffic Theory (ISTTT).

Yue Xie and Uday V. Shanbhag. On robust solutions to uncertain linear complementarity problems and their variants, 2015. URL https://arxiv.org/abs/1503.03490.

Weiliang Zeng, Tomio Miwa, and Takayuki Morikawa. Exploring traveler's risk-averse preference to travel time reliability from gps-based trip record. 01 2018.

A Appendix

OD pair	Path (node sequence)
OD $(1, 19)$	
(1,19)	$[1, 2, 6, 8, 16, 17, 19]$
(1,19)	$[1, 2, 6, 8, 7, 18, 16, 17, 19]$
(1,19)	$[1, 3, 4, 5, 6, 8, 16, 17, 19]$
(1,19)	$[1, 2, 6, 8, 7, 18, 20, 19]$
(1,19)	$[1, 3, 4, 5, 9, 10, 16, 17, 19]$
(1,19)	$[1, 3, 4, 11, 14, 15, 19]$
(1,19)	$[1, 3, 12, 11, 14, 15, 19]$
(1,19)	$[1, 3, 12, 13, 24, 21, 22, 15, 19]$
(1,19)	$[1, 3, 4, 5, 9, 10, 15, 19]$
(1,19)	$[1, 3, 4, 11, 10, 16, 17, 19]$
OD $(13, 8)$	
(13,8)	$[13, 12, 3, 4, 5, 6, 8]$
(13,8)	$[13, 24, 21, 20, 18, 7, 8]$
(13,8)	$[13, 12, 11, 4, 5, 6, 8]$
(13,8)	$[13, 12, 11, 10, 16, 8]$
(13,8)	$[13, 24, 21, 22, 20, 18, 7, 8]$
(13,8)	$[13, 12, 3, 1, 2, 6, 8]$
(13,8)	$[13, 24, 21, 22, 15, 19, 17, 16, 8]$
(13,8)	$[13, 24, 23, 22, 20, 18, 7, 8]$
(13,8)	$[13, 24, 21, 20, 18, 16, 8]$
(13,8)	$[13, 24, 23, 22, 15, 19, 17, 16, 8]$
OD $(12, 18)$	
(12,18)	$[12, 11, 10, 16, 18]$
(12,18)	$[12, 13, 24, 21, 20, 18]$
(12,18)	$[12, 3, 4, 5, 6, 8, 7, 18]$
(12,18)	$[12, 13, 24, 21, 22, 20, 18]$
(12,18)	$[12, 13, 24, 23, 22, 20, 18]$
(12,18)	$[12, 3, 4, 5, 6, 8, 16, 18]$
(12,18)	$[12, 11, 10, 17, 16, 18]$
(12,18)	$[12, 3, 4, 5, 9, 10, 16, 18]$
(12,18)	$[12, 11, 4, 5, 6, 8, 7, 18]$
(12,18)	$[12, 11, 10, 16, 8, 7, 18]$

Table A.1: Selected path sets for the Sioux Falls network (top-10 free-flow paths per OD pair).

A.1 Results

A.2 One-OD 3-paths network

A.3 $\bar{\alpha} = 0.3$

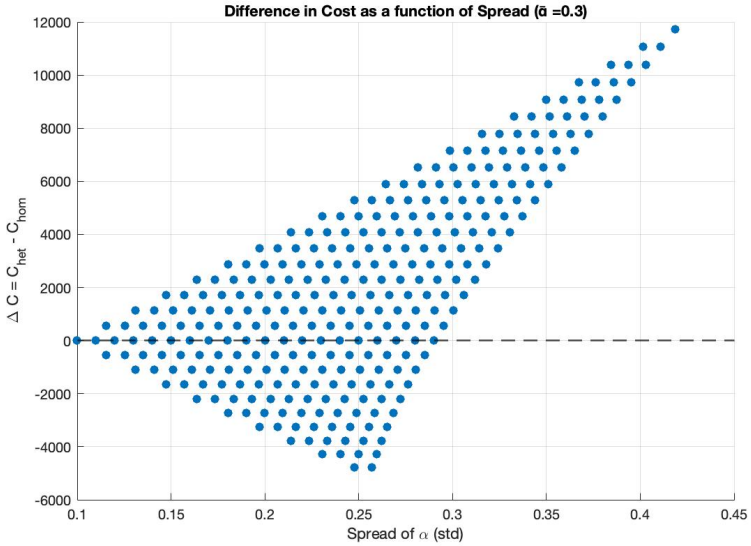

Figure A.1: Difference in total network costs homogeneous and heterogeneous against spread, for $\bar{\alpha} = 0.3$

Table A.2: Top 20 best heterogeneous configurations for the one-OD three-path network for $\bar{\alpha} = 0.3$

Alpha1	Alpha2	Alpha3	Spread	CostHet	ΔC	Improvement
0.01	0.39	0.50	0.257	1823541	-4791.202	4791.202
0.02	0.39	0.49	0.248	1823541	-4791.202	4791.202
0.01	0.38	0.51	0.259	1824049	-4283.077	4283.077
0.02	0.38	0.50	0.250	1824049	-4283.077	4283.077
0.03	0.38	0.49	0.240	1824049	-4283.077	4283.077
0.04	0.38	0.48	0.231	1824049	-4283.077	4283.077
0.01	0.37	0.52	0.262	1824563	-3768.894	3768.894
0.02	0.37	0.51	0.252	1824563	-3768.894	3768.894
0.03	0.37	0.50	0.243	1824563	-3768.894	3768.894
0.04	0.37	0.49	0.233	1824563	-3768.894	3768.894
0.05	0.37	0.48	0.223	1824563	-3768.894	3768.894
0.06	0.37	0.47	0.214	1824563	-3768.894	3768.894
0.01	0.36	0.53	0.265	1825083	-3248.654	3248.654
0.02	0.36	0.52	0.255	1825083	-3248.654	3248.654
0.03	0.36	0.51	0.246	1825083	-3248.654	3248.654
0.04	0.36	0.50	0.236	1825083	-3248.654	3248.654
0.05	0.36	0.49	0.226	1825083	-3248.654	3248.654
0.06	0.36	0.48	0.216	1825083	-3248.654	3248.654
0.07	0.36	0.47	0.207	1825083	-3248.654	3248.654
0.08	0.36	0.46	0.197	1825083	-3248.654	3248.654

Table A.3: Top 20 worst heterogeneous configurations for the one-OD three-path network for $\bar{\alpha} = 0.3$

Alpha1	Alpha2	Alpha3	Spread	CostHet	DeltaC	Improvement
0.01	0.11	0.78	0.419	1840058	11726.106	-11726.106
0.01	0.12	0.77	0.411	1839386	11054.423	-11054.423
0.02	0.12	0.76	0.401	1839386	11054.423	-11054.423
0.01	0.13	0.76	0.403	1838721	10388.798	-10388.798
0.02	0.13	0.75	0.394	1838721	10388.798	-10388.798
0.03	0.13	0.74	0.384	1838721	10388.798	-10388.798
0.01	0.14	0.75	0.395	1838061	9729.231	-9729.231
0.02	0.14	0.74	0.386	1838061	9729.231	-9729.231
0.03	0.14	0.73	0.376	1838061	9729.231	-9729.231
0.04	0.14	0.72	0.367	1838061	9729.231	-9729.231
0.01	0.15	0.74	0.387	1837407	9075.721	-9075.721
0.02	0.15	0.73	0.378	1837407	9075.721	-9075.721
0.03	0.15	0.72	0.369	1837407	9075.721	-9075.721
0.04	0.15	0.71	0.359	1837407	9075.721	-9075.721
0.05	0.15	0.7	0.35	1837407	9075.721	-9075.721
0.01	0.16	0.73	0.38	1836760	8428.269	-8428.269
0.02	0.16	0.72	0.37	1836760	8428.269	-8428.269
0.03	0.16	0.71	0.361	1836760	8428.269	-8428.269
0.04	0.16	0.7	0.352	1836760	8428.269	-8428.269
0.05	0.16	0.69	0.342	1836760	8428.269	-8428.269

A.4 $\bar{\alpha} = 0.5$

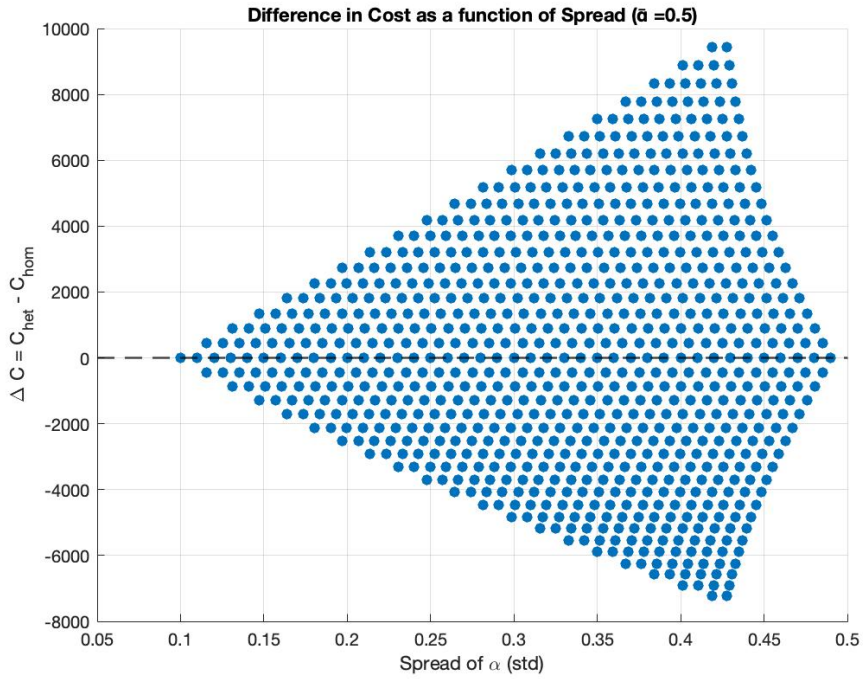

Figure A.2: Difference in total network costs between heterogeneous and homogeneous equilibria as a function of the spread of α for $\bar{\alpha} = 0.5$.

Table A.4: Top 20 best heterogeneous configurations for the one-OD three-path network for $\bar{\alpha} = 0.5$

Alpha1	Alpha2	Alpha3	Spread	CostHet	DeltaC	Improvement
0.01	0.69	0.8	0.428	1811114	-7237.356	7237.356
0.02	0.69	0.79	0.419	1811114	-7237.356	7237.356
0.01	0.68	0.81	0.429	1811440	-6910.962	6910.962
0.02	0.68	0.8	0.42	1811440	-6910.962	6910.962
0.03	0.68	0.79	0.411	1811440	-6910.962	6910.962
0.04	0.68	0.78	0.401	1811440	-6910.962	6910.962
0.01	0.67	0.82	0.431	1811772	-6578.51	6578.51
0.02	0.67	0.81	0.422	1811772	-6578.51	6578.51
0.03	0.67	0.8	0.412	1811772	-6578.51	6578.51
0.04	0.67	0.79	0.403	1811772	-6578.51	6578.51
0.05	0.67	0.78	0.394	1811772	-6578.51	6578.51
0.06	0.67	0.77	0.384	1811772	-6578.51	6578.51
0.01	0.66	0.83	0.433	1812111	-6240	6240
0.02	0.66	0.82	0.423	1812111	-6240	6240
0.03	0.66	0.81	0.414	1812111	-6240	6240
0.04	0.66	0.8	0.404	1812111	-6240	6240
0.05	0.66	0.79	0.395	1812111	-6240	6240
0.06	0.66	0.78	0.386	1812111	-6240	6240
0.07	0.66	0.77	0.376	1812111	-6240	6240
0.08	0.66	0.76	0.367	1812111	-6240	6240

Table A.5: Top 20 worst heterogeneous configurations for the one-OD three-path network for $\bar{\alpha} = 0.5$

Alpha1	Alpha2	Alpha3	Spread	CostHet	DeltaC	Improvement
0.2	0.31	0.99	0.428	1827775	9424.183	-9424.183
0.21	0.31	0.98	0.419	1827775	9424.183	-9424.183
0.19	0.32	0.99	0.429	1827225	8873.654	-8873.654
0.2	0.32	0.98	0.42	1827225	8873.654	-8873.654
0.21	0.32	0.97	0.411	1827225	8873.654	-8873.654
0.22	0.32	0.96	0.401	1827225	8873.654	-8873.654
0.18	0.33	0.99	0.431	1826680	8329.183	-8329.183
0.19	0.33	0.98	0.422	1826680	8329.183	-8329.183
0.2	0.33	0.97	0.412	1826680	8329.183	-8329.183
0.21	0.33	0.96	0.403	1826680	8329.183	-8329.183
0.22	0.33	0.95	0.394	1826680	8329.183	-8329.183
0.23	0.33	0.94	0.384	1826680	8329.183	-8329.183
0.17	0.34	0.99	0.433	1826142	7790.769	-7790.769
0.18	0.34	0.98	0.423	1826142	7790.769	-7790.769
0.19	0.34	0.97	0.414	1826142	7790.769	-7790.769
0.2	0.34	0.96	0.404	1826142	7790.769	-7790.769
0.21	0.34	0.95	0.395	1826142	7790.769	-7790.769
0.22	0.34	0.94	0.386	1826142	7790.769	-7790.769
0.23	0.34	0.93	0.376	1826142	7790.769	-7790.769
0.24	0.34	0.92	0.367	1826142	7790.769	-7790.769

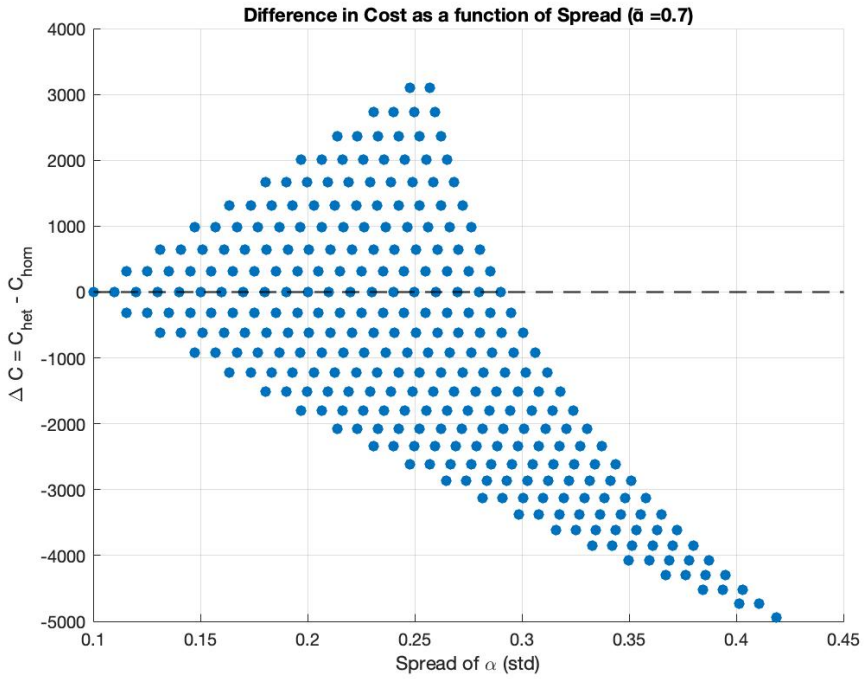

Figure A.3: Difference in total network costs between heterogeneous and homogeneous equilibria as a function of the spread of α for $\bar{\alpha} = 0.7$.

A.5 $\bar{\alpha} = 0.7$

Table A.6: Top 20 best heterogeneous configurations for the one-OD three-path network for $\bar{\alpha} = 0.7$

Alpha1	Alpha2	Alpha3	Spread	CostHet	DeltaC	Improvement
0.22	0.89	0.99	0.419	1805858	-4935.433	4935.433
0.23	0.88	0.99	0.411	1806063	-4730.192	4730.192
0.24	0.88	0.98	0.401	1806063	-4730.192	4730.192
0.24	0.87	0.99	0.403	1806274	-4518.894	4518.894
0.25	0.87	0.98	0.394	1806274	-4518.894	4518.894
0.26	0.87	0.97	0.384	1806274	-4518.894	4518.894
0.25	0.86	0.99	0.395	1806492	-4301.538	4301.538
0.26	0.86	0.98	0.386	1806492	-4301.538	4301.538
0.27	0.86	0.97	0.376	1806492	-4301.538	4301.538
0.28	0.86	0.96	0.367	1806492	-4301.538	4301.538
0.26	0.85	0.99	0.387	1806715	-4078.125	4078.125
0.27	0.85	0.98	0.378	1806715	-4078.125	4078.125
0.28	0.85	0.97	0.369	1806715	-4078.125	4078.125
0.29	0.85	0.96	0.359	1806715	-4078.125	4078.125
0.3	0.85	0.95	0.35	1806715	-4078.125	4078.125
0.27	0.84	0.99	0.38	1806945	-3848.654	3848.654
0.28	0.84	0.98	0.37	1806945	-3848.654	3848.654
0.29	0.84	0.97	0.361	1806945	-3848.654	3848.654
0.3	0.84	0.96	0.352	1806945	-3848.654	3848.654
0.31	0.84	0.95	0.342	1806945	-3848.654	3848.654

Table A.7: Top 20 worst heterogeneous configurations for the one-OD three-path network for $\bar{\alpha} = 0.7$

Alpha1	Alpha2	Alpha3	Spread	CostHet	DeltaC	Improvement
0.5	0.61	0.99	0.257	1813894	3101.106	-3101.106
0.51	0.61	0.98	0.248	1813894	3101.106	-3101.106
0.49	0.62	0.99	0.259	1813526	2732.308	-2732.308
0.5	0.62	0.98	0.25	1813526	2732.308	-2732.308
0.51	0.62	0.97	0.24	1813526	2732.308	-2732.308
0.52	0.62	0.96	0.231	1813526	2732.308	-2732.308
0.48	0.63	0.99	0.262	1813163	2369.567	-2369.567
0.49	0.63	0.98	0.252	1813163	2369.567	-2369.567
0.5	0.63	0.97	0.243	1813163	2369.567	-2369.567
0.51	0.63	0.96	0.233	1813163	2369.567	-2369.567
0.52	0.63	0.95	0.223	1813163	2369.567	-2369.567
0.53	0.63	0.94	0.214	1813163	2369.567	-2369.567
0.47	0.64	0.99	0.265	1812806	2012.885	-2012.885
0.48	0.64	0.98	0.255	1812806	2012.885	-2012.885
0.49	0.64	0.97	0.246	1812806	2012.885	-2012.885
0.5	0.64	0.96	0.236	1812806	2012.885	-2012.885
0.51	0.64	0.95	0.226	1812806	2012.885	-2012.885
0.52	0.64	0.94	0.216	1812806	2012.885	-2012.885
0.53	0.64	0.93	0.207	1812806	2012.885	-2012.885
0.54	0.64	0.92	0.197	1812806	2012.885	-2012.885

A.6 Two-OD 5-paths network

A.7 $\bar{\alpha} = 0.3$

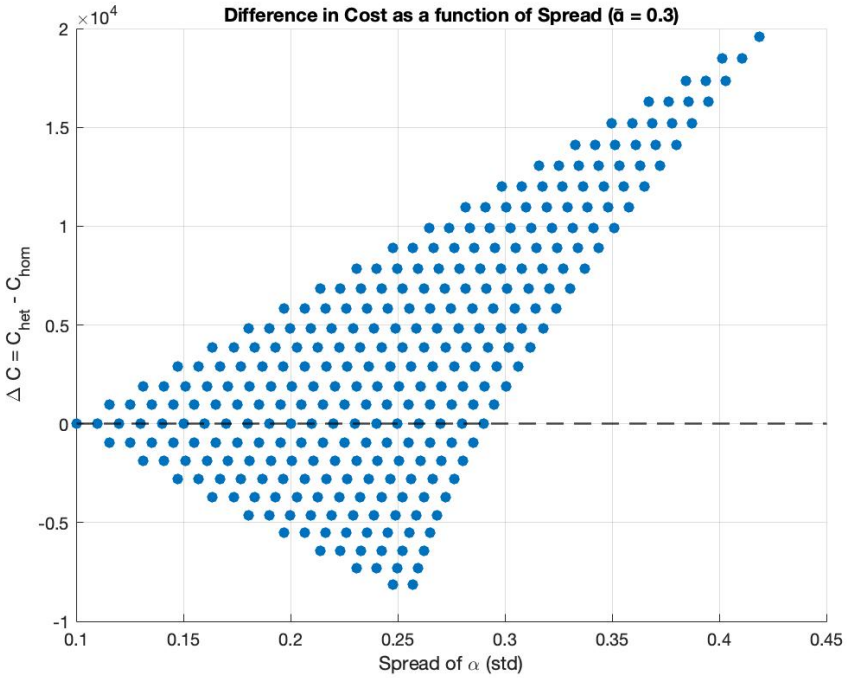

Figure A.4: Difference in total network costs between heterogeneous and homogeneous equilibria as a function of the spread of α for $\bar{\alpha} = 0.3$.

Table A.8: Top 20 best heterogeneous configurations for the two-OD five-path network for $\bar{\alpha} = 0.3$

Alpha1	Alpha2	Alpha3	Spread	CostHet	DeltaC	Improvement
0.01	0.39	0.5	0.257	3949537	-8160	8160
0.02	0.39	0.49	0.248	3949537	-8160	8160
0.01	0.38	0.51	0.259	3950409	-7289	7289
0.02	0.38	0.5	0.25	3950409	-7289	7289
0.03	0.38	0.49	0.24	3950409	-7289	7289
0.04	0.38	0.48	0.231	3950409	-7289	7289
0.01	0.37	0.52	0.262	3951289	-6409	6409
0.02	0.37	0.51	0.252	3951289	-6409	6409
0.03	0.37	0.5	0.243	3951289	-6409	6409
0.04	0.37	0.49	0.233	3951289	-6409	6409
0.05	0.37	0.48	0.223	3951289	-6409	6409
0.06	0.37	0.47	0.214	3951289	-6409	6409
0.01	0.36	0.53	0.265	3952178	-5520	5520
0.02	0.36	0.52	0.255	3952178	-5520	5520
0.03	0.36	0.51	0.246	3952178	-5520	5520
0.04	0.36	0.5	0.236	3952178	-5520	5520
0.05	0.36	0.49	0.226	3952178	-5520	5520
0.06	0.36	0.48	0.216	3952178	-5520	5520
0.07	0.36	0.47	0.207	3952178	-5520	5520
0.08	0.36	0.46	0.197	3952178	-5520	5520

Table A.9: Top 20 best heterogeneous configurations for the two-OD five-path network for $\bar{\alpha} = 0.3$

Alpha1	Alpha2	Alpha3	Spread	CostHet	DeltaC	Improvement
0.01	0.11	0.78	0.419	3977280	19583	-19583
0.01	0.12	0.77	0.411	3976170	18472	-18472
0.02	0.12	0.76	0.401	3976170	18472	-18472
0.01	0.13	0.76	0.403	3975069	17371	-17371
0.02	0.13	0.75	0.394	3975069	17371	-17371
0.03	0.13	0.74	0.384	3975069	17371	-17371
0.01	0.14	0.75	0.395	3973976	16278	-16278
0.02	0.14	0.74	0.386	3973976	16278	-16278
0.03	0.14	0.73	0.376	3973976	16278	-16278
0.04	0.14	0.72	0.367	3973976	16278	-16278
0.01	0.15	0.74	0.387	3972892	15194	-15194
0.02	0.15	0.73	0.378	3972892	15194	-15194
0.03	0.15	0.72	0.369	3972892	15194	-15194
0.04	0.15	0.71	0.359	3972892	15194	-15194
0.05	0.15	0.7	0.35	3972892	15194	-15194
0.01	0.16	0.73	0.38	3971817	14119	-14119
0.02	0.16	0.72	0.37	3971817	14119	-14119
0.03	0.16	0.71	0.361	3971817	14119	-14119
0.04	0.16	0.7	0.352	3971817	14119	-14119
0.05	0.16	0.69	0.342	3971817	14119	-14119

A.8 $\bar{\alpha} = 0.5$

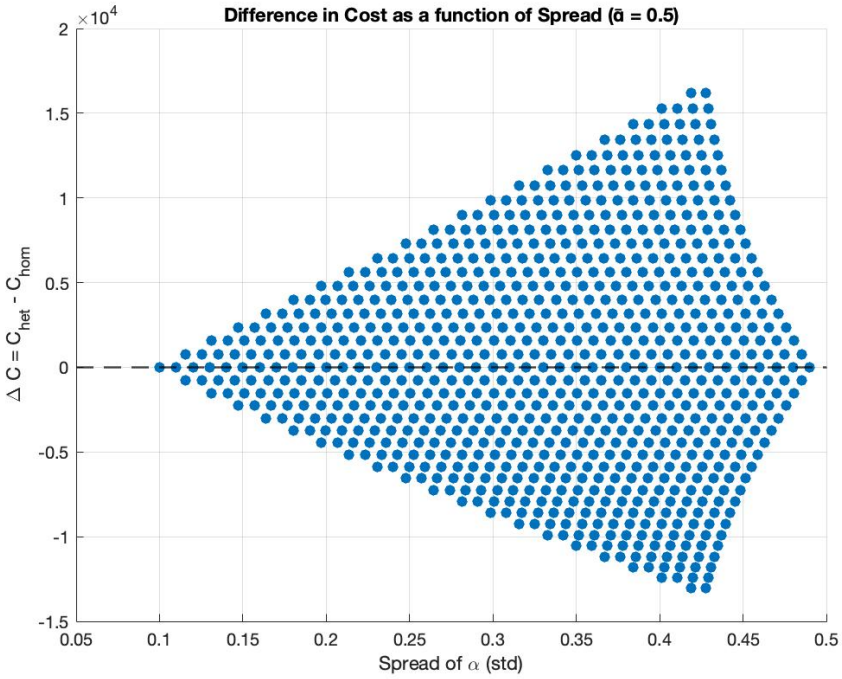

Figure A.5: Difference in total network costs between heterogeneous and homogeneous equilibria as a function of the spread of α for $\bar{\alpha} = 0.5$.

Table A.10: Top 20 best heterogeneous configurations for the twoo-OD five-path network for $\bar{\alpha} = 0.5$

Alpha1	Alpha2	Alpha3	Spread	CostHet	DeltaC	Improvement
0.01	0.69	0.8	0.428	3927515	-13022	13022
0.02	0.69	0.79	0.419	3927515	-13022	13022
0.01	0.68	0.81	0.429	3928121	-12417	12417
0.02	0.68	0.8	0.42	3928121	-12417	12417
0.03	0.68	0.79	0.411	3928121	-12417	12417
0.04	0.68	0.78	0.401	3928121	-12417	12417
0.01	0.67	0.82	0.431	3928735	-11802	11802
0.02	0.67	0.81	0.422	3928735	-11802	11802
0.03	0.67	0.8	0.412	3928735	-11802	11802
0.04	0.67	0.79	0.403	3928735	-11802	11802
0.05	0.67	0.78	0.394	3928735	-11802	11802
0.06	0.67	0.77	0.384	3928735	-11802	11802
0.01	0.66	0.83	0.433	3929359	-11179	11179
0.02	0.66	0.82	0.423	3929359	-11179	11179
0.03	0.66	0.81	0.414	3929359	-11179	11179
0.04	0.66	0.8	0.404	3929359	-11179	11179
0.05	0.66	0.79	0.395	3929359	-11179	11179
0.06	0.66	0.78	0.386	3929359	-11179	11179
0.07	0.66	0.77	0.376	3929359	-11179	11179
0.08	0.66	0.76	0.367	3929359	-11179	11179

Table A.11: Top 20 worst heterogeneous configurations for the two-OD five-path network for $\bar{\alpha} = 0.5$

Alpha1	Alpha2	Alpha3	Spread	CostHet	DeltaC	Improvement
0.2	0.31	0.99	0.428	3956756	16218	-16218
0.21	0.31	0.98	0.419	3956756	16218	-16218
0.19	0.32	0.99	0.429	3955822	15285	-15285
0.2	0.32	0.98	0.42	3955822	15285	-15285
0.21	0.32	0.97	0.411	3955822	15285	-15285
0.22	0.32	0.96	0.401	3955822	15285	-15285
0.18	0.33	0.99	0.431	3954898	14361	-14361
0.19	0.33	0.98	0.422	3954898	14361	-14361
0.2	0.33	0.97	0.412	3954898	14361	-14361
0.21	0.33	0.96	0.403	3954898	14361	-14361
0.22	0.33	0.95	0.394	3954898	14361	-14361
0.23	0.33	0.94	0.384	3954898	14361	-14361
0.17	0.34	0.99	0.433	3953982	13445	-13445
0.18	0.34	0.98	0.423	3953982	13445	-13445
0.19	0.34	0.97	0.414	3953982	13445	-13445
0.2	0.34	0.96	0.404	3953982	13445	-13445
0.21	0.34	0.95	0.395	3953982	13445	-13445
0.22	0.34	0.94	0.386	3953982	13445	-13445
0.23	0.34	0.93	0.376	3953982	13445	-13445
0.24	0.34	0.92	0.367	3953982	13445	-13445

A.9 $\bar{\alpha} = 0.7$

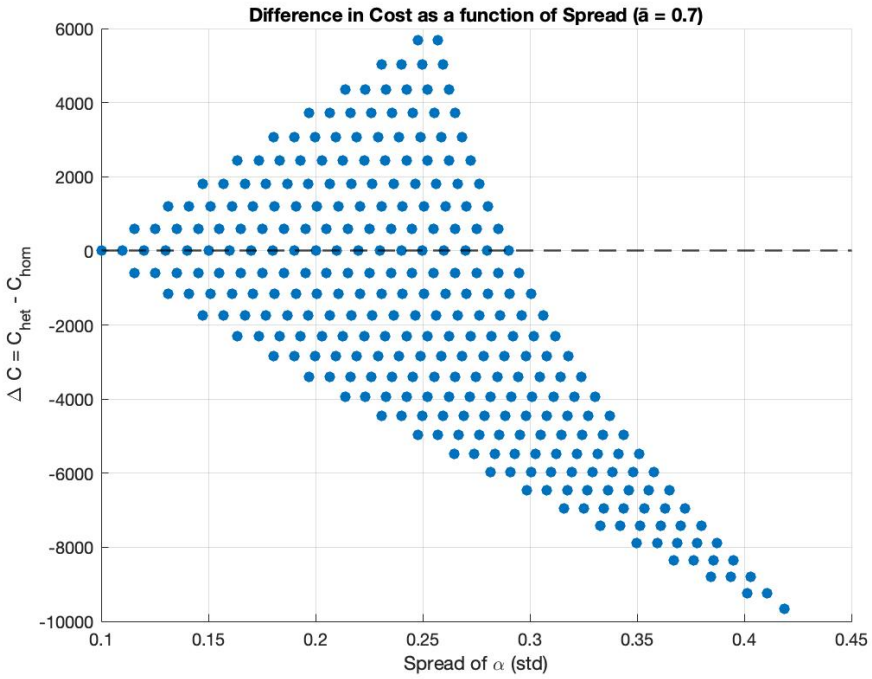

Figure A.6: Difference in total network costs between heterogeneous and homogeneous equilibria as a function of the spread of α for $\bar{\alpha} = 0.7$.

Table A.12: Top 20 best heterogeneous configurations for the two-OD five-path network for $\bar{\alpha} = 0.7$

Alpha1	Alpha2	Alpha3	Spread	CostHet	DeltaC	Improvement
0.22	0.89	0.99	0.419	3917260	-9658	9658
0.23	0.88	0.99	0.411	3917689	-9229	9229
0.24	0.88	0.98	0.401	3917689	-9229	9229
0.24	0.87	0.99	0.403	3918126	-8792	8792
0.25	0.87	0.98	0.394	3918126	-8792	8792
0.26	0.87	0.97	0.384	3918126	-8792	8792
0.25	0.86	0.99	0.395	3918572	-8346	8346
0.26	0.86	0.98	0.386	3918572	-8346	8346
0.27	0.86	0.97	0.376	3918572	-8346	8346
0.28	0.86	0.96	0.367	3918572	-8346	8346
0.26	0.85	0.99	0.387	3919028	-7890	7890
0.27	0.85	0.98	0.378	3919028	-7890	7890
0.28	0.85	0.97	0.369	3919028	-7890	7890
0.29	0.85	0.96	0.359	3919028	-7890	7890
0.3	0.85	0.95	0.35	3919028	-7890	7890
0.27	0.84	0.99	0.38	3919492	-7426	7426
0.28	0.84	0.98	0.37	3919492	-7426	7426
0.29	0.84	0.97	0.361	3919492	-7426	7426
0.3	0.84	0.96	0.352	3919492	-7426	7426
0.31	0.84	0.95	0.342	3919492	-7426	7426

Table A.13: Top 20 worst heterogeneous configurations for the two-OD five-path network for $\bar{\alpha} = 0.7$

Alpha1	Alpha2	Alpha3	Spread	CostHet	DeltaC	Improvement
0.5	0.61	0.99	0.257	3932608	5690	-5690
0.51	0.61	0.98	0.248	3932608	5690	-5690
0.49	0.62	0.99	0.259	3931941	5023	-5023
0.5	0.62	0.98	0.25	3931941	5023	-5023
0.51	0.62	0.97	0.24	3931941	5023	-5023
0.52	0.62	0.96	0.231	3931941	5023	-5023
0.48	0.63	0.99	0.262	3931282	4364	-4364
0.49	0.63	0.98	0.252	3931282	4364	-4364
0.5	0.63	0.97	0.243	3931282	4364	-4364
0.51	0.63	0.96	0.233	3931282	4364	-4364
0.52	0.63	0.95	0.223	3931282	4364	-4364
0.53	0.63	0.94	0.214	3931282	4364	-4364
0.47	0.64	0.99	0.265	3930632	3714	-3714
0.48	0.64	0.98	0.255	3930632	3714	-3714
0.49	0.64	0.97	0.246	3930632	3714	-3714
0.5	0.64	0.96	0.236	3930632	3714	-3714
0.51	0.64	0.95	0.226	3930632	3714	-3714
0.52	0.64	0.94	0.216	3930632	3714	-3714
0.53	0.64	0.93	0.207	3930632	3714	-3714
0.54	0.64	0.92	0.197	3930632	3714	-3714

A.10 Wheatstone Network

A.11 $\bar{\alpha} = 0.3$

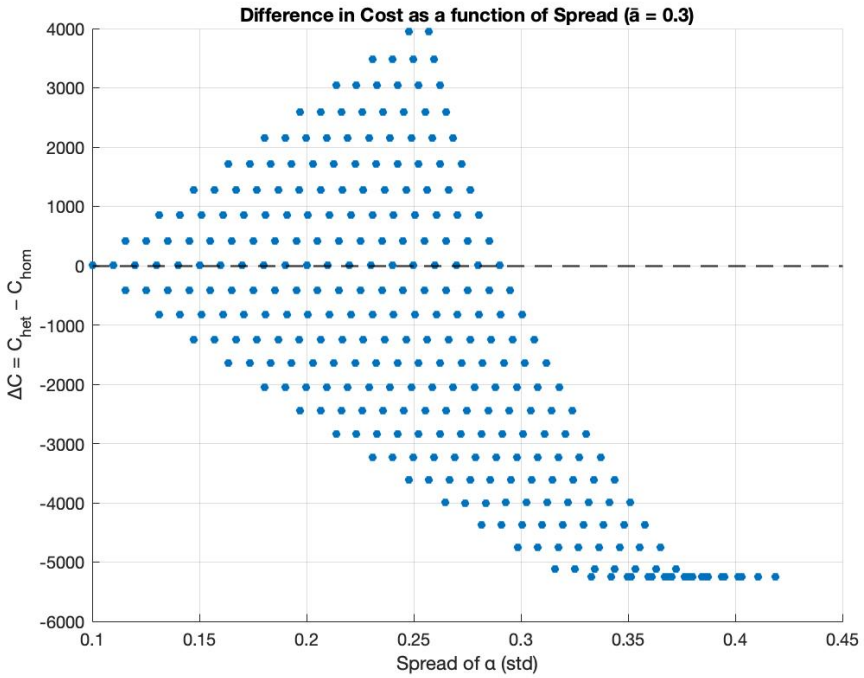

Figure A.7: Difference in total network costs between heterogeneous and homogeneous equilibria as a function of the spread of α for $\bar{\alpha} = 0.3$.

Table A.14: Top 20 best heterogeneous configurations for the Wheatstone network for $\bar{\alpha} = 0.3$

Alpha1	Alpha2	Alpha3	Spread	Extremeness	ShortcutShare	CostHet	DeltaC	Improvement
0.01	0.12	0.77	0.411	0.47	0.333	275555.556	-5244.444	5244.444
0.01	0.13	0.76	0.403	0.46	0.333	275555.556	-5244.444	5244.444
0.01	0.14	0.75	0.395	0.45	0.333	275555.556	-5244.444	5244.444
0.02	0.12	0.76	0.401	0.46	0.333	275555.556	-5244.444	5244.444
0.02	0.13	0.75	0.394	0.45	0.333	275555.556	-5244.444	5244.444
0.02	0.15	0.73	0.378	0.43	0.333	275555.556	-5244.444	5244.444
0.03	0.13	0.74	0.384	0.44	0.333	275555.556	-5244.444	5244.444
0.03	0.15	0.72	0.369	0.42	0.333	275555.556	-5244.444	5244.444
0.04	0.14	0.72	0.367	0.42	0.333	275555.556	-5244.444	5244.444
0.04	0.15	0.71	0.359	0.41	0.333	275555.556	-5244.444	5244.444
0.05	0.15	0.7	0.35	0.4	0.333	275555.556	-5244.444	5244.444
0.05	0.16	0.69	0.342	0.39	0.333	275555.556	-5244.444	5244.444
0.06	0.16	0.68	0.333	0.38	0.333	275555.556	-5244.444	5244.444
0.01	0.11	0.78	0.419	0.48	0.333	275555.557	-5244.443	5244.443
0.01	0.15	0.74	0.387	0.44	0.333	275555.557	-5244.443	5244.443
0.02	0.14	0.74	0.386	0.44	0.333	275555.557	-5244.443	5244.443
0.02	0.16	0.72	0.37	0.42	0.333	275555.557	-5244.443	5244.443
0.03	0.14	0.73	0.376	0.43	0.333	275555.557	-5244.443	5244.443
0.03	0.16	0.71	0.361	0.41	0.333	275555.557	-5244.443	5244.443
0.01	0.16	0.73	0.38	0.43	0.333	275555.558	-5244.442	5244.442

Table A.15: Top 20 worst heterogeneous configurations for the Wheatstone network for $\bar{\alpha} = 0.3$

Alpha1	Alpha2	Alpha3	Spread	Extremeness	ShortcutShare	CostHet	DeltaC	Improvement
0.01	0.39	0.5	0.257	0.29	0.445	284742	3942	-3942
0.02	0.39	0.49	0.248	0.28	0.445	284742	3942	-3942
0.01	0.38	0.51	0.259	0.29	0.44	284288	3488	-3488
0.02	0.38	0.5	0.25	0.28	0.44	284288	3488	-3488
0.03	0.38	0.49	0.24	0.27	0.44	284288	3488	-3488
0.04	0.38	0.48	0.231	0.26	0.44	284288	3488	-3488
0.01	0.37	0.52	0.262	0.29	0.435	283838	3038	-3038
0.02	0.37	0.51	0.252	0.28	0.435	283838	3038	-3038
0.03	0.37	0.5	0.243	0.27	0.435	283838	3038	-3038
0.04	0.37	0.49	0.233	0.26	0.435	283838	3038	-3038
0.05	0.37	0.48	0.223	0.25	0.435	283838	3038	-3038
0.06	0.37	0.47	0.214	0.24	0.435	283838	3038	-3038
0.01	0.36	0.53	0.265	0.29	0.43	283392	2592	-2592
0.02	0.36	0.52	0.255	0.28	0.43	283392	2592	-2592
0.03	0.36	0.51	0.246	0.27	0.43	283392	2592	-2592
0.04	0.36	0.5	0.236	0.26	0.43	283392	2592	-2592
0.05	0.36	0.49	0.226	0.25	0.43	283392	2592	-2592
0.06	0.36	0.48	0.216	0.24	0.43	283392	2592	-2592
0.07	0.36	0.47	0.207	0.23	0.43	283392	2592	-2592
0.08	0.36	0.46	0.197	0.22	0.43	283392	2592	-2592

A.12 $\bar{\alpha} = 0.5$

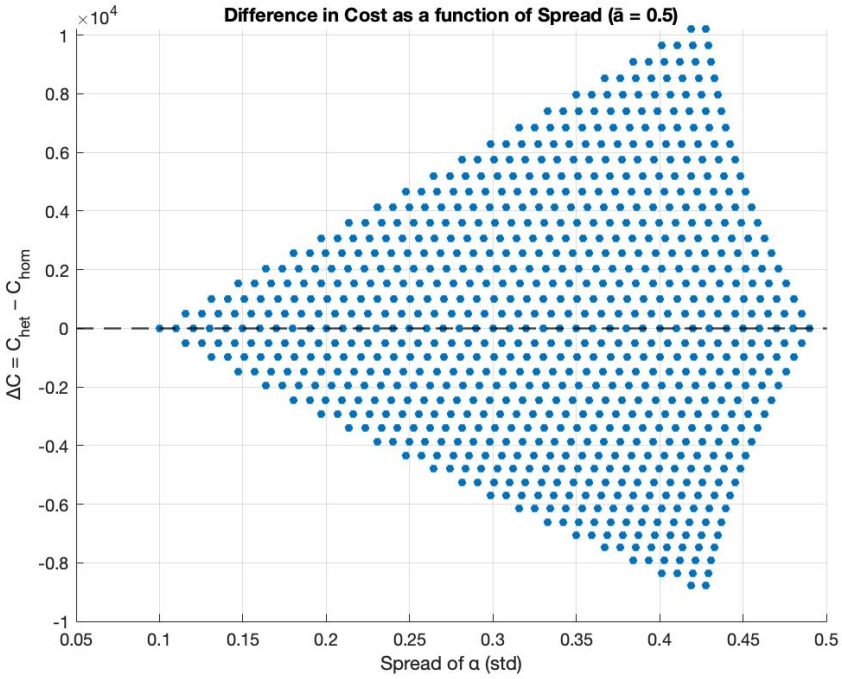

Figure A.8: Difference in total network costs between heterogeneous and homogeneous equilibria as a function of the spread of α for $\bar{\alpha} = 0.5$.

Table A.16: Top 20 best heterogeneous configurations for the Wheatstone network for $\bar{\alpha} = 0.5$

Alpha1	Alpha2	Alpha3	Spread	Extremeness	ShortcutShare	CostHet	DeltaC	Improvement
0.2	0.31	0.99	0.428	0.49	0.405	281222	-8778	8778
0.21	0.31	0.98	0.419	0.48	0.405	281222	-8778	8778
0.19	0.32	0.99	0.429	0.49	0.41	281648	-8352	8352
0.2	0.32	0.98	0.42	0.48	0.41	281648	-8352	8352
0.21	0.32	0.97	0.411	0.47	0.41	281648	-8352	8352
0.22	0.32	0.96	0.401	0.46	0.41	281648	-8352	8352
0.18	0.33	0.99	0.431	0.49	0.415	282078	-7922	7922
0.19	0.33	0.98	0.422	0.48	0.415	282078	-7922	7922
0.2	0.33	0.97	0.412	0.47	0.415	282078	-7922	7922
0.21	0.33	0.96	0.403	0.46	0.415	282078	-7922	7922
0.22	0.33	0.95	0.394	0.45	0.415	282078	-7922	7922
0.23	0.33	0.94	0.384	0.44	0.415	282078	-7922	7922
0.17	0.34	0.99	0.433	0.49	0.42	282512	-7488	7488
0.18	0.34	0.98	0.423	0.48	0.42	282512	-7488	7488
0.19	0.34	0.97	0.414	0.47	0.42	282512	-7488	7488
0.2	0.34	0.96	0.404	0.46	0.42	282512	-7488	7488
0.21	0.34	0.95	0.395	0.45	0.42	282512	-7488	7488
0.22	0.34	0.94	0.386	0.44	0.42	282512	-7488	7488
0.23	0.34	0.93	0.376	0.43	0.42	282512	-7488	7488
0.24	0.34	0.92	0.367	0.42	0.42	282512	-7488	7488

Table A.17: Top 20 worst heterogeneous configurations for the Wheatstone network for $\bar{\alpha} = 0.5$

Alpha1	Alpha2	Alpha3	Spread	Extremeness	ShortcutShare	CostHet	DeltaC	Improvement
0.01	0.69	0.8	0.428	0.49	0.595	300222	10222	-10222
0.02	0.69	0.79	0.419	0.48	0.595	300222	10222	-10222
0.01	0.68	0.81	0.429	0.49	0.59	299648	9648	-9648
0.02	0.68	0.8	0.42	0.48	0.59	299648	9648	-9648
0.03	0.68	0.79	0.411	0.47	0.59	299648	9648	-9648
0.04	0.68	0.78	0.401	0.46	0.59	299648	9648	-9648
0.01	0.67	0.82	0.431	0.49	0.585	299078	9078	-9078
0.02	0.67	0.81	0.422	0.48	0.585	299078	9078	-9078
0.03	0.67	0.8	0.412	0.47	0.585	299078	9078	-9078
0.04	0.67	0.79	0.403	0.46	0.585	299078	9078	-9078
0.05	0.67	0.78	0.394	0.45	0.585	299078	9078	-9078
0.06	0.67	0.77	0.384	0.44	0.585	299078	9078	-9078
0.01	0.66	0.83	0.433	0.49	0.58	298512	8512	-8512
0.02	0.66	0.82	0.423	0.48	0.58	298512	8512	-8512
0.03	0.66	0.81	0.414	0.47	0.58	298512	8512	-8512
0.04	0.66	0.8	0.404	0.46	0.58	298512	8512	-8512
0.05	0.66	0.79	0.395	0.45	0.58	298512	8512	-8512
0.06	0.66	0.78	0.386	0.44	0.58	298512	8512	-8512
0.07	0.66	0.77	0.376	0.43	0.58	298512	8512	-8512
0.08	0.66	0.76	0.367	0.42	0.58	298512	8512	-8512

A.13 $\bar{\alpha} = 0.7$

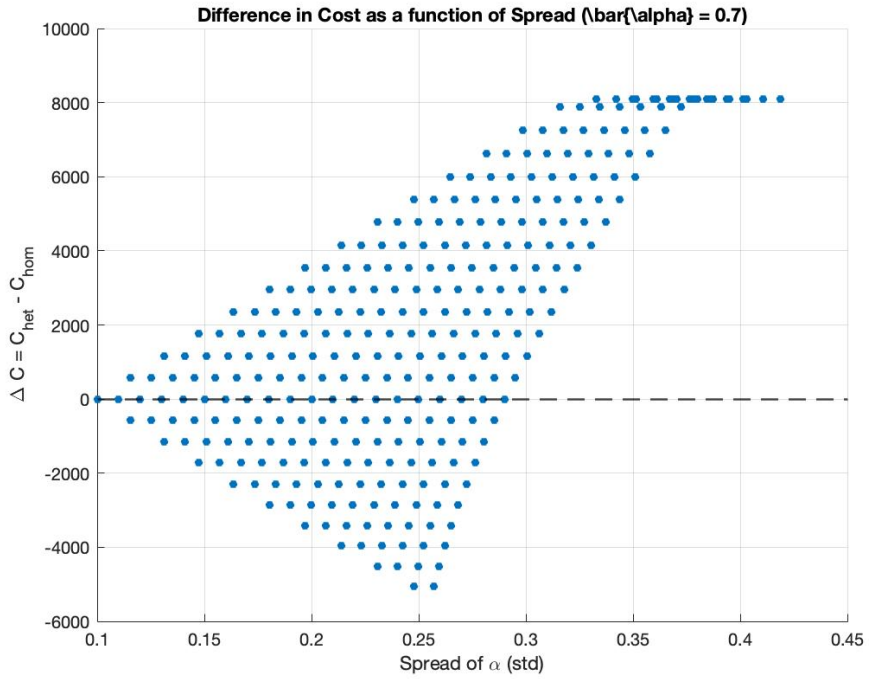

Figure A.9: Difference in total network costs between heterogeneous and homogeneous equilibria as a function of the spread of α for $\bar{\alpha} = 0.7$.

Table A.18: Top 20 best heterogeneous configurations for the Wheatstone network for $\bar{\alpha} = 0.7$

Alpha1	Alpha2	Alpha3	Spread	Extremeness	ShortcutShare	CostHet	DeltaC	Improvement
0.5	0.61	0.99	0.257	0.29	0.555	295742	-5058	5058
0.51	0.61	0.98	0.248	0.28	0.555	295742	-5058	5058
0.49	0.62	0.99	0.259	0.29	0.56	296288	-4512	4512
0.5	0.62	0.98	0.25	0.28	0.56	296288	-4512	4512
0.51	0.62	0.97	0.24	0.27	0.56	296288	-4512	4512
0.52	0.62	0.96	0.231	0.26	0.56	296288	-4512	4512
0.48	0.63	0.99	0.262	0.29	0.565	296838	-3962	3962
0.49	0.63	0.98	0.252	0.28	0.565	296838	-3962	3962
0.5	0.63	0.97	0.243	0.27	0.565	296838	-3962	3962
0.51	0.63	0.96	0.233	0.26	0.565	296838	-3962	3962
0.52	0.63	0.95	0.223	0.25	0.565	296838	-3962	3962
0.53	0.63	0.94	0.214	0.24	0.565	296838	-3962	3962
0.5	0.64	0.96	0.236	0.26	0.57	297391.998	-3408.002	3408.002
0.47	0.64	0.99	0.265	0.29	0.57	297392	-3408	3408
0.48	0.64	0.98	0.255	0.28	0.57	297392	-3408	3408
0.49	0.64	0.97	0.246	0.27	0.57	297392	-3408	3408
0.51	0.64	0.95	0.226	0.25	0.57	297392	-3408	3408
0.52	0.64	0.94	0.216	0.24	0.57	297392	-3408	3408
0.53	0.64	0.93	0.207	0.23	0.57	297392	-3408	3408
0.54	0.64	0.92	0.197	0.22	0.57	297392	-3408	3408

Table A.19: Top 20 worst heterogeneous configurations for the Wheatstone network for $\bar{\alpha} = 0.7$

Alpha1	Alpha2	Alpha3	Spread	Extremeness	ShortcutShare	CostHet	DeltaC	Improvement
0.26	0.87	0.97	0.384	0.44	0.667	308888.889	8088.889	-8088.889
0.28	0.84	0.98	0.37	0.42	0.667	308888.889	8088.889	-8088.889
0.29	0.84	0.97	0.361	0.41	0.667	308888.889	8088.889	-8088.889
0.3	0.84	0.96	0.352	0.4	0.667	308888.889	8088.889	-8088.889
0.31	0.84	0.95	0.342	0.39	0.667	308888.889	8088.889	-8088.889
0.32	0.84	0.94	0.333	0.38	0.667	308888.889	8088.889	-8088.889
0.22	0.89	0.99	0.419	0.48	0.667	308888.888	8088.888	-8088.888
0.24	0.87	0.99	0.403	0.46	0.667	308888.888	8088.888	-8088.888
0.25	0.86	0.99	0.395	0.45	0.667	308888.888	8088.888	-8088.888
0.26	0.86	0.98	0.386	0.44	0.667	308888.888	8088.888	-8088.888
0.27	0.84	0.99	0.38	0.43	0.667	308888.888	8088.888	-8088.888
0.27	0.86	0.97	0.376	0.43	0.667	308888.888	8088.888	-8088.888
0.28	0.86	0.96	0.367	0.42	0.667	308888.888	8088.888	-8088.888
0.23	0.88	0.99	0.411	0.47	0.667	308888.887	8088.887	-8088.887
0.24	0.88	0.98	0.401	0.46	0.667	308888.887	8088.887	-8088.887
0.26	0.85	0.99	0.387	0.44	0.667	308888.887	8088.887	-8088.887
0.27	0.85	0.98	0.378	0.43	0.667	308888.887	8088.887	-8088.887
0.28	0.85	0.97	0.369	0.42	0.667	308888.887	8088.887	-8088.887
0.29	0.85	0.96	0.359	0.41	0.667	308888.887	8088.887	-8088.887
0.3	0.85	0.95	0.35	0.4	0.667	308888.887	8088.887	-8088.887

A.14 Sioux Falls

$\bar{\alpha} = 0.3$

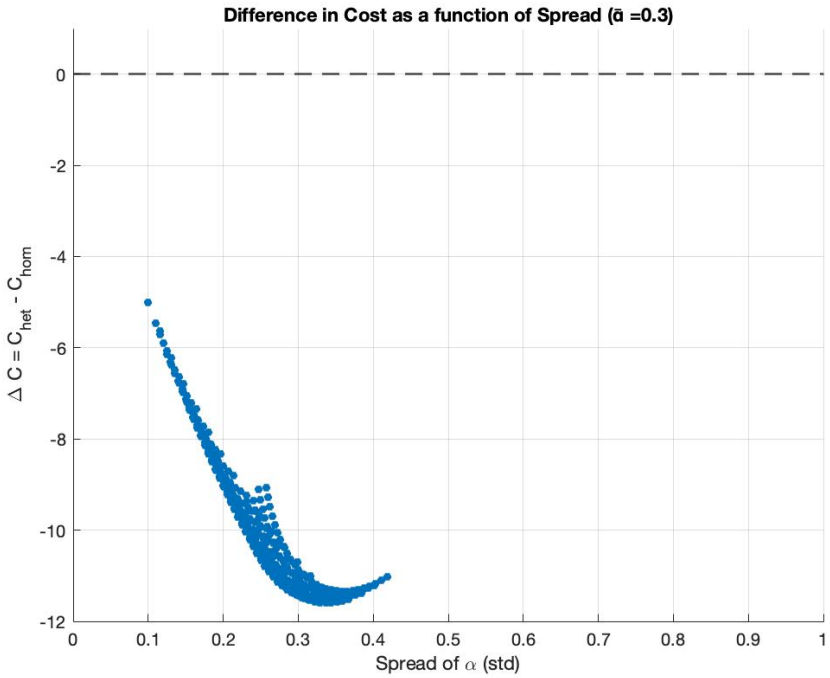

Figure A.10: Difference in total network costs between heterogeneous and homogeneous equilibria as a function of the spread of α for $\bar{\alpha} = 0.3$.

Table A.20: Top 20 best heterogeneous configurations for the Sioux Falls network for $\bar{\alpha} = 0.3$

Alpha1	Alpha2	Alpha3	Spread	Extremeness	Bottleneck	UncFlow	CostHet	DeltaC	Improvement
0.04	0.18	0.68	0.336	0.38	0.086	1059.015	82416.483	-11.594	11.594
0.04	0.17	0.69	0.344	0.39	0.086	1058.903	82416.488	-11.589	11.589
0.04	0.19	0.67	0.329	0.37	0.086	1059.126	82416.49	-11.587	11.587
0.04	0.16	0.7	0.352	0.4	0.086	1058.792	82416.503	-11.574	11.574
0.04	0.2	0.66	0.322	0.36	0.086	1059.237	82416.508	-11.569	11.569
0.04	0.15	0.71	0.359	0.41	0.086	1058.68	82416.529	-11.548	11.548
0.05	0.18	0.67	0.327	0.37	0.086	1058.951	82416.529	-11.547	11.547
0.05	0.17	0.68	0.335	0.38	0.086	1058.839	82416.529	-11.547	11.547
0.04	0.21	0.65	0.315	0.35	0.086	1059.349	82416.537	-11.54	11.54
0.05	0.16	0.69	0.342	0.39	0.086	1058.729	82416.538	-11.539	11.539
0.05	0.19	0.66	0.32	0.36	0.086	1059.06	82416.543	-11.534	11.534
0.03	0.18	0.69	0.346	0.39	0.086	1059.046	82416.554	-11.523	11.523
0.05	0.15	0.7	0.35	0.4	0.086	1058.62	82416.555	-11.522	11.522
0.03	0.19	0.68	0.339	0.38	0.086	1059.158	82416.557	-11.519	11.519
0.03	0.17	0.7	0.353	0.4	0.086	1058.935	82416.561	-11.516	11.516
0.04	0.14	0.72	0.367	0.42	0.086	1058.569	82416.567	-11.51	11.51
0.05	0.2	0.65	0.312	0.35	0.086	1059.17	82416.567	-11.509	11.509
0.03	0.2	0.67	0.332	0.37	0.086	1059.269	82416.572	-11.505	11.505
0.04	0.22	0.64	0.308	0.34	0.086	1059.46	82416.577	-11.5	11.5
0.03	0.16	0.71	0.361	0.41	0.086	1058.823	82416.581	-11.496	11.496

Table A.21: Top 20 worst heterogeneous configurations for the Sioux Falls network for $\bar{\alpha} = 0.3$

Alpha1	Alpha2	Alpha3	Spread	Extremeness	Bottleneck	UncFlow	CostHet	DeltaC	Improvement
0.2	0.3	0.4	0.1	0.1	0.086	1058.28	82423.068	-5.008	5.008
0.19	0.3	0.41	0.11	0.11	0.086	1058.412	82422.623	-5.454	5.454
0.19	0.29	0.42	0.115	0.12	0.086	1058.302	82422.448	-5.629	5.629
0.18	0.31	0.41	0.115	0.12	0.086	1058.655	82422.37	-5.707	5.707
0.18	0.3	0.42	0.12	0.12	0.086	1058.545	82422.187	-5.89	5.89
0.18	0.29	0.43	0.125	0.13	0.086	1058.435	82422.014	-6.062	6.062
0.17	0.31	0.42	0.125	0.13	0.086	1058.788	82421.941	-6.136	6.136
0.18	0.28	0.44	0.131	0.14	0.086	1058.325	82421.853	-6.223	6.223
0.17	0.3	0.43	0.13	0.13	0.086	1058.678	82421.76	-6.317	6.317
0.16	0.32	0.42	0.131	0.14	0.086	1059.031	82421.71	-6.367	6.367
0.17	0.29	0.44	0.135	0.14	0.086	1058.568	82421.59	-6.486	6.486
0.16	0.31	0.43	0.135	0.14	0.086	1058.921	82421.522	-6.555	6.555
0.17	0.28	0.45	0.141	0.15	0.086	1058.458	82421.433	-6.644	6.644
0.16	0.3	0.44	0.14	0.14	0.086	1058.811	82421.344	-6.733	6.733
0.15	0.32	0.43	0.141	0.15	0.086	1059.164	82421.298	-6.779	6.779
0.17	0.27	0.46	0.147	0.16	0.086	1058.348	82421.286	-6.791	6.791
0.16	0.29	0.45	0.145	0.15	0.086	1058.701	82421.177	-6.899	6.899
0.15	0.31	0.44	0.145	0.15	0.086	1059.054	82421.112	-6.965	6.965
0.14	0.33	0.43	0.147	0.16	0.086	1059.407	82421.09	-6.987	6.987
0.16	0.28	0.46	0.151	0.16	0.086	1058.591	82421.022	-7.054	7.054

$\bar{\alpha} = 0.5$

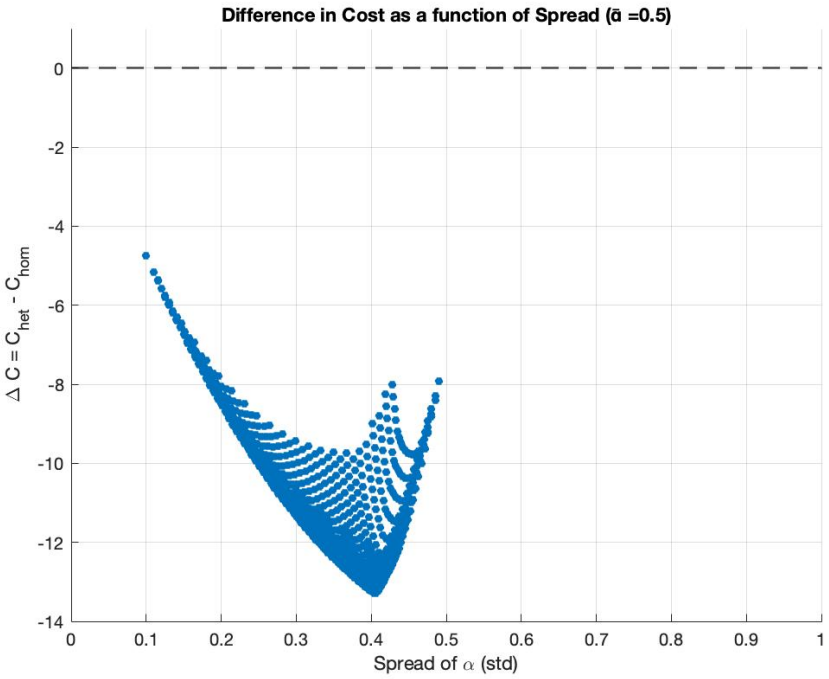

Figure A.11: Difference in total network costs between heterogeneous and homogeneous equilibria as a function of the spread of α for $\bar{\alpha} = 0.5$.

$\bar{\alpha} = 0.7$

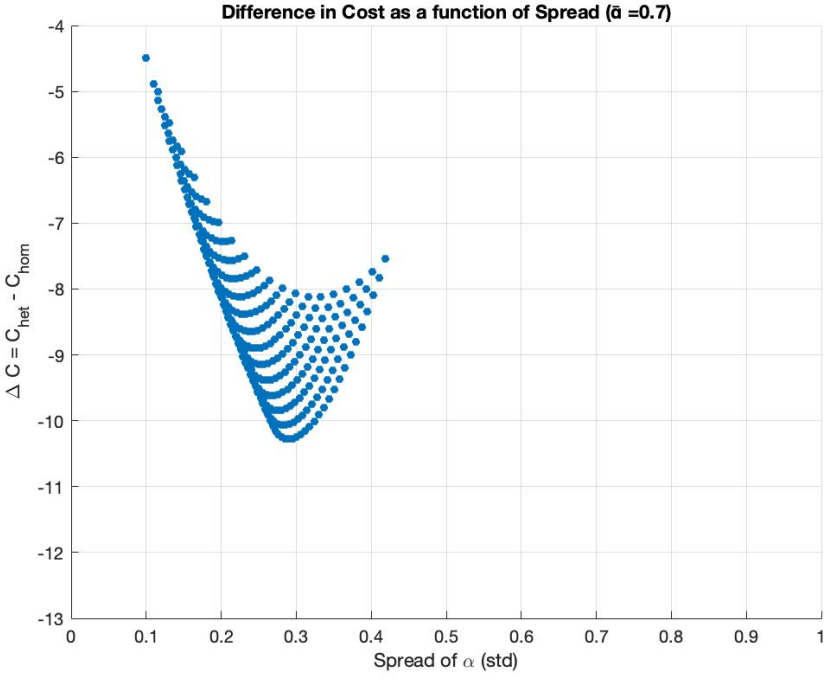

Figure A.12: Difference in total network costs between heterogeneous and homogeneous equilibria as a function of the spread of α for $\bar{\alpha} = 0.7$.

Table A.22: Top 20 best heterogeneous configurations for the Sioux Falls network for $\bar{\alpha} = 0.5$

Alpha1	Alpha2	Alpha3	Spread	Extremeness	Bottleneck	UncFlow	CostHet	DeltaC	Im
0.13	0.44	0.93	0.403	0.43	0.086	1082.117	82370.526	-13.285	13
0.14	0.42	0.94	0.406	0.44	0.086	1081.763	82370.526	-13.284	13
0.12	0.46	0.92	0.401	0.42	0.086	1082.47	82370.568	-13.242	13
0.15	0.4	0.95	0.409	0.45	0.086	1081.405	82370.579	-13.232	13
0.14	0.43	0.93	0.4	0.43	0.086	1081.874	82370.594	-13.217	13
0.12	0.45	0.93	0.407	0.43	0.086	1082.267	82370.607	-13.203	13
0.13	0.45	0.92	0.397	0.42	0.086	1082.227	82370.612	-13.198	13
0.15	0.41	0.94	0.403	0.44	0.086	1081.521	82370.618	-13.192	13
0.11	0.47	0.92	0.406	0.42	0.086	1082.653	82370.626	-13.185	13
0.13	0.43	0.94	0.41	0.44	0.086	1081.882	82370.632	-13.179	13
0.11	0.48	0.91	0.4	0.41	0.086	1082.823	82370.653	-13.158	13
0.14	0.44	0.92	0.393	0.42	0.086	1081.984	82370.669	-13.141	13
0.12	0.47	0.91	0.396	0.41	0.086	1082.58	82370.673	-13.137	13
0.15	0.42	0.93	0.396	0.43	0.086	1081.631	82370.675	-13.136	13
0.16	0.39	0.95	0.406	0.45	0.086	1081.168	82370.685	-13.126	13
0.1	0.49	0.91	0.405	0.41	0.086	1083.038	82370.687	-13.124	13
0.14	0.41	0.95	0.412	0.45	0.086	1081.497	82370.7	-13.111	13
0.16	0.38	0.96	0.413	0.46	0.086	1081.023	82370.707	-13.104	13
0.13	0.46	0.91	0.392	0.41	0.086	1082.337	82370.708	-13.103	13
0.16	0.4	0.94	0.399	0.44	0.086	1081.278	82370.723	-13.088	13

Table A.23: Top 20 worst heterogeneous configurations for the Sioux Falls network for $\bar{\alpha} = 0.5$

Alpha1	Alpha2	Alpha3	Spread	Extremeness	Bottleneck	UncFlow	CostHet	DeltaC	Im
0.4	0.5	0.6	0.1	0.1	0.086	1079.191	82379.063	-4.748	4.7
0.39	0.5	0.61	0.11	0.11	0.086	1079.324	82378.642	-5.168	5.1
0.38	0.51	0.61	0.115	0.12	0.086	1079.567	82378.456	-5.355	5.3
0.39	0.49	0.62	0.115	0.12	0.086	1079.214	82378.428	-5.383	5.3
0.38	0.5	0.62	0.12	0.12	0.086	1079.457	82378.233	-5.578	5.5
0.37	0.51	0.62	0.125	0.13	0.086	1079.7	82378.052	-5.759	5.7
0.38	0.49	0.63	0.125	0.13	0.086	1079.347	82378.021	-5.79	5.7
0.36	0.52	0.62	0.131	0.14	0.086	1079.943	82377.888	-5.923	5.9
0.37	0.5	0.63	0.13	0.13	0.086	1079.59	82377.832	-5.978	5.9
0.38	0.48	0.64	0.131	0.14	0.086	1079.237	82377.819	-5.991	5.9
0.36	0.51	0.63	0.135	0.14	0.086	1079.833	82377.66	-6.151	6.1
0.37	0.49	0.64	0.135	0.14	0.086	1079.48	82377.623	-6.188	6.1
0.35	0.52	0.63	0.141	0.15	0.086	1080.076	82377.502	-6.309	6.3
0.36	0.5	0.64	0.14	0.14	0.086	1079.723	82377.442	-6.369	6.3
0.37	0.48	0.65	0.141	0.15	0.086	1079.37	82377.424	-6.386	6.3
0.34	0.53	0.63	0.147	0.16	0.086	1080.318	82377.36	-6.451	6.4
0.35	0.51	0.64	0.145	0.15	0.086	1079.965	82377.276	-6.534	6.5
0.37	0.47	0.66	0.147	0.16	0.086	1079.259	82377.238	-6.573	6.5
0.36	0.49	0.65	0.145	0.15	0.086	1079.612	82377.235	-6.576	6.5
0.34	0.52	0.64	0.151	0.16	0.086	1080.208	82377.126	-6.685	6.6

Top 20 best heterogeneous configurations for the Sioux Falls network for $\bar{\alpha} = 0.7$

Alpha1	Alpha2	Alpha3	Spread	Extremeness	Bottleneck	UncFlow	CostHet	DeltaC	Improvement
0.41	0.7	0.99	0.29	0.29	0.086	1102.626	82336.954	-10.277	10.277
0.4	0.71	0.99	0.295	0.3	0.086	1102.869	82336.961	-10.271	10.271
0.42	0.69	0.99	0.285	0.29	0.086	1102.383	82336.963	-10.269	10.269
0.39	0.72	0.99	0.3	0.31	0.086	1103.112	82336.983	-10.249	10.249
0.43	0.68	0.99	0.281	0.29	0.086	1102.141	82336.987	-10.245	10.245
0.38	0.73	0.99	0.306	0.32	0.086	1103.355	82337.02	-10.212	10.212
0.44	0.67	0.99	0.276	0.29	0.086	1101.898	82337.026	-10.206	10.206
0.37	0.74	0.99	0.312	0.33	0.086	1103.598	82337.072	-10.16	10.16
0.45	0.66	0.99	0.272	0.29	0.086	1101.655	82337.081	-10.151	10.151
0.36	0.75	0.99	0.318	0.34	0.086	1103.841	82337.139	-10.092	10.092
0.46	0.65	0.99	0.269	0.29	0.086	1101.412	82337.15	-10.082	10.082
0.41	0.71	0.98	0.285	0.29	0.086	1102.736	82337.169	-10.063	10.063
0.42	0.7	0.98	0.28	0.28	0.086	1102.494	82337.17	-10.062	10.062
0.4	0.72	0.98	0.291	0.3	0.086	1102.979	82337.184	-10.048	10.048
0.43	0.69	0.98	0.275	0.28	0.086	1102.251	82337.186	-10.046	10.046
0.39	0.73	0.98	0.296	0.31	0.086	1103.222	82337.214	-10.018	10.018
0.44	0.68	0.98	0.271	0.28	0.086	1102.008	82337.215	-10.016	10.016
0.35	0.76	0.99	0.324	0.35	0.086	1104.084	82337.223	-10.009	10.009
0.47	0.64	0.99	0.265	0.29	0.086	1101.169	82337.236	-9.996	9.996
0.38	0.74	0.98	0.302	0.32	0.086	1103.465	82337.259	-9.973	9.973

Top 20 worst heterogeneous configurations for the Sioux Falls network for $\bar{\alpha} = 0.7$

Alpha1	Alpha2	Alpha3	Spread	Extremeness	Bottleneck	UncFlow	CostHet	DeltaC	Improvement
0.6	0.7	0.8	0.1	0.1	0.086	1100.103	82342.744	-4.488	4.488
0.59	0.7	0.81	0.11	0.11	0.086	1100.236	82342.35	-4.881	4.881
0.58	0.71	0.81	0.115	0.12	0.086	1100.479	82342.229	-5.003	5.003
0.59	0.69	0.82	0.115	0.12	0.086	1100.126	82342.095	-5.137	5.137
0.58	0.7	0.82	0.12	0.12	0.086	1100.369	82341.966	-5.266	5.266
0.57	0.71	0.82	0.125	0.13	0.086	1100.611	82341.852	-5.38	5.38
0.56	0.72	0.82	0.131	0.14	0.086	1100.854	82341.754	-5.478	5.478
0.58	0.69	0.83	0.125	0.13	0.086	1100.258	82341.713	-5.518	5.518
0.57	0.7	0.83	0.13	0.13	0.086	1100.501	82341.592	-5.64	5.64
0.56	0.71	0.83	0.135	0.14	0.086	1100.744	82341.485	-5.747	5.747
0.58	0.68	0.84	0.131	0.14	0.086	1100.148	82341.472	-5.759	5.759
0.55	0.72	0.83	0.141	0.15	0.086	1100.987	82341.394	-5.838	5.838
0.57	0.69	0.84	0.135	0.14	0.086	1100.391	82341.341	-5.891	5.891
0.54	0.73	0.83	0.147	0.16	0.086	1101.23	82341.317	-5.915	5.915
0.56	0.7	0.84	0.14	0.14	0.086	1100.634	82341.227	-6.004	6.004
0.55	0.71	0.84	0.145	0.15	0.086	1100.877	82341.127	-6.105	6.105
0.57	0.68	0.85	0.141	0.15	0.086	1100.281	82341.104	-6.128	6.128
0.54	0.72	0.84	0.151	0.16	0.086	1101.12	82341.043	-6.189	6.189
0.56	0.69	0.85	0.145	0.15	0.086	1100.524	82340.98	-6.252	6.252
0.53	0.73	0.84	0.157	0.17	0.086	1101.363	82340.974	-6.258	6.258

B Matlab Codes

```
clear; close all; clc;
clear; close all; clc;

% Homogeneous CVaR-based Wardrop equilibrium (one OD, three
    parallel paths)

%% Parameters
nEdges = 3;
nPaths = 3;
nOD    = 1;

alphaGrid = 0.1:0.1:1;
demandOD  = 260;

t_ff = [1000; 950; 3000];

R_diag = [40; 60; 80];
R      = diag(R_diag);

gamma = [3000; 0; 0];
EU    = 0.5;

%% Matrices
Q = eye(nEdges);
B = [1 1 1];

A11 = Q' * R * Q;
A12 = -B';
A21 = B;
A22 = zeros(nOD, nOD);

A = [A11, A12;
     A21, A22];

%% Storage
nAlpha = numel(alphaGrid);

h_hom_store      = zeros(nAlpha, nPaths);   % homogeneous
    equilibrium path flows
Ecost_total_store = zeros(nAlpha, 1);       % total expected
    network cost

%% Loop over alpha
for ia = 1:nAlpha
    alpha = alphaGrid(ia);

    % Perceived (CVaR-based) constant costs
    % CVaR_alpha(U), U~Unif[0,1] = 1 - alpha/2
    cvarU  = 1 - alpha/2;
```

```
    c_cvar = t_ff + [gamma(1)*cvarU; 0; 0];

    % Vecotor q
    q = [c_cvar; -demandOD];

    % Solve homogeneous Wardrop equilibrium as convex QP
    cvx_begin quiet
        variable x_hom(nPaths + nOD)
        minimize( x_hom' * A * x_hom + q' * x_hom )
        subject to
            x_hom >= 0;
            A * x_hom + q >= 0;
    cvx_end

    h_hom = x_hom(1:nPaths);                % homogeneous
       equilibrium path flows
    h_hom_store(ia, :) = h_hom.';

    % Expected physical path costs
    Ecost_path = zeros(nPaths, 1);
    Ecost_path(1) = t_ff(1) + R_diag(1)*h_hom(1) + gamma(1)*EU;
    Ecost_path(2) = t_ff(2) + R_diag(2)*h_hom(2);
    Ecost_path(3) = t_ff(3) + R_diag(3)*h_hom(3);

    Ecost_total_store(ia) = sum(h_hom .* Ecost_path);
end

%% Plots

% Homogeneous equilibrium path flows
figure; hold on;
for p = 1:nPaths
    plot(alphaGrid, h_hom_store(:, p), 'LineWidth', 1.5);
end
xlabel('Risk aversion parameter \alpha');
ylabel('Path flow h_p^{\mathrm{hom}}');
legend('Path 1','Path 2','Path 3','Location','best');
title('Homogeneous CVaR-based Wardrop equilibrium');
grid on; hold off;

% Total expected network cost
figure;
plot(alphaGrid, Ecost_total_store, '-o', 'LineWidth', 1.5);
xlabel('Risk aversion parameter \alpha');
ylabel('Total expected network cost');
title('Homogeneous network: total expected cost');
grid on;
```

Listing 1: Homogeneous CVaR-based Wardrop equilibrium (one OD, three parallel paths)

```
clear; close all; clc;
```

```
format long
cvx_solver sedumi
cvx_precision high

% Heterogeneous CVaR-based Wardrop equilibrium (one OD, three parallel paths)

%% Parameters
nGroups = 3;
nPaths  = 3;
nOD     = 1;

alpha_bar = 0.3;      % homogeneous mean risk aversion \bar{\alpha}
minGap    = 0.1;      % minimum separation between group alphas
rng(1);               % reproducibility (plotting order etc.)

d_total = 260;                                  % total OD demand
d_group = (d_total/nGroups) * ones(nGroups,1);  % equal demand per group

%% Cost parameters
t_ff  = [1000; 950; 3000];          % free-flow travel times t_ff
R     = diag([40; 60; 80]);         % congestion matrix R (diagonal)
gamma = [3000; 0; 0];               % uncertainty amplitude (only path 1 uncertain)
EU    = 0.5;                        % E[U] for U~Unif[0,1]

%% Network matrices
Q = eye(nPaths);                    % edge path incidence (identity for 3-path network)
B = ones(1,nPaths);                 % OD path incidence

% A in A x + q (LCP / VI operator)
A11 = kron(ones(nGroups), Q'*R*Q);
A12 = -blkdiag(B',B',B');
A21 =  blkdiag(B,B,B);
A22 = zeros(nGroups);
A   = [A11 A12; A21 A22];

n_var = nGroups*nPaths + nGroups;

%% ================================================================
% 1) ALL UNIQUE DISCRETE CONFIGURATIONS
% ================================================================

step = 0.01;

valsInt   = 1:99;
```

```
barInt    = round(alpha_bar * 100);
minGapInt = round(minGap * 100);

all_cfg_int = [];   % store sorted triples as integers

for i = 1:numel(valsInt)
    a1i = valsInt(i);
    for j = 1:numel(valsInt)
        a2i = valsInt(j);

        % a1 + a2 + a3 = 3*alpha_bar
        a3i = 3*barInt - a1i - a2i;

        % bounds
        if a3i < 1 || a3i > 99
            continue;
        end

        aa = sort([a1i a2i a3i]);

        % minimum separation constraint
        if min(diff(aa)) < minGapInt
            continue;
        end

        all_cfg_int = [all_cfg_int; aa];
    end
end

all_cfg_int = unique(all_cfg_int, 'rows');
alpha_cfg   = all_cfg_int / 100;

nCfg = size(alpha_cfg,1);
fprintf('Total number of UNIQUE heterogeneous configurations = %d
    \n', nCfg);

assert(size(unique(alpha_cfg,'rows'),1) == nCfg, 'Duplicates
    still present in alpha_cfg!');

spread  = std(alpha_cfg, 0, 2);
extreme = max(abs(alpha_cfg - alpha_bar), [], 2); %#ok<NASGU>

fprintf('Std(alpha) range: [%.6f, %.6f]\n', min(spread), max(
    spread));
fprintf('Min pairwise alpha gap: %.6f\n', min(min(diff(sort(
    alpha_cfg,2),1,2))));

%% ============================================================
% 2) HOMOGENEOUS RISK AVERSION (alpha = alpha_bar for all groups)
% ============================================================

```

```
q_hom = zeros(n_var,1);
for g = 1:nGroups
    q_hom((g-1)*nPaths + (1:nPaths)) = t_ff + gamma*(1 -
       alpha_bar/2);
end
q_hom(nGroups*nPaths + (1:nGroups)) = -d_group;

cvx_begin quiet
    variable x_hom(n_var)
    minimize( x_hom'*A*x_hom + q_hom'*x_hom )
    subject to
        x_hom >= 0;
        A*x_hom + q_hom >= 0;
cvx_end

H_hom = reshape(x_hom(1:nGroups*nPaths), nPaths, nGroups); %
   nPaths x nGroups
h_hom = sum(H_hom,2);                                      %
   nPaths x 1

C_path_hom = t_ff + diag(R).*h_hom + gamma*EU;
C_hom      = sum(h_hom .* C_path_hom);

fprintf('Computed homogeneous benchmark: C_hom = %.6f\n', C_hom);

%% ================================================================
% 3) HETEROGENEOUS CASES (STORE FLOWS FOR BEST / WORST)
% ================================================================

C_het = zeros(nCfg,1);

bestDelta  = +Inf;
worstDelta = -Inf;

best_idx  = NaN;
worst_idx = NaN;

H_best  = NaN(nPaths,nGroups);
H_worst = NaN(nPaths,nGroups);

h_best  = NaN(nPaths,1);
h_worst = NaN(nPaths,1);

for c = 1:nCfg
    q_het = zeros(n_var,1);

    for g = 1:nGroups
        alpha_g = alpha_cfg(c,g);
        q_het((g-1)*nPaths + (1:nPaths)) = t_ff + gamma*(1 -
           alpha_g/2);
    end
```

```
    q_het(nGroups*nPaths + (1:nGroups)) = -d_group;

    cvx_begin quiet
        variable x_het(n_var)
        minimize( x_het'*A*x_het + q_het'*x_het )
        subject to
            x_het >= 0;
            A*x_het + q_het >= 0;
    cvx_end

    H_het = reshape(x_het(1:nGroups*nPaths), nPaths, nGroups);
    h_het = sum(H_het,2);

    C_path_het = t_ff + diag(R).*h_het + gamma*EU;
    C_het(c)   = sum(h_het .* C_path_het);

    delta = C_het(c) - C_hom;

    if delta < bestDelta
        bestDelta = delta;
        best_idx  = c;
        H_best    = H_het;
        h_best    = h_het;
    end

    if delta > worstDelta
        worstDelta = delta;
        worst_idx  = c;
        H_worst    = H_het;
        h_worst    = h_het;
    end
end


DeltaC_raw = C_het - C_hom;
DeltaC     = round(DeltaC_raw, 3);
DeltaC(abs(DeltaC) < 1e-3) = 0;

Improvement = -DeltaC;                  % since Improvement =
   C_hom - C_het


%% ============================================================
% 3.6 PRINT FLOWS FOR BEST AND WORST CONFIGURATIONS
% ============================================================

pathNames  = strcat("Path", string(1:nPaths));
groupNames = strcat("Group", string(1:nGroups));

fprintf('\n===== BEST configuration (min DeltaC) =====\n');
fprintf('Index: %d\n', best_idx);
```

```
fprintf('Alphas (sorted): [%.2f %.2f %.2f]\n', alpha_cfg(best_idx,1), alpha_cfg(best_idx,2), alpha_cfg(best_idx,3));
fprintf('DeltaC (rounded): %.3f\n', bestDelta);

T_h_best = table(h_best, 'RowNames', cellstr(pathNames));
T_H_best = array2table(H_best, 'RowNames', cellstr(pathNames), 'VariableNames', cellstr(groupNames));

disp('--- BEST total flow per path (h_best) ---');
disp(T_h_best);
disp('--- BEST per group per path (H_best) ---');
disp(T_H_best);

fprintf('\n===== WORST configuration (max DeltaC) =====\n');
fprintf('Index: %d\n', worst_idx);
fprintf('Alphas (sorted): [%.2f %.2f %.2f]\n', alpha_cfg(worst_idx,1), alpha_cfg(worst_idx,2), alpha_cfg(worst_idx,3));
fprintf('DeltaC (rounded): %.3f\n', worstDelta);

T_h_worst = table(h_worst, 'RowNames', cellstr(pathNames));
T_H_worst = array2table(H_worst, 'RowNames', cellstr(pathNames), 'VariableNames', cellstr(groupNames));

disp('--- WORST total flow per path (h_worst) ---');
disp(T_h_worst);
disp('--- WORST per group per path (H_worst) ---');
disp(T_H_worst);

%% ============================================================
% TABLE RESULTS + TOP CONFIGURATIONS
% ============================================================

ResultsTable = table( ...
    alpha_cfg(:,1), alpha_cfg(:,2), alpha_cfg(:,3), ...
    round(spread,3), ...
    round(C_het), ...
    DeltaC, ...
    round(Improvement,3), ...
    'VariableNames', {'Alpha1','Alpha2','Alpha3', ...
                      'Spread', ...
                      'CostHet','DeltaC','Improvement'} );

ResultsTable = sortrows(ResultsTable, 'Improvement', 'descend');
writetable(ResultsTable, 'All_Configurations_Results_ThreePaths.csv');

disp(ResultsTable(1:min(20,height(ResultsTable)), :));

T_best = sortrows(ResultsTable, 'Improvement', 'descend');
topK = min(100, height(T_best));
Top20_Best = T_best(1:topK,:);
```

```
236
237 disp('=====␣TOP␣BEST␣configurations␣(lowest␣DeltaC)␣=====');
238 disp(Top20_Best);
239
240 T_worst = sortrows(ResultsTable, 'Improvement', 'ascend');
241 topK2 = min(100, height(T_worst));
242 Top20_Worst = T_worst(1:topK2,:);
243
244 disp('=====␣TOP␣WORST␣configurations␣(highest␣DeltaC)␣=====');
245 disp(Top20_Worst);
246
247 writetable(Top20_Best,  'Top20_Best_3Paths.csv');
248 writetable(Top20_Worst, 'Top20_Worst_3Paths.csv');
249
250 %% ============================================================
251 % SUMMARY STATS (EXPORT)
252 % ============================================================
253
254 fprintf('\n===␣Heterogeneity␣Summary␣===\n');
255 fprintf('Homogeneous␣cost␣C_hom␣=␣%.6f\n', C_hom);
256 fprintf('Mean␣ C ␣(rounded)␣=␣%.3f\n', mean(DeltaC));
257 fprintf('%%␣cases␣better␣than␣homogeneous␣=␣%.2f%%\n', 100*mean(
       DeltaC < 0));
258 fprintf('Best␣ C ␣(rounded)␣=␣%.3f\n', min(DeltaC));
259 fprintf('Worst␣ C ␣(rounded)␣=␣%.3f\n', max(DeltaC));
260 fprintf('============================\n');
261
262 SummaryTable = table( ...
263     nCfg, ...
264     C_hom, ...
265     mean(DeltaC), ...
266     100*mean(DeltaC < 0), ...
267     min(DeltaC), ...
268     max(DeltaC), ...
269     min(spread), ...
270     max(spread), ...
271     'VariableNames', {'NumConfigs','C_hom','MeanDeltaC','
          PctBetterThanHom', ...
272                       'BestDeltaC','WorstDeltaC','MinSpread','
                             MaxSpread'} );
273
274 writetable(SummaryTable, 'SummaryStats_3Paths.csv');
275
276 disp('=====␣SUMMARY␣STATS␣=====');
277 disp(SummaryTable);
278
279 %% ============================================================
280 % PLOTS
281 % ============================================================
282
283 % (1)   Cost   vs Spread
```

```
figure;
scatter(spread, DeltaC, 40, 'filled');
xlabel('Spread␣of␣\alpha␣(std)');
ylabel('\Delta␣C␣=␣C_{het}␣-␣C_{hom}');
title(sprintf('Difference␣in␣Cost␣as␣a␣function␣of␣Spread␣(  ␣=␣
   %.1f)', alpha_bar));
grid on;
yline(0,'k--','LineWidth',1.2);

% (2) Distribution of  Cost
figure;
histogram(DeltaC,30);
xline(0,'k--','LineWidth',1.5);
xlabel('\Delta␣C');
ylabel('Frequency');
title(sprintf('Distribution␣of␣\\Delta␣C␣(  ␣=␣%.1f)', alpha_bar)
   );
grid on;
```

Listing 2: Heterogeneous CVaR-based Wardrop equilibrium (one OD, three parallel paths)

```

% Homogeneous CVaR-based Wardrop equilibrium (two OD pairs, five
   paths)

%% Parameters
nEdges = 5;                          %  each path corresponds to
   one edge
nPaths = 5;                          %  five parallel paths
nOD    = 2;                          %  two OD pairs)

n_var = nPaths + nOD;                % decision variables: x = [h;
    v]

alphaGrid = 0.1:0.1:1.0;             % risk parameter alpha in
   CVaR_alpha
nAlpha    = numel(alphaGrid);

demandOD = [260; 170];               % OD demands (OD1: A->B, OD2:
    B->A)

% MATRICES DEFINITION
%  O D path  incidence
B = [1 1 1 0 0;
     0 0 0 1 1];


% MATRICE R
R = zeros(nPaths);
R(1,1) = 40;
R(1,4) = 20;
```

```
R(2,2) = 60;
R(2,5) = 20;
R(3,3) = 80;
R(4,1) = 8;
R(4,4) = 80;
R(5,2) = 4;
R(5,5) = 100;

Q = eye(nEdges);                        %  e d g e path  incidence

% Free-flow constants t_ff per path
t_ff = [1000; 950; 3000; 1000; 1300];

% (only paths 1 and 4 uncertain)
gamma = [3000; 0; 0; 4000; 0];
EU    = 0.5;                            % E[U] for U~Unif[0,1]

%% Matrix (A in A x + q)
A11 = Q' * R * Q;
A12 = -B';
A21 =  B;
A22 = zeros(nOD,nOD);

A = [A11, A12;
     A21, A22];

%% Storage
h_hom_store         = zeros(nAlpha, nPaths);    % equilibrium path
    flows h^{hom} for each alpha
Ecost_path_store    = zeros(nAlpha, nPaths);    % expected
   physical path costs E[C_p]
Ecost_total_store   = zeros(nAlpha, 1);         % total expected
   network cost

%% Loop over alpha
for ia = 1:nAlpha
    alpha = alphaGrid(ia);

    % CVaR_alpha(U), U~Unif[0,1] = 1 - alpha/2
    cvarU = 1 - alpha/2;

    % Perceived (CVaR-based) constant costs: t_ff + gamma .*
       CVaR_alpha[U]
    c_cvar = t_ff + gamma * cvarU;

    % q vector with x = [h; v]
    q = [c_cvar; -demandOD];

    % Solve homogeneous Wardrop equilibrium as convex QP
    cvx_begin quiet
        variable x_hom(n_var)
```

```
        minimize( x_hom' * A * x_hom + q' * x_hom )
        subject to
            x_hom >= 0;
            A * x_hom + q >= 0;
    cvx_end

    h_hom = x_hom(1:nPaths);                    % path flows
    h_hom_store(ia,:) = h_hom.';

    % Expected physical path costs (no CVaR term): E[C] = t_ff +
       R h + gamma E[U]
    Ecost_path = R*h_hom + t_ff + gamma*EU;

    Ecost_path_store(ia,:)  = Ecost_path.';
    Ecost_total_store(ia,1) = sum(h_hom .* Ecost_path);
end

figure; hold on;
for p = 1:nPaths
    plot(alphaGrid, h_hom_store(:,p), 'LineWidth', 1.5);
end
xlabel('Risk aversion parameter \alpha');
ylabel('Flow h_p');
legend('Path 1','Path 2','Path 3','Path 4','Path 5','Location','
   best');
title('Effect of \alpha on path usage');
grid on; hold off;


figure; hold on;
for p = 1:nPaths
    plot(alphaGrid, Ecost_path_store(:,p), 'LineWidth', 1.5);
end
xlabel('\alpha');
ylabel('Expected path cost E[C_p]');
legend('Path 1','Path 2','Path 3','Path 4','Path 5','Location','
   best');
title('Expected path costs vs \alpha');
grid on; hold off;
```

Listing 3: Homogeneous CVaR-based Wardrop equilibrium (two OD pairs, five paths)

```

    clear; close all; clc;
format long

cvx_solver sedumi
cvx_precision high

% Heterogeneous CVaR-based Wardrop equilibrium (two OD pairs,
   five paths)
```

```
9
10 %% Parameters
11 nGroups = 3;                          % number of user groups
12 nPaths  = 5;                          % number of paths
13 nOD     = 2;                          % number of OD pairs
14
15 alpha_bar = 0.3;                      % homogeneous mean risk
       aversion \bar{\alpha}
16 minGap    = 0.10;                     % minimum separation between
       group alphas
17
18 %% OD demands
19 demandOD = [260; 170];                                  % total
       demand per OD
20 d_group  = (1/nGroups) * demandOD;                      % equal
       split across groups (nOD x 1)
21
22 %% Cost parameters
23 t_ff = [1000; 950; 3000; 1000; 1300];                   % free-flow
       constants t_ff
24
25 % Congestion matrix R ( p a t h path  interactions)
26 R = zeros(nPaths);
27 R(1,1)= 40;
28 R(1,4)=20;
29 R(2,2)= 60;
30 R(2,5)=20;
31 R(3,3)= 80;
32 R(4,1)=  8;
33 R(4,4)=80;
34 R(5,2)=  4;
35 R(5,5)=100;
36
37 gamma = [3000; 0; 0; 4000; 0];                          %
       uncertainty amplitudes
38 EU    = 0.5;                                           % E[U]
39
40 %% Incidence matrices
41 Q = eye(nPaths);                                        %
       e d g e path  incidence
42 B = [1 1 1 0 0;
43      0 0 0 1 1];                                        %  O D path
           incidence
44
45 %% A matrix for K groups and W ODs (A x + q)
46 A11 = kron(ones(nGroups), Q' * R * Q);                  % (K*P)x(K*
       P)
47 A12 = -blkdiag(B', B', B');                            % (K*P)x(K*
       W)
48 A21 =  blkdiag(B,  B,  B);                             % (K*W)x(K*
       P)
```

```
A22 = zeros(nGroups*nOD);                                    % (K*W)x(K*W)

A = [A11 A12;
     A21 A22];

n_var = nGroups*nPaths + nGroups*nOD;

%% ================================================================
% 1) ALL UNIQUE DISCRETE CONFIGURATIONS
% ================================================================

step = 0.01;

valsInt   = 1:99;
barInt    = round(alpha_bar * 100);
minGapInt = round(minGap * 100);

all_cfg_int = [];                                            % store sorted integer triples

for i = 1:numel(valsInt)
    a1i = valsInt(i);
    for j = 1:numel(valsInt)
        a2i = valsInt(j);

        % enforce mean exactly: a1 + a2 + a3 = 3*alpha_bar
        a3i = 3*barInt - a1i - a2i;

        % bounds (must be 1..99)
        if a3i < 1 || a3i > 99
            continue;
        end

        aa = sort([a1i a2i a3i]);

        % minimum separation constraint
        if min(diff(aa)) < minGapInt
            continue;
        end

        all_cfg_int = [all_cfg_int; aa];
    end
end

all_cfg_int = unique(all_cfg_int, 'rows');
alpha_cfg   = all_cfg_int / 100;

nCfg = size(alpha_cfg,1);
fprintf('Total number of UNIQUE heterogeneous configurations = %d\n', nCfg);
```

```
97
98  spread  = std(alpha_cfg, 0, 2);
99  extreme = max(abs(alpha_cfg - alpha_bar), [], 2);
100
101 fprintf('Mean(alpha) check (min/max): [%.6f, %.6f]\n', min(mean(
        alpha_cfg,2)), max(mean(alpha_cfg,2)));
102 fprintf('Std(alpha) range: [%.6f, %.6f]\n', min(spread), max(
        spread));
103 fprintf('Min pairwise alpha gap: %.6f\n\n', min(min(diff(sort(
        alpha_cfg,2),1,2))));
104
105 %% ================================================================
106 % 2) HOMOGENEOUS BENCHMARK (alpha = alpha_bar for all groups)
107 % ================================================================
108
109 q_hom = zeros(n_var,1);
110
111 for g = 1:nGroups
112     q_hom((g-1)*nPaths + (1:nPaths)) = t_ff + gamma*(1 -
            alpha_bar/2);
113 end
114
115 for g = 1:nGroups
116     idxv = nGroups*nPaths + (g-1)*nOD + (1:nOD);
117     q_hom(idxv) = -d_group;
118 end
119
120 cvx_begin quiet
121     variable x_hom(n_var)
122     minimize( x_hom'*A*x_hom + q_hom'*x_hom )
123     subject to
124         x_hom >= 0;
125         A*x_hom + q_hom >= 0;
126 cvx_end
127
128 H_hom = reshape(x_hom(1:nGroups*nPaths), nPaths, nGroups);   %
        nPaths x nGroups
129 h_hom = sum(H_hom,2);                                       %
        nPaths x 1
130
131 C_path_hom = t_ff + R*h_hom + gamma*EU;                     %
        expected physical costs
132 C_hom      = sum(h_hom .* C_path_hom);
133
134 fprintf('Computed homogeneous benchmark: C_hom = %.6f\n', C_hom);
135
136 %% ================================================================
137 % 3) HETEROGENEOUS CASES (STORE FLOWS FOR BEST / WORST)
138 % ================================================================
139
140 C_het = zeros(nCfg,1);
```

```
141
142 bestDelta  = +Inf;
143 worstDelta = -Inf;
144
145 best_idx  = NaN;
146 worst_idx = NaN;
147
148 H_best  = NaN(nPaths,nGroups);
149 H_worst = NaN(nPaths,nGroups);
150
151 h_best  = NaN(nPaths,1);
152 h_worst = NaN(nPaths,1);
153
154 for c = 1:nCfg
155     q_het = zeros(n_var,1);
156
157     for g = 1:nGroups
158         alpha_g = alpha_cfg(c,g);
159         q_het((g-1)*nPaths + (1:nPaths)) = t_ff + gamma*(1 -
               alpha_g/2);
160     end
161
162     for g = 1:nGroups
163         idxv = nGroups*nPaths + (g-1)*nOD + (1:nOD);
164         q_het(idxv) = -d_group;
165     end
166
167     cvx_begin quiet
168         variable x_het(n_var)
169         minimize( x_het'*A*x_het + q_het'*x_het )
170         subject to
171             x_het >= 0;
172             A*x_het + q_het >= 0;
173     cvx_end
174
175     H_het = reshape(x_het(1:nGroups*nPaths), nPaths, nGroups); %
          nPaths x nGroups
176     h_het = sum(H_het,2);                                      %
          nPaths x 1
177
178     C_path_het = t_ff + R*h_het + gamma*EU;
179     C_het(c)   = sum(h_het .* C_path_het);
180
181     delta = C_het(c) - C_hom;
182
183     if delta < bestDelta
184         bestDelta = delta;
185         best_idx  = c;
186         H_best    = H_het;
187         h_best    = h_het;
188     end
```

```
189
190     if delta > worstDelta
191         worstDelta = delta;
192         worst_idx  = c;
193         H_worst    = H_het;
194         h_worst    = h_het;
195     end
196 end
197
198 DeltaC      = C_het - C_hom;
199 Improvement = C_hom - C_het;
200
201 %% ============================================================
202 % 3.6 PRINT FLOWS FOR BEST AND WORST CONFIGURATIONS
203 % ============================================================
204
205 pathNames  = strcat("Path", string(1:nPaths));
206 groupNames = strcat("Group", string(1:nGroups));  % Group1=lowest
        alpha (alphas are sorted)
207
208 fprintf('\n=====␣BEST␣configuration␣(min␣DeltaC)␣=====\n');
209 fprintf('Index:␣%d\n', best_idx);
210 fprintf('Alphas␣(sorted):␣[%.2f␣%.2f␣%.2f]\n', alpha_cfg(best_idx
       ,1), alpha_cfg(best_idx,2), alpha_cfg(best_idx,3));
211 fprintf('DeltaC:␣%.6f\n', bestDelta);
212
213 T_h_best = table(h_best, 'RowNames', cellstr(pathNames));
214 T_H_best = array2table(H_best, 'RowNames', cellstr(pathNames), '
       VariableNames', cellstr(groupNames));
215
216 disp('---␣BEST␣total␣flow␣per␣path␣(h_best)␣---');
217 disp(T_h_best);
218 disp('---␣BEST␣per␣group␣per␣path␣(H_best)␣---');
219 disp(T_H_best);
220
221 fprintf('\n=====␣WORST␣configuration␣(max␣DeltaC)␣=====\n');
222 fprintf('Index:␣%d\n', worst_idx);
223 fprintf('Alphas␣(sorted):␣[%.2f␣%.2f␣%.2f]\n', alpha_cfg(
       worst_idx,1), alpha_cfg(worst_idx,2), alpha_cfg(worst_idx,3));
224 fprintf('DeltaC:␣%.6f\n', worstDelta);
225
226 T_h_worst = table(h_worst, 'RowNames', cellstr(pathNames));
227 T_H_worst = array2table(H_worst, 'RowNames', cellstr(pathNames),
       'VariableNames', cellstr(groupNames));
228
229 disp('---␣WORST␣total␣flow␣per␣path␣(h_worst)␣---');
230 disp(T_h_worst);
231 disp('---␣WORST␣per␣group␣per␣path␣(H_worst)␣---');
232 disp(T_H_worst);
233
234 %% ============================================================
```

```
% 4) TABLE RESULTS + TOP-20 CONFIGURATIONS (BEST / WORST)
% ============================================================

ResultsTable = table( ...
    alpha_cfg(:,1), alpha_cfg(:,2), alpha_cfg(:,3), ...
    round(spread,3), ...
    round(C_het), round(DeltaC), round(Improvement), ...
    'VariableNames', {'Alpha1','Alpha2','Alpha3', ...
                      'Spread', ...
                      'CostHet','DeltaC','Improvement'} );

ResultsTable = sortrows(ResultsTable, 'Improvement', 'descend');
writetable(ResultsTable, 'All_Configurations_Results_FivePaths.
    csv');

Top20_Best  = ResultsTable(1:min(20,height(ResultsTable)), :);

ResultsTable_worst = sortrows(ResultsTable, 'Improvement', '
    ascend');
Top20_Worst = ResultsTable_worst(1:min(20,height(
    ResultsTable_worst)), :);

disp('=====␣TOP-20␣BEST␣configurations␣(highest␣Improvement)␣
    =====');
disp(Top20_Best);

disp('=====␣TOP-20␣WORST␣configurations␣(lowest␣Improvement)␣
    =====');
disp(Top20_Worst);

writetable(Top20_Best,  'Top20_Best_5Paths.csv');
writetable(Top20_Worst, 'Top20_Worst_5Paths.csv');

%% ============================================================
% 5) PLOTS
% ============================================================

figure;
scatter(spread, DeltaC, 40, 'filled');
xlabel('Spread␣of␣\alpha␣(std)');
ylabel('\Delta␣C␣=␣C_{het}␣-␣C_{hom}');
title(sprintf('Difference␣in␣Cost␣as␣a␣function␣of␣Spread␣(  ␣=␣
    %.1f)', alpha_bar));
grid on;
yline(0,'k--','LineWidth',1.2);

figure;
histogram(DeltaC,30);
xline(0,'k--','LineWidth',1.5);
xlabel('\Delta␣C');
ylabel('Frequency');
```

```
title(sprintf('Distribution␣of␣\\Delta␣C␣(\\bar{\\alpha}␣=␣%.1f)'
    , alpha_bar));
grid on;

%% ============================================================
% 6) SUMMARY STATS (same format as 3-path case)
% ============================================================

fprintf('\n===␣Heterogeneity␣Summary␣===\n');
fprintf('Homogeneous␣cost␣C_hom␣=␣%.6f\n', C_hom);
fprintf('Mean␣ C ␣␣␣=␣%.6f\n', mean(DeltaC));
fprintf('%%␣cases␣better␣than␣homogeneous␣=␣%.2f%%\n', 100*mean(
   round(DeltaC) < 0));
fprintf('Best␣ C ␣=␣%.6f\n', min(DeltaC));
fprintf('Worst␣ C ␣=␣%.6f\n', max(DeltaC));
fprintf('============================\n');

SummaryTable = table( ...
    nCfg, ...
    C_hom, ...
    mean(DeltaC), ...
    100*mean(round(DeltaC) < 0), ...
    min(DeltaC), ...
    max(DeltaC), ...
    min(spread), ...
    max(spread), ...
    'VariableNames', {'NumConfigs','C_hom','MeanDeltaC','
       PctBetterThanHom', ...
                      'BestDeltaC','WorstDeltaC','MinSpread','
                         MaxSpread'} );

writetable(SummaryTable, 'SummaryStats_5Paths.csv');

disp('=====␣SUMMARY␣STATS␣=====');
disp(SummaryTable);

%% ============================================================
% OD contributions (unchanged logic; names aligned)
% ============================================================

C_path_best  = t_ff + R*h_best  + gamma*EU;
C_path_worst = t_ff + R*h_worst + gamma*EU;

dC_OD1_mean = mean(C_path_worst(1:3)) - mean(C_path_best(1:3));
dC_OD2_mean = mean(C_path_worst(4:5)) - mean(C_path_best(4:5));

fprintf('\n===␣Which␣OD␣drives␣ b e s t worst ␣cost␣change?␣===\n');
fprintf('  ␣mean␣path␣cost␣OD1␣(paths␣1-3):␣%.6f\n', dC_OD1_mean)
   ;
fprintf('  ␣mean␣path␣cost␣OD2␣(paths␣4-5):␣%.6f\n', dC_OD2_mean)
   ;
```

```
325
326 if dC_OD1_mean > dC_OD2_mean
327     fprintf('=> OD1 shows the larger cost shift between best and
        worst.\n');
328 elseif dC_OD2_mean > dC_OD1_mean
329     fprintf('=> OD2 shows the larger cost shift between best and
        worst.\n');
330 else
331     fprintf('=> OD1 and OD2 show the same mean cost shift.\n');
332 end
333 fprintf('================================================\n');
334
335 h1_hom   = h_hom(1:3);   h2_hom   = h_hom(4:5);
336 h1_best  = h_best(1:3);  h2_best  = h_best(4:5);
337 h1_worst = h_worst(1:3); h2_worst = h_worst(4:5);
338
339 C_OD1_hom   = sum(h1_hom   .* C_path_hom(1:3));
340 C_OD2_hom   = sum(h2_hom   .* C_path_hom(4:5));
341
342 C_OD1_best  = sum(h1_best  .* C_path_best(1:3));
343 C_OD2_best  = sum(h2_best  .* C_path_best(4:5));
344
345 C_OD1_worst = sum(h1_worst .* C_path_worst(1:3));
346 C_OD2_worst = sum(h2_worst .* C_path_worst(4:5));
347
348 dC_OD1_best  = C_OD1_best  - C_OD1_hom;
349 dC_OD2_best  = C_OD2_best  - C_OD2_hom;
350
351 dC_OD1_worst = C_OD1_worst - C_OD1_hom;
352 dC_OD2_worst = C_OD2_worst - C_OD2_hom;
353
354 fprintf('\n=== OD contributions vs HOMOGENEOUS ===\n');
355 fprintf('BEST - HOM:   C_OD1 = %.6f | C_OD2 = %.6f | Share OD1
    = %.2f%%\n', ...
356     dC_OD1_best, dC_OD2_best, 100*abs(dC_OD1_best)/(abs(
        dC_OD1_best)+abs(dC_OD2_best)));
357 fprintf('WORST - HOM:  C_OD1 = %.6f | C_OD2 = %.6f | Share OD1
    = %.2f%%\n', ...
358     dC_OD1_worst, dC_OD2_worst, 100*abs(dC_OD1_worst)/(abs(
        dC_OD1_worst)+abs(dC_OD2_worst)));
359 fprintf('========================================\n');
360
361 h_hom
```

Listing 4: Heterogeneous CVaR-based Wardrop equilibrium (two OD pairs, five paths)

```
1     clear; close all; clc;
2
3 % Homogeneous CVaR-based Wardrop equilibrium (Braess/Wheatstone,
    one OD)
4
```

```
%% Parameters
nEdges = 5;
nPaths = 3;                              % p1=O-A-D, p2=O-B-D, p3=O-A
   -B-D
nOD    = 1;

%  P a t h edge  incidence Q (nEdges x nPaths)
Q = [1 0 1;
     1 0 0;
     0 1 0;
     0 1 1;
     0 0 1];

B = [1 1 1];                             %  O D path  incidence
demandOD = 4000;                         % total OD demand

%% Edge cost data (affine)
a  = [1/100; 0; 0; 1/100; 0];            % slope per edge
t_ff = [0; 45; 45; 0; 0];                % free-flow / constant term
    per edge

R = diag(a);

%% A matrix in A x + q
A11 = Q' * R * Q;
A12 = -B';
A21 =  B;
A22 = zeros(nOD,nOD);

A = [A11, A12;
     A21, A22];

n_var = nPaths + nOD;

%% Uncertainty (shortcut edge e5 only)
Umax = zeros(nEdges,1);
Umax(5) = 1;                             % U5 ~ Unif[0,1]
gamma = 20;                              % u5 = gamma * U5
EU    = 0.5;                             % E[U]

alphaGrid = 0.1:0.1:1.0;
nAlpha    = numel(alphaGrid);

h_hom_store        = zeros(nPaths, nAlpha);  % path flows per
   alpha
Ecost_total_store  = zeros(nAlpha, 1);       % total expected
   physical cost
shortcut_share     = zeros(nAlpha, 1);       % h_3 / demand

cvar_u_edge = @(alpha) gamma * (1 - alpha/2) .* Umax;  %
   CVaR_alpha(gamma*U)
```

```
51
52 %% Solve for each alpha
53 cvx_solver sedumi
54 cvx_precision high
55
56 for ia = 1:nAlpha
57     alpha = alphaGrid(ia);
58
59     % perceived edge constants: t_ff + CVaR term
60     t_cvar_edge = t_ff + cvar_u_edge(alpha);
61
62     % perceived path constants
63     t_cvar_path = Q' * t_cvar_edge;
64
65     q = [t_cvar_path; -demandOD];
66
67     cvx_begin quiet
68         variable x_hom(n_var)
69         minimize( x_hom' * A * x_hom + q' * x_hom )
70         subject to
71             x_hom >= 0;
72             A*x_hom + q >= 0;
73     cvx_end
74
75     h_hom = x_hom(1:nPaths);
76     h_hom_store(:, ia) = h_hom;
77
78     % expected physical system cost (mean uncertainty, not CVaR)
79     ell = Q*h_hom;                                          % edge
       flows
80     c_edge = a .* ell + t_ff + gamma*EU*Umax;               %
       expected edge costs
81
82     Ecost_total_store(ia) = sum(ell .* c_edge);
83     shortcut_share(ia)    = h_hom(3) / demandOD;
84 end
85
86 %% Plots
87 figure; hold on;
88 plot(alphaGrid, h_hom_store(1,:), '-o', 'LineWidth', 1.8);
89 plot(alphaGrid, h_hom_store(2,:), 'LineWidth', 1.8);
90 plot(alphaGrid, h_hom_store(3,:), 'LineWidth', 1.8);
91 xlabel('Risk␣aversion␣parameter␣\alpha');
92 ylabel('Flow␣h_p');
93 legend('Path␣1:␣O-A-D','Path␣2:␣O-B-D','Path␣3:␣O-A-B-D','
   Location','best');
94 title('Effect␣of␣\alpha␣on␣path␣usage');
95 grid on; hold off;
96
97 figure;
98 plot(alphaGrid, Ecost_total_store, '-o', 'LineWidth', 1.8);
```

```
xlabel('Risk aversion parameter \alpha');
ylabel('Total expected network cost');
title('Effect of \alpha on total expected network cost');
grid on;

figure;
plot(alphaGrid, shortcut_share, '-o', 'LineWidth', 1.8);
xlabel('Risk aversion parameter \alpha');
ylabel('Shortcut share (h_3 / d)');
title('Effect of \alpha on shortcut usage');
grid on;
```

Listing 5: Homogeneous CVaR-based Wardrop equilibrium (Wheatstone Network)

```
    clear; close all; clc;
format short g

% Heterogeneous CVaR-based Wardrop equilibrium (Braess/Wheatstone, one OD)

%% Tolerance
tol = 1e-3;                             % treat |x|<tol as zero

%% Parameters
alpha_bar = 0.7;                        % benchmark mean risk aversion \bar{\alpha}
nGroups   = 3;                          % number of groups (K=3)
minGap    = 0.1;                        % minimum separation between group alphas

demandOD  = 4000;                       % total OD demand
d_group   = (demandOD/nGroups) * ones(nGroups,1);

gamma = 20;                             % u5 = gamma * U, U~Unif[0,1]

%% Network definition (Braess/Wheatstone)
nEdges = 5;
nPaths = 3;                             % p1=O-A-D, p2=O-B-D, p3=O-A-B-D
nOD    = 1;

Q = [1 0 1;
     1 0 0;
     0 1 0;
     0 1 1;
     0 0 1];                            % edge path incidence (nEdges x nPaths)

B = [1 1 1];                            % OD path incidence

%% Edge costs: J_e(ell_e,u_e) = a_e*ell_e + t_ff_e + u_e
```

```
a     = [1/100; 0; 0; 1/100; 0];
t_ff  = [0;     45; 45; 0;    0];

R = diag(a);
A_base = Q' * R * Q;                    % path-level congestion
    block

%% Uncertainty on shortcut edge e5 only
Umax = zeros(nEdges,1);
Umax(5) = 1;                            % U5~Unif[0,1]

EU = 0.5;
mean_u_edge = gamma * EU * Umax;        % E[u] at edge level
cvar_u_edge = @(alpha) gamma * (1 - alpha/2) .* Umax;

%% ============================================================
% 1) ALL UNIQUE alpha CONFIGURATIONS (0.01 grid, fixed mean,
    minGap)
% ============================================================

step = 0.01;

valsInt   = 1:(1/step - 1);                    % 1..99
barInt    = round(alpha_bar / step);
minGapInt = round(minGap / step);

maxCand = numel(valsInt)^2;
all_cfg_int = zeros(maxCand, 3);
cnt = 0;

for i = 1:numel(valsInt)
    a1i = valsInt(i);
    for j = 1:numel(valsInt)
        a2i = valsInt(j);

        a3i = nGroups*barInt - a1i - a2i;
        if a3i < 1 || a3i > (1/step - 1)
            continue;
        end

        aa = sort([a1i a2i a3i]);
        if min(diff(aa)) < minGapInt
            continue;
        end

        cnt = cnt + 1;
        all_cfg_int(cnt,:) = aa;
    end
end

all_cfg_int = all_cfg_int(1:cnt,:);
```

```
all_cfg_int = unique(all_cfg_int, 'rows');

alpha_cfg = all_cfg_int * step;
nCfg = size(alpha_cfg,1);

spread  = std(alpha_cfg, 0, 2);
extreme = max(abs(alpha_cfg - alpha_bar), [], 2);

fprintf('Total number of UNIQUE heterogeneous configurations = %d
    \n', nCfg);
fprintf('Std(alpha) range: [%.6f, %.6f]\n', min(spread), max(
    spread));

sortedA = sort(alpha_cfg, 2);
minPairwiseGap = min(min(diff(sortedA,1,2)));
fprintf('Min pairwise alpha gap: %.6f\n\n', minPairwiseGap);

assert(size(unique(alpha_cfg,'rows'),1) == nCfg, 'Duplicates
    still present in alpha_cfg!');

%% ================================================================
% 2) STACKED MATRIX (A x + q) for nGroups groups
% ================================================================

B_stack  = kron(eye(nGroups), B);            % (K*nOD) x (K*
    nPaths)
A11 = kron(ones(nGroups), A_base);           % (K*nPaths) x (K*
    nPaths)
A12 = -B_stack';
A21 =  B_stack;
A22 = zeros(nGroups*nOD);

A = [A11 A12;
     A21 A22];

n_var = nGroups*nPaths + nGroups*nOD;

cvx_solver sedumi
cvx_precision high

%% ================================================================
% 3) HOMOGENEOUS BENCHMARK (alpha_k = alpha_bar)
% ================================================================

q_hom = zeros(n_var, 1);

for g = 1:nGroups
    t_cvar_edge = t_ff + cvar_u_edge(alpha_bar);
    t_cvar_path = Q' * t_cvar_edge;

    idxh = (g-1)*nPaths + (1:nPaths);
```

```
    q_hom(idxh) = t_cvar_path;

    idxv = nGroups*nPaths + (g-1)*nOD + (1:nOD);
    q_hom(idxv) = -d_group(g);
end

cvx_begin quiet
    variable x_hom(n_var)
    minimize( x_hom' * A * x_hom + q_hom' * x_hom )
    subject to
        x_hom >= 0;
        A*x_hom + q_hom >= 0;
cvx_end

H_hom = reshape(x_hom(1:nGroups*nPaths), nPaths, nGroups);
h_hom = sum(H_hom, 2);

ell_hom = Q * h_hom;
c_edge_hom = a .* ell_hom + t_ff + mean_u_edge;
C_hom = sum(ell_hom .* c_edge_hom);

H_hom(abs(H_hom) < tol) = 0;
h_hom(abs(h_hom) < tol) = 0;
ell_hom(abs(ell_hom) < tol) = 0;
if abs(C_hom) < tol, C_hom = 0; end

shortcut_share_hom = h_hom(3) / demandOD;
if abs(shortcut_share_hom) < tol, shortcut_share_hom = 0; end

fprintf('Homogeneous benchmark (alpha_k = %.2f): C_hom = %.6f | shortcut share = %.4f\n\n', ...
    alpha_bar, C_hom, shortcut_share_hom);

%% ============================================================
% 4) HETEROGENEOUS CASES (track best/worst)
% ============================================================

C_het  = zeros(nCfg,1);
DeltaC = zeros(nCfg,1);

shortcut_share = zeros(nCfg,1);
shortcut_flow  = zeros(nCfg,1);

bestDelta  = +Inf;
worstDelta = -Inf;

best_idx  = NaN;
worst_idx = NaN;

H_best  = NaN(nPaths,nGroups);
H_worst = NaN(nPaths,nGroups);
```

```
178
179 h_best  = NaN(nPaths,1);
180 h_worst = NaN(nPaths,1);
181
182 for c = 1:nCfg
183     q_het = zeros(n_var, 1);
184
185     for g = 1:nGroups
186         alpha_g = alpha_cfg(c, g);
187
188         t_cvar_edge = t_ff + cvar_u_edge(alpha_g);
189         t_cvar_path = Q' * t_cvar_edge;
190
191         idxh = (g-1)*nPaths + (1:nPaths);
192         q_het(idxh) = t_cvar_path;
193
194         idxv = nGroups*nPaths + (g-1)*nOD + (1:nOD);
195         q_het(idxv) = -d_group(g);
196     end
197
198     cvx_begin quiet
199         variable x_het(n_var)
200         minimize( x_het' * A * x_het + q_het' * x_het )
201         subject to
202             x_het >= 0;
203             A*x_het + q_het >= 0;
204     cvx_end
205
206     H_het = reshape(x_het(1:nGroups*nPaths), nPaths, nGroups);
207     h_het = sum(H_het, 2);
208
209     ell = Q * h_het;
210     c_edge = a .* ell + t_ff + mean_u_edge;
211
212     C_het(c)  = sum(ell .* c_edge);
213     DeltaC(c) = C_het(c) - C_hom;
214
215     shortcut_flow(c)  = h_het(3);
216     shortcut_share(c) = h_het(3) / demandOD;
217
218     H_het(abs(H_het) < tol) = 0;
219     h_het(abs(h_het) < tol) = 0;
220     ell(abs(ell) < tol) = 0;
221
222     if abs(C_het(c)) < tol,  C_het(c)  = 0; end
223     if abs(DeltaC(c)) < tol, DeltaC(c) = 0; end
224     if abs(shortcut_flow(c)) < tol,  shortcut_flow(c)  = 0; end
225     if abs(shortcut_share(c)) < tol, shortcut_share(c) = 0; end
226
227     if DeltaC(c) < bestDelta
228         bestDelta = DeltaC(c);
```

```
229         best_idx  = c;
230         H_best    = H_het;
231         h_best    = sum(H_het,2);
232     end
233
234     if DeltaC(c) > worstDelta
235         worstDelta = DeltaC(c);
236         worst_idx  = c;
237         H_worst    = H_het;
238         h_worst    = sum(H_het,2);
239     end
240 end
241
242 Improvement = C_hom - C_het;
243
244 Improvement(abs(Improvement) < tol) = 0;
245 C_het(abs(C_het) < tol) = 0;
246 DeltaC(abs(DeltaC) < tol) = 0;
247
248 %% ============================================================
249 % 4b) PRINT FLOWS: HOM, BEST, WORST
250 % ============================================================
251
252 pathNames  = strcat("Path", string(1:nPaths));
253 groupNames = strcat("Group", string(1:nGroups));
254
255 fprintf('\n=====␣HOMOGENEOUS␣benchmark␣=====\n');
256 fprintf('All␣groups␣alpha␣=␣%.2f\n', alpha_bar);
257 fprintf('C_hom␣=␣%.6f\n', C_hom);
258 fprintf('h_hom␣=␣[%.3f␣%.3f␣%.3f]\n', h_hom(1), h_hom(2), h_hom
    (3));
259
260 T_h_hom = table(h_hom, 'RowNames', cellstr(pathNames));
261 T_H_hom = array2table(H_hom, 'RowNames', cellstr(pathNames), '
    VariableNames', cellstr(groupNames));
262 disp('---␣HOM␣total␣flow␣per␣path␣(h_hom)␣---'); disp(T_h_hom);
263 disp('---␣HOM␣per␣group␣per␣path␣(H_hom)␣---'); disp(T_H_hom);
264
265 fprintf('\n=====␣BEST␣heterogeneous␣configuration␣(min␣DeltaC)␣
    =====\n');
266 fprintf('Index:␣%d\n', best_idx);
267 fprintf('Alphas␣(sorted):␣[%.2f␣%.2f␣%.2f]\n', alpha_cfg(best_idx
    ,1), alpha_cfg(best_idx,2), alpha_cfg(best_idx,3));
268 fprintf('DeltaC:␣%.6f\n', bestDelta);
269 fprintf('C_het(best)␣=␣%.6f\n', C_het(best_idx));
270 fprintf('h_best␣=␣[%.3f␣%.3f␣%.3f]\n', h_best(1), h_best(2),
    h_best(3));
271
272 T_h_best = table(h_best, 'RowNames', cellstr(pathNames));
273 T_H_best = array2table(H_best, 'RowNames', cellstr(pathNames), '
    VariableNames', cellstr(groupNames));
```

```
disp('--- BEST total flow per path (h_best) ---'); disp(T_h_best);
disp('--- BEST per group per path (H_best) ---'); disp(T_H_best);

fprintf('\n===== WORST heterogeneous configuration (max DeltaC) =====\n');
fprintf('Index: %d\n', worst_idx);
fprintf('Alphas (sorted): [%.2f %.2f %.2f]\n', alpha_cfg(worst_idx,1), alpha_cfg(worst_idx,2), alpha_cfg(worst_idx,3));
fprintf('DeltaC: %.6f\n', worstDelta);
fprintf('C_het(worst) = %.6f\n', C_het(worst_idx));
fprintf('h_worst = [%.3f %.3f %.3f]\n', h_worst(1), h_worst(2), h_worst(3));

T_h_worst = table(h_worst, 'RowNames', cellstr(pathNames));
T_H_worst = array2table(H_worst, 'RowNames', cellstr(pathNames), 'VariableNames', cellstr(groupNames));
disp('--- WORST total flow per path (h_worst) ---'); disp(T_h_worst);
disp('--- WORST per group per path (H_worst) ---'); disp(T_H_worst);

%% ================================================================
% 5) TABLES: TOP-20 BEST / WORST
% ================================================================

ResultsTable = table( ...
    alpha_cfg(:,1), alpha_cfg(:,2), alpha_cfg(:,3), ...
    spread, extreme, shortcut_share, ...
    C_het, DeltaC, Improvement, ...
    'VariableNames', {'Alpha1','Alpha2','Alpha3', ...
                      'Spread','Extremeness','ShortcutShare', ...
                      'CostHet','DeltaC','Improvement'} );

varsToClean = {'Spread','Extremeness','ShortcutShare','CostHet','DeltaC','Improvement'};
for vv = 1:numel(varsToClean)
    col = ResultsTable.(varsToClean{vv});
    col(abs(col) < tol) = 0;
    ResultsTable.(varsToClean{vv}) = col;
end

T_best  = sortrows(ResultsTable, 'DeltaC', 'ascend');
T_worst = sortrows(ResultsTable, 'DeltaC', 'descend');

Top20_Best  = T_best(1:min(20,height(T_best)),:);
Top20_Worst = T_worst(1:min(20,height(T_worst)),:);

disp('===== TOP 20 BEST configurations (lowest DeltaC) =====');
disp(Top20_Best);
disp('===== TOP 20 WORST configurations (highest DeltaC) =====');
```

```
disp(Top20_Worst);

writetable(Top20_Best,  'Braess_Top20_Best.csv');
writetable(Top20_Worst, 'Braess_Top20_Worst.csv');

%% ================================================================
% 6) PLOTS
% ================================================================

figure;
scatter(spread, DeltaC, 25, 'filled');
xlabel('Spread of \alpha (std)');
ylabel('\Delta C = C_{het} - C_{hom}');
title(sprintf('Difference in Cost as a function of Spread (\\bar{\\alpha} = %.1f)', alpha_bar));
grid on; yline(0,'k--','LineWidth',1.2);

figure;
scatter(extreme, DeltaC, 25, spread, 'filled');
cb = colorbar; ylabel(cb,'Spread');
xlabel('Extremeness  max | \alpha_g - \bar{\alpha} |');
ylabel('\Delta C');
title(sprintf('Difference in Cost as a function of Extremeness (\\bar{\\alpha} = %.1f)', alpha_bar));
grid on; yline(0,'k--','LineWidth',1.2);

figure;
scatter(shortcut_share, DeltaC, 25, spread, 'filled');
cb = colorbar; ylabel(cb,'Spread');
xlabel('Shortcut share');
ylabel('\Delta C');
title(sprintf('Difference in Cost as a function of Shortcut Usage (\\bar{\\alpha} = %.1f)', alpha_bar));
grid on; yline(0,'k--','LineWidth',1.2);

figure;
histogram(DeltaC, 30);
xline(0,'k--','LineWidth',1.5);
xlabel('\Delta C'); ylabel('Frequency');
title(sprintf('Distribution of \\Delta C (\\bar{\\alpha} = %.1f)', alpha_bar));
grid on;

%% ================================================================
% 7) SUMMARY STATS
% ================================================================

fprintf('\n=== Heterogeneity Summary (Braess, alpha_bar=%.2f) ===\n', alpha_bar);
fprintf('gamma = %.6f (edge e5 only)\n', gamma);
fprintf('Benchmark cost C_hom = %.6f\n', C_hom);
```

```
fprintf('Mean C = %.6f\n', mean(DeltaC));
fprintf('%% cases better than benchmark = %.2f%%\n', 100*mean(
    DeltaC < 0));
fprintf('Best C = %.6f\n', min(DeltaC));
fprintf('Worst C = %.6f\n', max(DeltaC));
fprintf('Benchmark shortcut share = %.4f\n', shortcut_share_hom);
fprintf('Mean heterogeneous shortcut share = %.4f\n', mean(
    shortcut_share));
fprintf('=====================================================\n'
    );
```

Listing 6: Heterogeneous CVaR-based Wardrop equilibrium (Wheatstone Network)

```
[caption={ Homogeneous CVaR-based Wardrop equilibrium (Sioux
    Falls Network)}]
    %% Sioux Falls Homogeneous Network

clear; clc;

%% 1. Load network data
Sioux_data = readtable('SiouxFalls_net.csv');
start_node    = Sioux_data.A;
end_node      = Sioux_data.B;
freeflow_time = Sioux_data.a0;      % t0

G = digraph(start_node, end_node, freeflow_time);

%% 2. OD pairs + path enumeration settings
OD_pairs = [1 19; 13 8; 12 18];
nOD      = size(OD_pairs, 1);
K        = 10;                      % Number of top paths per OD
maxLen   = 15;                      % Maximum path length

k_shortest = struct('origin',cell(nOD,1), 'destination',cell(nOD
    ,1), 'paths',cell(nOD,1), 'costs',cell(nOD,1));

fprintf('\n=== Top-%d free-flow paths per OD pair ===\n', K);

%% 3. Enumerate paths and keep top-K
for r = 1:nOD
    o = OD_pairs(r,1);
    d = OD_pairs(r,2);

    path_list = allpaths(G, o, d, 'MaxPathLength', maxLen);
    nPathsOD  = numel(path_list);

    if nPathsOD == 0
        fprintf('OD %d -> %d: no path found.\n', o, d);
        continue;
    end

    path_cost = zeros(nPathsOD,1);
```

```
38      for p = 1:nPathsOD
39          nodes_on_path = path_list{p};
40          e_idx = findedge(G, nodes_on_path(1:end-1), nodes_on_path
                (2:end));
41          path_cost(p) = sum(G.Edges.Weight(e_idx));
42      end
43
44      k_use = min(K, nPathsOD);
45      [~, best_idx] = mink(path_cost, k_use);
46
47      k_shortest(r).origin      = o;
48      k_shortest(r).destination = d;
49      k_shortest(r).paths       = path_list(best_idx);
50      k_shortest(r).costs       = path_cost(best_idx);
51
52      fprintf('\nOD␣%d␣->␣%d:\n', o, d);
53      for j = 1:k_use
54          fprintf('%2d)␣cost␣=␣%.3f␣|␣path:␣%s\n', j, k_shortest(r)
                .costs(j), mat2str(k_shortest(r).paths{j}));
55      end
56  end
57
58  %% 4. Build  p a t h edge  incidence matrix Q
59  nEdges = numedges(G);
60  totalPaths = 0;
61  for r = 1:nOD
62      totalPaths = totalPaths + numel(k_shortest(r).paths);
63  end
64  nPaths = totalPaths;
65
66  Q = zeros(nEdges, nPaths);
67  col_OD   = zeros(nPaths, 2);
68  col_rank = zeros(nPaths, 1);
69
70  colIdx = 1;
71  for r = 1:nOD
72      paths_r = k_shortest(r).paths;
73      for j = 1:numel(paths_r)
74          nodes_on_path = paths_r{j};
75          e_idx = findedge(G, nodes_on_path(1:end-1), nodes_on_path
                (2:end));
76
77          Q(e_idx, colIdx) = 1;
78          col_OD(colIdx,:) = [k_shortest(r).origin, k_shortest(r).
                destination];
79          col_rank(colIdx) = j;
80
81          colIdx = colIdx + 1;
82      end
83  end
84
```

```
fprintf('\nIncidence matrix Q size: %d edges   %d paths\n',
    nEdges, nPaths);

%% ==================== VI SETUP ====================
demand = [300; 600; 200]; % Demand for each OD pair
B = zeros(nOD, nPaths);

for p = 1:nPaths
    odp = col_OD(p,:);
    rMatch = find(OD_pairs(:,1)==odp(1) & OD_pairs(:,2)==odp(2),
        1);
    B(rMatch, p) = 1;
end

b_e = 100;
t0  = G.Edges.Weight(:);  % free-flow time per edge

% Capacities
c_e = [25900.20; 23403.47; 25900.20; 4958.18; 23403.47; 17110.52;
    23403.47; 17110.52; ...
    17782.79; 4908.83; 17782.79; 4948.00; 10000.00; 4958.18;
        4948.00; 4898.59; ...
    7841.81; 23403.47; 4898.59; 7841.81; 5050.19; 5045.82;
        10000.00; 5050.19; 13915.79; ...
    13915.79; 10000.00; 13512.00; 4854.92; 4993.51; 4908.83;
        10000.00; 4908.83; 4876.51; ...
    23403.47; 4908.83; 25900.20; 25900.20; 5091.26; 4876.51;
        5127.53; 4924.79; ...
    13512.00; 5127.53; 14564.75; 9599.18; 5045.82; 4854.92;
        5229.91; 19679.90; ...
    4993.51; 5229.91; 4823.95; 23403.47; 19679.90; 23403.47;
        14564.75; 4823.95; ...
    5002.61; 23403.47; 5002.61; 5059.91; 5075.70; 5059.91;
        5229.91; 4885.36; ...
    9599.18; 5075.70; 5229.91; 5000.00; 4924.79; 5000.00;
        5078.51; 5091.26; ...
    4885.36; 5078.51];

R = diag(b_e * (t0 ./ c_e));

% VI matrix A (previously M)
A11 = Q' * R * Q;
A12 = -B';
A21 = B;
A22 = zeros(nOD, nOD);
A   = [A11, A12;
       A21, A22];


alpha_grid = 0:0.1:1;
nA = numel(alpha_grid);
```

```
125
126 H_store  = zeros(nPaths, nA);  % equilibrium path flows per alpha
127 TC_store = zeros(nA, 1);       % expected ACTUAL total cost per
       alpha
128
129 n = nPaths + nOD;
130
131 fprintf('\n=== Solving VI for alpha = 0:0.1:1 ===\n');
132
133 for ia = 1:nA
134     alpha = alpha_grid(ia);
135
136     % Perceived edge cost for routing decisions in the VI
137     cvar_u = zeros(nEdges, 1);
138     cvar_u = (0.25 * (2 - alpha)) .* t0;  % Uncertainty for edges
139
140     perc_cost = t0 + cvar_u;     % perceived edge cost
141     c_path    = Q' * perc_cost;  % perceived path cost
142     q         = [c_path; -demand];
143
144     % Solve VI/QP (CVX)
145     cvx_begin quiet
146         variable x_hom(n)
147         minimize( x_hom' * A * x_hom + q' * x_hom )
148         subject to
149             x_hom >= 0;
150             A * x_hom + q >= 0;
151     cvx_end
152
153     h_star = x_hom(1:nPaths);
154     H_store(:, ia) = h_star;
155
156     % Expected ACTUAL total cost for plotting
157     ell = Q * h_star;
158     f_cong = t0 .* (1 + b_e * (ell ./ c_e));
159     u_mean = 0.25 * t0;   % Uncertainty mean
160
161     % Total expected system cost: sum_e l_e * (f_cong + u_mean)
162     TC_store(ia) = sum(ell .* (f_cong + u_mean));
163     fprintf('alpha = %.1f |  Actual Total Cost = %.6g \n', alpha,
           TC_store(ia));
164 end
165
166 %% ================== PLOTS ==================
167
168 % Plot 1: Path usage
169 figure; hold on;
170 for p = 1:nPaths
171     plot(alpha_grid, H_store(p,:), 'LineWidth', 1.5);
172 end
173 hold off;
```

```
174
175 xlabel('Risk aversion parameter \alpha');
176 ylabel('Flow h_p');
177 title('Effect of \alpha on path usage');
178 grid on;
179
180 % Plot 2: Expected actual total cost vs alpha
181 figure;
182 plot(alpha_grid, TC_store, '-o', 'LineWidth', 1.5);
183 xlabel('Risk aversion parameter \alpha');
184 ylabel('Total network cost');
185 title('Effect of \alpha on total network cost');
186 grid on;
```

```
1 [caption={Heterogeneous CVaR-based Wardrop equilibrium (Sioux
     Falls Network)}]
2     %% Sioux Falls     Heterogeneous Risk
3
4 clear; close all; clc;
5
6 %% ============================================================
7 %  0) USER SETTINGS
8 %% ============================================================
9 alpha_bar = 0.7;      % homogeneous benchmark mean alpha
10 K         = 3;        % number of risk groups
11 N_cfg     = 400;      % (will be overwritten after enumeration)
12 minGap    = 0.10;     % minimum separation between alpha values
13 rng(1);               % reproducibility
14
15 Kpaths = 10;
16 maxLen = 15;
17
18 %% ============================================================
19 %  1) BUILD TOP-K PATHS + INCIDENCE
20 %% ============================================================
21 Sioux_data = readtable('SiouxFalls_net.csv');
22
23 start_node    = Sioux_data.A;
24 end_node      = Sioux_data.B;
25 freeflow_time = Sioux_data.a0;
26
27 G = digraph(start_node, end_node, freeflow_time);
28
29 OD_pairs = [1 19; 13 8; 12 18];
30 nOD      = size(OD_pairs,1);
31
32 k_shortest = struct('origin',cell(nOD,1), 'destination',cell(nOD
     ,1), ...
33                     'paths',cell(nOD,1), 'costs',cell(nOD,1));
34
35 fprintf('\n=== Top-%d free-flow paths per OD pair ===\n', Kpaths)
```

```
    ;
36
37 for r = 1:nOD
38     o = OD_pairs(r,1);
39     d = OD_pairs(r,2);
40
41     path_list = allpaths(G, o, d, 'MaxPathLength', maxLen);
42     nPathsOD  = numel(path_list);
43
44     if nPathsOD == 0
45         fprintf('OD %d -> %d: no path found.\n', o, d);
46         k_shortest(r).origin      = o;
47         k_shortest(r).destination = d;
48         k_shortest(r).paths       = {};
49         k_shortest(r).costs       = [];
50         continue;
51     end
52
53     path_cost = zeros(nPathsOD,1);
54     for p = 1:nPathsOD
55         nodes_on_path = path_list{p};
56         e_idx = findedge(G, nodes_on_path(1:end-1), nodes_on_path
               (2:end));
57         path_cost(p) = sum(G.Edges.Weight(e_idx));
58     end
59
60     k_use = min(Kpaths, nPathsOD);
61     [~, best_idx] = mink(path_cost, k_use);
62
63     k_shortest(r).origin      = o;
64     k_shortest(r).destination = d;
65     k_shortest(r).paths       = path_list(best_idx);
66     k_shortest(r).costs       = path_cost(best_idx);
67
68     fprintf('\nOD %d -> %d:\n', o, d);
69     for j = 1:k_use
70         fprintf('%2d) cost = %.3f | path: %s\n', j, k_shortest(r)
               .costs(j), mat2str(k_shortest(r).paths{j}));
71     end
72 end
73
74 %% --- Build Q (edge path) and bookkeeping ---
75 nEdges = numedges(G);
76 totalPaths = 0;
77
78 for r = 1:nOD
79     totalPaths = totalPaths + numel(k_shortest(r).paths);
80 end
81 P = totalPaths;
82
83 Q = zeros(nEdges, P);
```

```
col_OD   = zeros(P, 2);
col_rank = zeros(P, 1);

colIdx = 1;
for r = 1:nOD
    paths_r = k_shortest(r).paths;
    for j = 1:numel(paths_r)
        nodes_on_path = paths_r{j};
        e_idx = findedge(G, nodes_on_path(1:end-1), nodes_on_path
           (2:end));

        Q(e_idx, colIdx) = 1;
        col_OD(colIdx,:) = [k_shortest(r).origin, k_shortest(r).
           destination];
        col_rank(colIdx) = j;

        colIdx = colIdx + 1;
    end
end

fprintf('\nIncidence matrix Q size: %d edges    %d paths\n',
   nEdges, P);

%% --- Build B (OD path) ---
B = zeros(nOD, P);
for p = 1:P
    odp = col_OD(p,:);
    rMatch = find(OD_pairs(:,1)==odp(1) & OD_pairs(:,2)==odp(2),
       1);
    B(rMatch,p) = 1;
end

%% ============================================================
%  2) MODEL PARAMETERS (same as homogeneous Sioux Falls setup)
%% ============================================================
d = [300; 600; 200];
d_group = (1/K) * d;

b_e = 100;
t0  = G.Edges.Weight(:);

c_e = [25900.20; 23403.47; 25900.20; 4958.18; 23403.47; 17110.52;
    23403.47; 17110.52;...
    17782.79; 4908.83; 17782.79; 4948.00; 10000.00; 4958.18;
       4948.00; 4898.59;...
    7841.81; 23403.47; 4898.59; 7841.81; 5050.19; 5045.82;
       10000.00; 5050.19; 13915.79];
c_e = c_e(:);

R = diag(b_e * (t0 ./ c_e));
Mbase = Q' * R * Q;
```

```
128
129 % Uncertain edges: incident to nodes 10, 16, 17
130 nodes_unc = [10 16 17];
131 edges_uncertainty = [];
132 for v = nodes_unc
133     edges_uncertainty = [edges_uncertainty; inedges(G,v);
        outedges(G,v)];
134 end
135 edges_uncertainty = unique(edges_uncertainty);
136 isUnc = false(nEdges,1);
137 isUnc(edges_uncertainty) = true;
138
139 u_mean_edge = zeros(nEdges,1);
140 u_mean_edge(isUnc) = 0.25 * t0(isUnc);
141
142 %% ============================================================
143 %  3) ALL UNIQUE DISCRETE CONFIGURATIONS
144 %% ============================================================
145 step = 0.01;
146 valsInt   = 1:99;
147 barInt    = round(alpha_bar * 100);
148 minGapInt = round(minGap * 100);
149
150 all_cfg_int = [];
151
152 for i = 1:numel(valsInt)
153     a1i = valsInt(i);
154     for j = 1:numel(valsInt)
155         a2i = valsInt(j);
156
157         a3i = 3*barInt - a1i - a2i;
158
159         if a3i < 1 || a3i > 99
160             continue;
161         end
162
163         aa = sort([a1i a2i a3i]);
164
165         if min(diff(aa)) < minGapInt
166             continue;
167         end
168
169         all_cfg_int = [all_cfg_int; aa];
170     end
171 end
172
173 all_cfg_int = unique(all_cfg_int, 'rows');
174 alpha_cfg = all_cfg_int / 100;
175 N_cfg = size(alpha_cfg, 1);
176
177 fprintf('\nTotal number of UNIQUE heterogeneous configurations =
```

```
    %d\n', N_cfg);
178
179 assert(size(unique(alpha_cfg,'rows'),1) == N_cfg, 'Duplicates␣
    still␣present␣in␣alpha_cfg!');
180
181 spread  = std(alpha_cfg, 0, 2);
182 extreme = max(abs(alpha_cfg - alpha_bar), [], 2);
183
184 fprintf('Std(alpha)␣range:␣[%.6f,␣%.6f]\n', min(spread), max(
    spread));
185
186 %% ============================================================
187 %  4) BUILD VI MATRICES (homogeneous + heterogeneous)
188 %% ============================================================
189 M_hom = [Mbase, -B';
190          B,     zeros(nOD)];
191
192 M11_het = kron(ones(K), Mbase);
193 B_het   = kron(eye(K), B);
194 M12_het = -B_het';
195 M21_het =  B_het;
196 M22_het = zeros(K*nOD);
197
198 M_het = [M11_het, M12_het;
199          M21_het, M22_het];
200
201 n_var_hom = P + nOD;
202 n_var_het = K*P + K*nOD;
203
204 %% ============================================================
205 %  5) HOMOGENEOUS BASELINE
206 %% ============================================================
207 cvar_u = zeros(nEdges,1);
208 cvar_u(isUnc) = (0.25 * (2 - alpha_bar)) .* t0(isUnc);
209 perc_edge_cost = t0 + cvar_u;
210 perc_path_cost = Q' * perc_edge_cost;
211
212 q_hom = [perc_path_cost; -d];
213
214 cvx_solver sedumi
215 cvx_precision high
216 cvx_begin quiet
217     variable x_hom(n_var_hom)
218     minimize( x_hom' * M_hom * x_hom + q_hom' * x_hom )
219     subject to
220         x_hom >= 0;
221         M_hom * x_hom + q_hom >= 0;
222 cvx_end
223
224 h_hom = x_hom(1:P);
225 ell_h = Q * h_hom;
```

```
f_cong_h = t0 .* (1 + b_e * (ell_h ./ c_e));
C_hom = sum( ell_h .* (f_cong_h + u_mean_edge) );

fprintf('Homogeneous cost C_hom (alpha_bar=%.2f) = %.6g\n',
    alpha_bar, C_hom);

%% ============================================================
%  6) HETEROGENEOUS RUNS + METRICS
%% ============================================================
C_het = zeros(N_cfg,1);
deltaC = zeros(N_cfg,1);
bneckUtil = zeros(N_cfg,1);
uncFlow = zeros(N_cfg,1);

bestDelta  = +Inf;
worstDelta = -Inf;

best_idx  = NaN;
worst_idx = NaN;

H_best  = NaN(P,K);
H_worst = NaN(P,K);
h_best  = NaN(P,1);
h_worst = NaN(P,1);

for c = 1:N_cfg
    a_vec = alpha_cfg(c,:);

    q = zeros(n_var_het,1);

    for kk = 1:K
        a_k = a_vec(kk);
        cvar_u_k = zeros(nEdges,1);
        cvar_u_k(isUnc) = (0.25 * (2 - a_k)) .* t0(isUnc);
        perc_edge_cost_k = t0 + cvar_u_k;
        perc_path_cost_k = Q' * perc_edge_cost_k;

        idx = (kk-1)*P + (1:P);
        q(idx) = perc_path_cost_k;
    end

    for kk = 1:K
        idxv = K*P + (kk-1)*nOD + (1:nOD);
        q(idxv) = -d_group;
    end

    cvx_begin quiet
        variable x(n_var_het)
        minimize( x' * M_het * x + q' * x )
        subject to
            x >= 0;
```

```
            M_het * x + q >= 0;
    cvx_end

    H = reshape(x(1:K*P), P, K);
    H(abs(H) < 1e-6) = 0;
    h_tot = sum(H,2);
    h_tot(abs(h_tot) < 1e-6) = 0;

    ell = Q * h_tot;
    f_cong = t0 .* (1 + b_e * (ell ./ c_e));
    C_het(c) = sum( ell .* (f_cong + u_mean_edge) );

    deltaC(c) = C_het(c) - C_hom;

    util = ell ./ c_e;
    bneckUtil(c) = max(util);
    uncFlow(c)   = sum(ell(isUnc));

    if deltaC(c) < bestDelta
        bestDelta = deltaC(c);
        best_idx  = c;
        H_best    = H;
        h_best    = h_tot;
    end

    if deltaC(c) > worstDelta
        worstDelta = deltaC(c);
        worst_idx  = c;
        H_worst    = H;
        h_worst    = h_tot;
    end
end

Improvement = C_hom - C_het;

%% ============================================================
%  6.6) PRINT FLOWS FOR BEST AND WORST CONFIGURATIONS
%% ============================================================
pathNames   = strcat("Path", string(1:P));
groupNames  = strcat("Group", string(1:K));

fprintf('\n=====␣BEST␣configuration␣(min␣DeltaC)␣=====\n');
fprintf('Index:␣%d\n', best_idx);
fprintf('Alphas␣(sorted):␣[%.2f␣%.2f␣%.2f]\n', alpha_cfg(best_idx
   ,1), alpha_cfg(best_idx,2), alpha_cfg(best_idx,3));
fprintf('DeltaC:␣%.6f\n', bestDelta);

T_h_best = table(h_best, 'RowNames', cellstr(pathNames));
T_H_best = array2table(H_best, 'RowNames', cellstr(pathNames), '
   VariableNames', cellstr(groupNames));

```

```
disp('--- BEST total flow per path (h_best) ---');
disp(T_h_best);
disp('--- BEST per group per path (H_best) ---');
disp(T_H_best);

fprintf('\n===== WORST configuration (max DeltaC) =====\n');
fprintf('Index: %d\n', worst_idx);
fprintf('Alphas (sorted): [%.2f %.2f %.2f]\n', alpha_cfg(
    worst_idx,1), alpha_cfg(worst_idx,2), alpha_cfg(worst_idx,3));
fprintf('DeltaC: %.6f\n', worstDelta);

T_h_worst = table(h_worst, 'RowNames', cellstr(pathNames));
T_H_worst = array2table(H_worst, 'RowNames', cellstr(pathNames),
    'VariableNames', cellstr(groupNames));

disp('--- WORST total flow per path (h_worst) ---');
disp(T_h_worst);
disp('--- WORST per group per path (H_worst) ---');
disp(T_H_worst);

%% ================================================================
%  7) SUMMARY STATS
%% ================================================================
fprintf('\n=== Heterogeneity Summary (Sioux Falls) ===\n');
fprintf('Homogeneous cost C_hom = %.6f\n', C_hom);
fprintf('Mean  C  = %.6f\n', mean(deltaC));
fprintf('%% cases better than homogeneous = %.2f%%\n', 100*mean(
    deltaC < 0));
fprintf('Best  C  (most negative) = %.6f\n', min(deltaC));
fprintf('Worst  C  (most positive) = %.6f\n', max(deltaC));
fprintf('=========================================\n');
```